รายงานวิจัยฉบับสมบูรณ์

การฟลูอิไดเซชันที่ถูกช่วยด้วยเสียงของอนุภาคละเอียด
(SOUND ASSISTED FLUIDIZATION OF FINE PARTICLES)

โดย

ผู้ช่วยศาสตราจารย์ ดร. ปริมานันท์ เชิญธงไชย

15 ธันวาคม พ.ศ. 2560

สัญญาเลขที่ RSA5780008

รายงานวิจัยฉบับสมบรูณ์

การฟลูอิไดเซชันที่ถูกช่วยด้วยเสียงของอนุภาคละเอียด
(SOUND ASSISTED FLUIDIZATION OF FINE PARTICLES)

ผู้ช่วยศาสตราจารย์ ดร. ปริมานันท์ เชิญธงไชย

ภาควิชาเคมีอุตสาหกรรม คณะวิทยาศาสตร์

มหาวิทยาลัยเชียงใหม่

(ความเห็นในรายงานนี้เป็นของผู้วิจัย สกว. และมหาวิทยาลัยเชียงใหม่ไม่จำเป็นต้องเห็นด้วยเสมอไป)

ACKNOWLEGMENT

Thailand Research Fund and Chiang Mai University are gratefully acknowledged for their financial support (Contract number: RSA5780008). In addition, I would like to acknowledge also Faculty of Science, Chiang Mai University and all staffs for all kinds of their supports. Finally, I would like to express my sincere thanks to all undergraduate students who have helped in this project.

TABLE OF CONTENTS

LIST OF FIGURES

LIST OF TABLES

บทคัดย่อ

งานวิจัยนี้มีจุดประสงค์เพื่อศึกษาพฤติกรรมทางไฮโดรไดนามิกส์ของอนุภาคละเอียด (อนุภาค เกลดาร์ท กลุ่ม เอ) ของการฟลูอิไดเซชันที่ถูกช่วยด้วยเสียงภายใต้อิทธิพลของคลื่นนิ่งที่แฝงไว้ซึ่งคุณสมบัติต่างๆ ของคลื่นเสียงและเพื่อพัฒนาความสัมพันธ์ทางคณิตศาสตร์ที่ใช้อธิบายพฤติกรรมทางไฮโดรไดนามิกส์ของอนุภาคละเอียด ในงานนี้คุณสมบัติของคลื่นเสียงที่ใช้คือที่ระดับความดันเสียง 80 เดซิเบลและความถี่ช่วง 50–500 เฮิร์ต พฤติกรรมทางไฮโดรไดนามิกส์ที่ศึกษาได้แก่ ความดันลดคร่อมเบดความดันลดคร่อมเบดนิ่ง ความเร็วเริ่มต้นของการฟลูอิไดเซชัน ความเร็วสมบรูณ์ของการฟลูอิไดเซขัน (ความเร็วต่ำสุดของการฟลูอิไดเซขัน) และลักษณะเฉพาะการขยายตัวของเบด โดยวิธีการทดลองที่ใช้ศึกษาคือการทดลองฟลูอิไดเซชันและดีฟลูอิไดเซชัน และการทดลอง 1–วาล์ว และ 2–วาล์วเบดคอลแลปส์ นอกจากนี้เพื่อให้ได้ข้อมูลการขยายตัวของเบดทีถูกต้อง กราฟเบดคอลแลปส์จะถูกแปลผลโดยใช้แบดคอลแลปส์โมเดล

สำหรับการฟลูอิไดเซชันที่สมบรูณ์พบว่าความดันลดคร่อมเบดจะเท่ากับน้ำหนักเบดต่อพื้นที่หน้าตัดเบดเสมอ แต่ความดันลดครอมเบดนิ่งจะเพิ่มขึ้นตามความถี่เสียงที่เพิ่มขึ้นเมื่อเทียบกับการฟลูอิไดเซชันพื้นฐาน ซึ่งพิสูจน์ว่าเสียงส่งแรงกระทำต่อเบดของอนุภาค นอกจากนี้ยังพบว่าเมื่อเพิ่มความถี่เสียงความเร็วต่ำสุดของการฟลูอิไดเซขันจะลดลงจนถึงค่าต่ำสุดที่ความถี่เสียงวิกฤต 50 เฮิร์ต หลังจากจุดนี้การเพิ่มความถี่เสียงจะทำให้ความเร็วต่ำสุดของการฟลูอิไดเซขันเพิ่มขึ้นและคงที่ในที่สุด รูปแบบการเปลี่ยนแปลงความเร็วต่ำสุดของการฟลูอิไดเซขันตามความถี่เสียงเช่นนี้พบว่าสอดคล้องกับลักษณะเฉพาะของคลื่นนิ่งที่ตัวกลางฟลูอิไดเซชัน ซึ่งค่าเฉลี่ยของระดับความดันเสียงของคลื่นนิ่งจะมีการเพิ่มขึ้นแบบเอ็กซ์โพเนนเชียลเมื่อค่าความถี่เสียงเข้าใกล้ค่าวิกฤตและและมีลักษณะเป็นรอบสำหรับแต่ละเลขฮาโมนิกส์ ซึ่งความสัมพันธ์นี้ยังชี้ให้เห็นว่าค่าต่ำสุดของความเร็วต่ำสุดของการฟลูอิไดเซขันมีได้หลายค่าตามรูปแบบการเปลี่ยนแปลงที่มีลักษณะเป็นรอบของคลื่นนิ่งในฟลูอิไดซ์เบดตามคุณสมบัติของคลื่นเสียง สุดท้ายความสัมพันธ์ทางคณิตศาสตร์สำหรับความดันลดคร่อมเบดนิ่งของการฟลูอิไดเซชันที่ถูกช่วยด้วยเสียงได้ถูกเสนอโดยอยู่บนฐานของสมการเออร์กัน และสมการปรับปรุงของสมการ

เออร์กัน ที่พิจารณาความเร็วในการสั่นสะเทือนของก๊าซภายใต้รูปแบบการเคลื่อนที่ของคลื่นนิ่งในฟลูอิไดซ์เบดร่วมด้วย

ลักษณะเฉพาะการขยายตังของเบดของอนุภาคเกลดาร์ทกลุ่ม เอ ในการฟลูอิไดเซชันที่ถูกช่วยด้วยเสียงได้แก่ สัดส่วนช่องว่างในเบดทั้งหมด และสัดส่วนช่องว่างในวัฏภาคแน่นมีการเปลี่ยนแปลงตามความเร็วในท่อเปล่าที่ทางเข้าในลักษณะเดียวกันกับการฟลูอิไดเซชันพื้ฐาน นอกจากนี้ยังพบว่าสัดส่วนช่องว่างในการฟลูอิไดเซชันที่ถูกช่วยด้วยเสียงจะมีค่าต่ำกว่าสัดส่วนช่องว่างในการฟลูอิไดเซชันพื้นฐานและไม่ขึ้นอยู่กับความถี่เสียง และยังพบว่าความสัมพันธ์ระหว่างสัดส่วนช่องว่างในวัฏภาคแน่นและความเร็วในท่อเปล่าในวัฏภาคแน่นที่ความถี่เสียงต่างๆกระจายอยู่บนแนวโน้มเดียวกันกับความสัมพันธ์ดังกล่าวของการฟลูอิไดเซชันพื้นฐาน และยังพบว่าจุดต่ำสุดของการเกิดฟองก๊าซจะไม่ขึ้นอยู่กับแรงสั่นสะเทือนของเสียง เมื่อระบุโดยใช้กราฟลักษณะเฉพาะของความสมพันธ์ระหว่างสัดส่วนช่องว่างในวัฏภาคแน่นและความเร็วในท่อเปล่าในวัฏภาคแน่น สิ่งที่พบเหล่านี้ชี้ให้เห็นว่าแรงสั่นสะเทือนของเสียงมีแนวโน้มที่จะสร้างวัฏภาคช่องว่างหรือวัฏภาคฟองก๊าซในฟลูอิไดซ์เบดมากกว่าที่จะเปลี่ยนแปลงความสัมพันธ์ทางไฮโดรไดนามิกส์ในวัฏภาคแน่น ดังนั้นสมดุลแรงสำหรับการฟลูอิไดเซชันที่ถูกช่วยด้วยเสียงจึงเหมือนกับสมดุลแรงสำหรับการฟลูอิไดเซชันพื้นฐาน และเช่นกันสำหรับเกณฑ์ตัดสินความเสถียรของอนุภาคเบด ในงานวิจัยนี้ยังได้พิสูจน์ให้เห็นว่าความสัมพันธ์ปรับปรุงของเออร์กันสำหรับการฟลูอิไดเซชันพื้นฐานสามารถใช้อธิบายกราฟลักษณะเฉพาะของความสมพันธ์ระหว่างสัดส่วนช่องว่างในวัฏภาคแน่น และความเร็วในท่อเปล่าในวัฏภาคแน่นของการฟลูอิไดเซชันที่ถูกช่วยด้วยเสียงได้เป็นอย่างดีในทำนองเดียวกันกับเกณฑ์ตัดสินความเสถียรของอนุภาคเบดเสนอโดย เชิญธงไชยและบรานดานิ ใน ปี ค.ศ. 2013

คำสำคัญ: เสียง; ฟลูอิไดเซชัน; ไฮโดรไดนามิกส์

ABSTRACT

Objectives of this work were to investigate hydrodynamics behaviors of a sound-assisted fluidization of fine powder (Geldart's group A powder) under effects of standing wave characteristics in which the wave properties were embedded and to develop mathematical models to describe the hydrodynamics behaviors of this fine powder in the sound assisted fluidization. The sound wave properties used in this work were a sound frequency ranging from 0-500 Hz at a fixed sound pressure level of 80 dB and the hydrodynamics behaviors observed were a total bed pressure drop, a fixed bed pressure drop, an incipient fluidization velocity, a complete fluidization velocity (a minimum fluidization velocity) and bed expansion characteristics. Experimental methods used for the study of fluidization hydrodynamics behaviorswerefluidization and de-fluidization experiments and 1-valve and 2-valve bed collapse experiment. And, to obtain an accurate bed expansion data, a bed collapse model was used for a correct interpretation of bed collapse curves.

It was found that, for full fluidization, the total bed pressure drop was always equaled to weight of a bed per cross section area but the fixed bed pressure drop increased with sound frequency, in comparison with a conventional fluidization. This was proved that the sound wave also associated its force on the particle bed. In addition, with increasing sound wave frequency, the minimum fluidization velocity was decreased and reached the local minimum value at sound critical frequency of 50 Hz. After this point, the further increase in the sound frequency caused the minimum fluidization velocity to be increased again and, then, leveled off. This pattern of variation was found to be consistent with the standing wave characteristics in fluidization medium, where an average magnitude of the sound pressure level varied exponentially around the critical

frequency and periodically for each harmonic number. It was also pointed out that the local minimum of the minimum fluidization velocity can be multiple values according to this periodic variation pattern of the standing wave in the fluidized bed with the sound wave properties. Finally, by taken into account the gas oscillation velocity caused by a particular pattern of the standing wave travelling inside the fluidized bed, the fixed bed pressure drop correlations based on revised Ergun equation and Ergun equation, including their empirical closure equations, were proposed.

Bed expansion characteristics of the Geldart,group A powder in the sound assisted fluidization were as follows; a total bed voidage and a dense bed voidage for the sound assisted fluidization were varied with an inlet superficial velocity in the same fashion as those for a conventional fluidization. Besides, the voidage with respect to the inlet superficial velocity of the sound assisted fluidization was found to be lower, in comparison with those of the conventional fluidization and was independent with the sound frequency. In addition, dense phase voidage and its superficial velocity relations of the sound assisted fluidization at different sound frequency were approximately on the same trend as that for the conventional fluidization. Finally, a minimum bubbling point, defined using the dense phase voidage and dense phase superficial velocity characteristic curve, was also unaffected by the sound vibration force. These findings suggested that a sound vibrational force tended to create more cavity or bubble phase in the fluidized bed, rather than changing a hydrodynamics relation in the dense phase. Therefore, the same equilibrium of force as that of the conventional fluidization can still be applied for the sound assisted fluidization, as well as stability criteria. Finally, it was proved that the modified revised Ergun drag force correlation, applicable for the conventional fluidization, can describe well the dense phase voidage and the dense

phase superficial velocity characteristic curves of the sound assisted fluidization. Likewise, the stability criterion purposed by Cherntongchai and Brandani (2013) can predict excellently the minimum bubbling points for the sound assisted fluidized bed.

KEYWORDS: Sound; Fluidization; Hydrodynamics

EXECUTIVE SUMMARY

1. Objectives

1.1 To extend level of understanding on hydrodynamics behaviors fine particles in sound assisted fluidization.

1.2 To develop mathematical models to describe the hydrodynamics behaviors of the fine particles in the sound assisted fluidization.

2. Research overview

Sound-assisted fluidization is a modification of conventional fluidization by implementing sound vibrational force. And, the additional equipment is a sound wave generator, connected to a sound amplifier and a loudspeaker.Then, the sound wave which is a pressure wave will propagate through a bed of particles and break up the inter-particle forces, resulting in better fluidization quality, smaller agglomerate size, particle elutriation reduction, and change in the fluidization hydrodynamics.

The characteristics of sound-assisted fluidization are implicitly related to the characteristics of a standing wave traveling through the fluidizing bed, which has been thoroughly described by Herrera et al. (2002). However, the knowledge has never been used to explain the fluidization characteristics observed. In this work, we applied the knowledge regarding the standing wave characteristics to explain the influence of sound frequency on the minimum fluidization velocity of sound-assisted fluidization of Geldart's group A powder. In addition, fixed bed pressure drop correlations for sound-assisted fluidization were also developed, where gas oscillation velocity, varied according to the characteristics of the standing wave, was taken into account.

Bed expansion characteristics in the sound assisted fluidization require a further interesting investigation. We, therefore, underwent a research work to discover intrinsic bed expansion characteristics of Geldart's group A powder in the sound assisted fluidization. To obtain accurate bed expansion characteristics, the 1-valve and 2-valve bed collapse experiment and the bed collapse model (Cherntongchai and Brandani, 2005) were used to interpret correctly the bed collapse curves. Finally, the drag force correlation and the minimum bubbling criterion for the description of the bed expansion characteristics of Geldart's group A powder in the sound assisted fluidization werevalidated.

3. Research scope

This research work is a basic research divided into two parts. One is an experimental part and another is a theoretical part. A focus of an investigation is on hydrodynamics of fine particles (Geldart's group A powder) in sound assisted fluidization under following operating condition parameters;

3.1 An inlet superficial velocity for the flow regime ranging from fixed bed to bubbling bed (≈ 0-50 L/min)

3.2 A sound pressure level (80 dB)

3.3 A sound frequency (50 Hz-500 Hz)

4. Outputs

4.1 International conference

- Cherntongchai, P., Hydrodynamics of Sound Assisted Fluidization of Rigid-microsized Powder, 2017AIChE Annual Meeting, October 29 - November 3, 2017, Minneapolis, MN, USA.(Oral presentation)

4.2 International publications

- Cherntongchai P., Chaiwattana S., Leruk R., Panyaruean J., Sriboonnak S., Influence of Standing Wave Characteristics on Hydrodynamics Behaviors in Sound Assisted Fluidization of Geldart’s Group A Powder, Chemical Engineering Science. (Submitted).
- Cherntongchai P., Chaiwattana S., Leruk R., Bed expansion characteristics in Sound Assisted Fluidization of Geldart’s Group A powder, Chemical Engineering Science. (Submitted)

NOMENCLATURES

A	=	Constant depending on boundary condition
Ar	=	Archimedes number
Area	=	Bed cross section area (m^2)
B	=	Constant depending on boundary condition
C_D	=	Drag coefficient
C_o	=	Standing wave velocity in fluidization media (m/s)
d_P	=	Mean particle size (m)
F_D	=	Drag force of particles in suspension/volume (kg/m^2s^2)
f	=	Sound frequency (Hz)
f_c	=	Critical frequency (Hz)
g	=	Acceleration of gravity (m^2/s)
h	=	Total bed height (m)
i	=	1, 2, 3, … n
K_g	=	Bulk modulus of nitrogen gas = 117×10^3 Pa
K_p	=	Bulk modulus of glass bead = 40×10^9 Pa
k	=	Wave number = $2\pi f/C_o$
L	=	Bed height (m)
L_c	=	Column height (m)
L_o	=	Total bed height from distributor (m)
L_1	=	Height of Zone1 from distributor (m)
L_2	=	Height of Zone 2 from distributor (m)
n	=	Harmonic number
n’	=	Richardson and Zaki index
P_{atm}	=	Atmospheric pressure (Pa)

P_{fs} = Source amplitude at surface boundary at x=h (Pa)

P_{ref} = 2×10^{-5} Pa

P_{rms} = Root mean square of sound pressure (Pa)

p = Pressure (Pa)

P_w = Absolute pressure in a windbox (Pa)

Q_V = Volumetric flow rate of gas through discharge valve (m^3/s)

$Q_{Windbox}$ = Volumetric flow rate of gas at windbox pressure (m^3/s)

Re_P = Particle Reynold number = $\frac{d_P U \rho_F}{\mu_F}$

SPL = Sound pressure level (dB)

t = Time (s)

t_{bub} = Bubble escape time (s)

U = Superficial velocity (m/s)

U_A = Amplitude of gas oscillation velocity (4.83×10^{-8} m/s)

U_D = Dynamic wave velocity (m/s)

U_d = Dense phase superficial velocity (m/s)

U_{dis} = Superficial velocity of gas flowing through a distributor (m/s)

U_{mb} = Minimum bubbling velocity (m/s)

U_{ref} = Reference velocity (m/s)

U_t = Terminal falling velocity (m/s)

U_o = Inlet superficial velocity (m/s)

U_1 = Zone 1 superficial velocity (m/s)

U_ε = Continuity wave velocity (m/s)

u_{ac} = Gas oscillation velocity (m/s)

$\bar{u}_{ac}$ = Average gas oscillation velocity over distance Δx(m/s)

V_w = Windbox volume (m^3)

x = Axial displacement of wave propagation (m)

Greek letters

β = Exponential factor for modified revised Ergun correlation

ΔP = Piezometric pressure drop (Pa)

ΔP_{ac} = Pressure drop due to acoustic force(Pa)

ΔP_d = Pressure drop due to drag force(Pa)

δ = Characteristic length (m)

ε = Bed voidage

ε_d = Dense phase voidage

ε_{fixed} = Fixed bed voidage

ε_{mb} = Minimum bubbling voidage

ε_{mf} = Minimum fluidization voidage

ε_o = Total bed voidage

ε_1 = Zone 1 bed voidage

ε_2 = Zone 2 bed voidage

ρ_F = Fluid density(kg/m^3)

ρ_g = Gas density of nitrogen = 1.21 kg/m^3

ρ_P = Particle density of glass bead = 2432 kg/m^3

θ = Phase angle

ω = Angular frequency

μ_F = Fluid viscosity (kg/m.s)

CHAPTER 1: INTRODUCTION

1.1 Introduction

Sound-assisted fluidization is a modification of conventional fluidization by implementing sound vibrational force. And, the additional equipment is a sound wave generator, connected to a sound amplifier and a loudspeaker. Sound waves from the loudspeaker can be directed to a fluidized bed from either the top or thebottom of a column. Then, the sound wave which is a pressure wave will propagate through a bed of particles and break up the inter-particle forces, resulting in better fluidization quality, smaller agglomerate size, particle elutriation reduction, and change in the fluidization hydrodynamics.

Sound-assisted fluidization has been successfully used to improvethe qualityof fluidizationsince 1955 by Morsefor the fluidization of Geldart's group C/A powders, as well as in the works of Kaliyaperumal et al. (2011),Langde et al. (2011), Russo et al. (1995), and Xu et al. (2006). Zhu et al. (2004) was the first to report better fluidization quality in sound-assisted fluidized bed of nanoparticles, followed by Guo et al. (2005), Guo et al. (2006), and Liu et al. (2007). The sound-assisted fluidization of Geldart's group B powder was also investigated byEscudero and Heindel (2013) and Leu et al. (1997) and it was concluded that the sound wave field helped to improve the ease of fluidization.

Numerous hydrodynamic investigations of sound-assisted fluidization have been reported, except bed expansion characteristics. In general, it has been known that characteristics of sound-assisted fluidization are implicitly related to the characteristics of a standing wave traveling through the fluidizing bed, which has been thoroughly described by Herrera et al. (2002). However, the knowledge has never been used to explain the fluidization characteristics observed. For the bed expansion characteristic, there is much more comprehension for a further interesting investigation and an accurate expansion data is required. Therefore, in this work, the aim was to apply the knowledge regarding the standing wave characteristics to explain the influence of sound frequency on the minimum fluidization velocity of sound-assisted fluidization of Geldart's group A powder. In addition, fixed bed pressure drop correlations for sound-assisted fluidization were developed, where gas oscillation velocity, varied according to the characteristics of the standing wave, was taken into account. Besides, intrinsic bed expansion characteristics of Geldart's group A powder in the sound assisted fluidization was also discovered. To obtain accurate bed expansion characteristics, the 1-valve and 2-valve bed collapse experiment and the bed collapse model (Cherntongchai and Brandani, 2005) were used to interpret correctly the bed collapse curves. Finally, for the description of the bed expansion characteristics of Geldart's group A powder in the sound assisted fluidization, the drag force correlation and the minimum bubbling criterion were validated.

1.2Objectives

- To extend level of understanding on hydrodynamics behaviors fine particles in sound assisted fluidization.
- To develop mathematical models to describe the hydrodynamics behaviors of the fine particles in the sound assisted fluidization.

1.3Research scope

This research work is a basic research divided into two parts. One is an experimental part and another is a theoretical part. A focus of an investigation is on hydrodynamics of fine particles (Geldart's group A powder) in sound assisted fluidization under following operating condition parameters;

- An inlet superficial velocity for the flow regime ranging from fixed bed to bubbling bed (≈ 0-50 L/min)
- A sound pressure level (80 dB)
- A sound frequency (50 Hz-500 Hz)

CHAPTER 2: LITERATURE REVIEW

2.1 Minimum fluidization point in sound assisted fluidization

Transition from the fixed to the fluidized bed under the effect of sound waves appeared as a range from the incipient fluidization stage to the complete fluidization stage, reported by Xu et al. (2006). And, the minimum fluidization point has been generally defined to be at the point of complete fluidization (Escudero and Heindel, (2013); Guo et al.,(2006);Si et al., 2015),apart from the work of Xu et al. (2006), who defined the minimum fluidization velocity to be at the intersecting point of the defluidization curve with the constant pressure line, and the work of Kaliyaperumal et al. (2011), who proposed a novel curve-fitting iteration method to define the minimum fluidization point. In any case, it has been observed that inthe presence of sound, there is significant reduction in the minimum fluidization velocity (Kaliyaperumal et al., 2011; Leu et al., 1997;Si et al., 2015; Zhu et al., 2004).

Variation in minimum fluidization under the influence of the properties of sound waves can be summarized as follows: All previous works have reported that an increase in the sound frequency causes the minimum fluidization point to decrease to the local minima and, then, increase with increase in the sound frequency (Escudero and Heindel, 2013; Guo et al., 2005; Guo et al., 2006; Kaliyaperumal et al., 2011; Liu et al., 2007; Russo et al., 1995;Si et al., 2015; Xu et al., 2006; Zhu et al., 2004;).And, the common explanation involves the resonance behavior between the natural frequency of the fixed bed and the sound frequency. Under the effect of the sound pressure level, it has been reported, as the sound pressure level increases, the minimum fluidization decreases (Escudero and Heindel, 2013; Guo et al., 2005; Kaliyaperumal et al., 2011; Russo et al., 1995;Si et al., 2015; Xu et al., 2006) because the vibrational forces help to loosen the bed and reduce the energy required for particle fluidization.

Russo et al. (1995)studied the effect of particle loading on sound-assisted fluidization of Geldart's group C powder and reported that with increase in particle loading, the minimum fluidization velocity was observed to increase. They explained that the more the particle loading, the more the sound attenuation and the more the decrease in the sound pressure level, resulting in an increase in the minimum fluidization velocity.

2.2 Fixed bed pressure drop in sound assisted fluidization

It is well-known that the fixed bed pressure drop undergoes variation in accordance with the sound wave properties. For example, Xu et al. (2006) reported that the fixed bed pressure drop increased significantly with sound frequency for Geldart's group A powders. In order to describe the variation of the fixed bed pressure drop with respect to sound frequency, the force-balance principle as well as the drag force correlation and the acoustic force correlation should be taken into consideration. To the best of the researchers' knowledge, there is no previous report that has purposed an appropriate correlation for the prediction of the fixed bed pressure drop in sound-assisted fluidization. Instead, there have been a number of previous works using the principle of force-balance and the related force correlations for describing sound-assisted fluidization. For example, Russo et al. (1995) developed the cluster/subcluster oscillator model to predict the agglomeration size of Geldart's group C powder in sound-assisted fluidization and implemented Stokes' law to identify the drag force due to gas flow in an acoustic field. Likewise, Si and Guo (2008)and Urciuolo et al. (2008) also used Stokes' law for drag force under fluid velocity and gas oscillation velocity in force-balance analysis. Wang et al. (2011)used the Ergun equation for drag force correlation and applied the gas oscillation velocity in the same equation for the acoustic force in order to establish the equation of motion for cohesive powder.

2.3 Bed expansion characteristics in sound assisted fluidization

There are still very limit numbers of research works investigating the bed expansion characteristics of the particle bed in the sound assisted fluidization. Currently, there are some of the work used a visual observation to obtain a bed expansion ratio and a bed collapse experiment to obtain a bed collapse time and a shape of a bed collapse curve in order to determine a fluidization quality. Russo et al. (1995) studied an influence of a particle loading, a sound pressure level and a sound frequency on the bed expansion ratio of Geldart's group C powder, to determine the fluidization quantity. It was found from this work that, in relation to an inlet superficial velocity, the bed expansion ratio was found to non-monotonically increase with increasing the inlet superficial velocity and, hence, the fluidization quality. Herrera and Levy (2001) investigated the effect of the sound pressure level on the homogeneous bed expansion and the minimum bubbling point for Geldart's group A powder. The increase of the bed height and the minimum bubbling velocity with increasing the sound pressure level was reported. And, a change in a void structure under the sound vibrational force was an underlined explanation. Zhu et al. (2004) studied the effect of the sound pressure level and the sound frequency on the bed expansion for nanoparticle agglomerates. With an application sound, the bed expansion increased due to the breakup of the large agglomerate under the combined effect of hydrodynamics forces and acoustic excitations. Guo et al. (2006) carried out the bed collapse experiment and used the bed collapse time to identify the de-aeration characteristic of silica nanoparticle with different surface properties in the sound assisted fluidization. It was pointed out that there was a greater bed collapse time under the sound vibrational force. This was due to the more reduction in the van der waals forces between the nanoparticles and the better fluidization quality. Ammendola and Chirone (2010) studied aeration and a mixing behavior of the nano-sized powders under the sound vibration. The bed expansion ratio was also used for an index of the fluidization quality. Under the influence of sound, the fluidization quality was improved. Similar to the previous reports, the higher the sound intensity, the higher the bed expansion, as far as the sound pressure level was higher enough to compensate the sound attenuation. In addition, the optimum sound frequency, giving the maximum bed expansion, was also found. Ammendola et al. (2011) focused on the aeration behavior of the binary mixtures of nanoparticle under acoustic field and reported the better fluidization quality in term of the bed expansion ratio. In this work, they also worked with the homogenous bed expansion data using the Richardson and Zaki correlation at $n \approx 5$ in order to estimate the terminal falling velocity of the agglomerate. Kaliyaperumal et al. (2011) observed the bed expansion ratio for the nano and sub-micron powder under the acoustic vibration to determine the fluidization quality. Similarly, the bed expansion ratio increased with the sound pressure level and was raised with increasing inlet superficial velocity. This was due to the reorientation of the bed voidage under the vibration induced the sound excitation. In addition, the maximum bed expansion ratio was found at a resonance sound frequency. Langde and Sonolikar (2011) investigated the bed expansion of Geldart group C/A powder under the sound field. They reported that the expansion ratio increase non-monotonically with the inlet superficial velocity. Also, the bed expansion ratio was reported to increase with the sound pressure level due to the breaking up of the interparticle forces at higher sound intensity. As a result, more void was created. Under the influence of the sound frequency, the bed expansion ratio reached the maximum point at a certain frequency (120 Hz), where the sound oscillation was the highest and for other sound frequency the bed expansion was approximately the same. Raganati et al. (2014) studied the effect of the CO_2 partial pressure, the sound pressure level and the sound frequency on the fluidization quality using the bed expansion ratio for the CO_2adsorption on the fine activated carbon. It was pointed out the bed expansion ratio increased with the sound pressure level after the threshold value where the sound intensity overcame the attenuation effect. Under the effect of the sound frequency, the optimum frequency was found for the best fluidization quality and the maximum aggregate break-up. Either too low or too high sound frequency, the fluidization quality failed out on the same range. The explanation given was that for too high frequencies the acoustic filed is not able to propagate inside the bed and to promote the break-up of aggregates. On the other hand, for too low frequency, the relative motion between the smaller and the larger sub-aggregates, leading the large aggregates to be broken up, was practically absent.

CHAPTER 3: THOERY

3.1 Standing wave characteristics in sound-assisted fluidized bed

The concept of pressure wave propagation in fluidization was used to describe sound wave propagation in the fluidization medium. Considering Herrera et al. (2002), they assumed that sound propagation was an adiabatic one-dimensional process; the wave equation in terms of pressure is written as follows:

$$\frac{\partial^2 p}{\partial x^2} = \frac{1}{\varepsilon^2}\frac{\partial^2 p}{\partial t^2} \tag{3.1}$$

A known solution to the above equation is as follows:

$$p(x,t) = Ae^{-j(\omega t - kx)} \tag{3.2}$$

Transmission of a sound wave in the sound-assisted fluidization system consists of traveling of the sound wave in two media, confined in a vertical column (Fig.3.1). One is the top end, where the sound wave is supplied, which was the nitrogen media (in this study), and the other is the bottom end which is the heavier fluidization media supported by a rigid porous distributor. As the sound wave travels through the nitrogen, the incident pressure wave (p_{i1}) reaches the interface between the nitrogen and the fluidized bed. A fraction of the incident wave is reflected (p_{r1}) and the rest (p_t) travels downward through the bed and reaches the distributor. Once the incident wave in the fluidized bed (p_{i2}) reaches the rigid distributor, the reflected wave (P_{r2}) travels backward. The incident wave and the reflected wave then combine to form a steady wave called the "standing wave." The sum of the incident and the reflected waves within the fluidized bed in the form of the total pressure is illustrated in Eq. (3.3):

$$p(x,t) = Ae^{-j(\omega t - kx)} + Be^{-j(\omega t - kx + \theta)} \tag{3.3}$$

The amplitude $|p(x,t)|$ can be written as follows:

$$|p(x,t)| = \sqrt{(A+B)^2 \cos^2(-kx + \frac{\theta}{2}) + (A-B)^2 \sin^2(-kx + \frac{\theta}{2})} \tag{3.4}$$

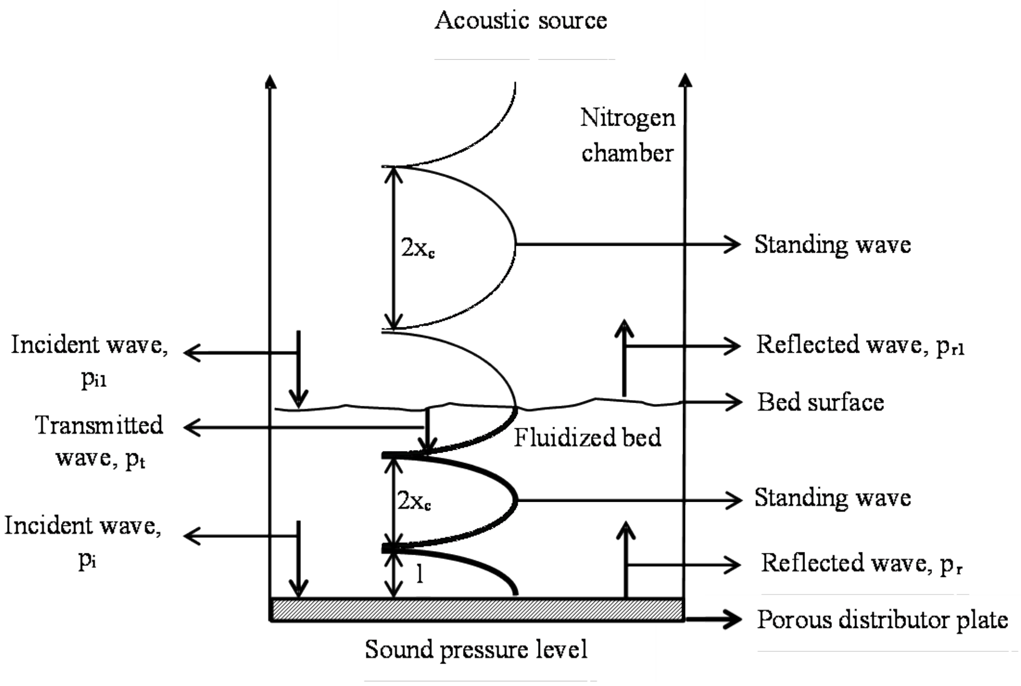

Fig. 3.1 Standing wave pattern in the fluidization media

When the reflecting boundary is solid, the incident and the reflected amplitude are equal; therefore, A=B. In addition, assuming that the incident and the reflected waves were in phase (θ=0), the resulting standing wave amplitude becomes

$$|p(x,t)| = 2A\sqrt{\cos^2 kx} \tag{3.5}$$

At x=h, the pressure was

$$p(h,t) = P_{fs} \cos \omega t \tag{3.6}$$

$P_{fs}$is related to the sound pressure level as

$$SPL = -20 \log \left[\frac{p_{rms}}{p_{ref}} \right] \tag{3.7}$$

$$P_{rms} = \frac{|p(x,t)|}{\sqrt{2}} = \frac{P}{\sqrt{2}} \tag{3.8}$$

Thus, the pressure distribution becomes

$$p(x,t) = P_{fs}\sqrt{\frac{\cos^2 kx}{\cos^2 kh}}\cos\omega t \tag{3.9}$$

And,

$$|p(x,t)| = P_{fs}\sqrt{\frac{\cos^2 kx}{\cos^2 kh}} \tag{3.10}$$

$|p(x,t)|$ is very large when cos(kh) = 0, which occurs at

$$kh = (2n-1)\frac{\pi}{2}, \text{for } n = 1,2... \tag{3.11}$$

This point is called the "critical state," and the critical frequency can be calculated as follows:

$$f_c = \frac{(2n-1)}{4}\frac{C_o}{h}, \text{for } n = 1,2... \tag{3.12}$$

$$C_o = \sqrt{\frac{\left[\frac{\varepsilon}{K_g} + \frac{(1-\varepsilon)}{K_p}\right]^{-1}}{\varepsilon\rho_g + (1-\varepsilon)\rho_p}} \tag{3.13}$$

The value of $|p(x,t)|$ can be interchanged using Eqs. (3.7), (3.8), and (3.10), and this would also enable the gas oscillation velocity ($u_{ac}(x,t)$) along the bed height to be calculated thus:

$$u_{ac}(x,t) = U_A \sin(2\pi ft) = U_A \sin(kx) \tag{3.14}$$

And,

$$SPL = 20\log\left[\frac{U_A}{\sqrt{2}U_{ref}}\right] \tag{3.15}$$

Finally, the point is reached at whichit is possible to explain the characteristics of fluidization under the influence of sound wave properties using the value of $|p(x,t)|$ or $u_{ac}(x,t)$ of the standing wave.

3.2 1-valve and 2-valve bed collapse model

1-valve and 2-valve bed collapse model was developed by Cherntongchai and Brandani 2005 for a correct interpretation of 1-valve and 2-valve bed collapse curves.

1-valve bed collapse experiment is carried out by abruptly shut down an inlet valve. For 2-valve bed collapse experiment, there is a discharged valve attached at a windbox. This valve is synchronized with the inlet valve. Once the inlet valve is abruptly shut down, the discharge valve is opened to vent gas in a bed and the windbox. For both cases, a bed surface starts to collapse with a lapse of time once the valves were energized and a bed collapse structure is presented in Fig. 3.2. From $0 \le t \le t_{bub}$(Fig. 3.2(a)), so called "a bubble escape stage", remained bubbles will escape from the collapsing bed. The collapsing bed is comprised of 3zones. Zone 0 ($\varepsilon = \varepsilon_o$) is the bubbling bed zone, extended from L_o to L_1. This zone is diminished with time due to the escape of the bubbles and the falling down of L_o together with the growing up of L_1. Zone 1 ($\varepsilon = \varepsilon_1 = \varepsilon_d$) is the homogeneous expanded zone, extended from L_1 to L_2, where both L_1 and L_2 moved upward. Zone 2 ($\varepsilon = \varepsilon_2 = \varepsilon_{fixed}$) is the fixed bed zone, formed up from t=0 and growth upward all along the collapsing process. At t= t_{bub}, all bubbles disappear and the bed collapse structure is of 2 zone as shown in Fig. 3.2(b). From $t \ge t_{bub}$(Fig. 3.2(c)), at this stage is called "a sedimentation stage". L_1 is falling down while L_2 keep growing upward. And, the bed collapse process ends when $L_1 = L_2$. During the entire bed collapse process, the gas flows through the bed are from the gas residue in the windbox and the gas generated at the interface L_2, due to the change in the bed voidage between zone 1 and zone 2. For 1-valve bed collapse process, the gas always flows in an upward direction. On the other hand, for 2-valve bed collapse process, the gas from the windbox and the gas generated at the interface can flow in both upward and downward directions, due to the characteristic of the discharge valve.

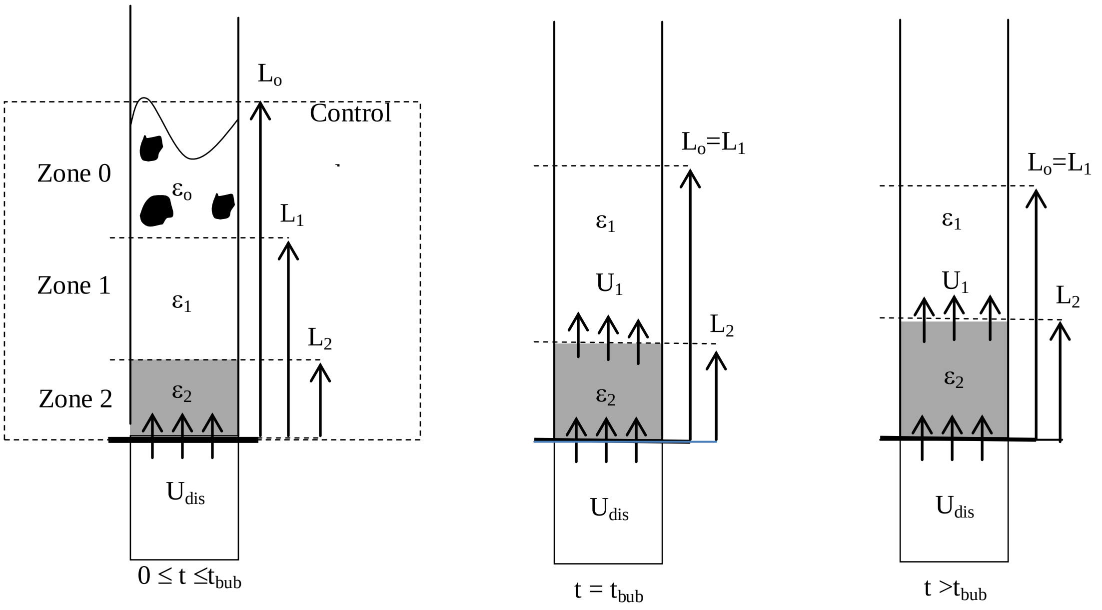

(a) (b) (c)

Fig. 3.2 Schematic of (a) bubble escape stage, (b) and (c) sedimentation stage for 1-valve bed collapse experiment

The main assumptions of the model equations are; one dimensional system, ideal gas, incompressible fluid in the bed section, compressible fluid in the windbox, negligible inertial effects, a constant voidage fraction ε_1 ($\varepsilon_1 = \varepsilon_d$) according to a gas velocity U_d ($U_1 = U_d$).

The bed collapse model can be summarized as follows;

3.2.1 Sedimentation stage

1-valve configuration

$$\frac{dL_1}{dt} = U_{dis} - U_d \tag{3.16}$$

$$\frac{dL_2}{dt} = \frac{(1-\varepsilon_1)(U_{dis} - U_d)}{(\varepsilon_1 - \varepsilon_2)} \tag{3.17}$$

$$-\frac{dp_W}{dt} = \frac{p_W}{V_W} U_{dis} Area \tag{3.18}$$

The bed collapse model can be solved through integration of Eqs. (3.16) - (3.18), simultaneously. U_{dis} can be calculated from the knowledge of the distributor pressure drop, determined from the collapsing bed momentum balance (Eq. (3.19)). The initial condition for L_1 is L_o and for L_2 is zero:

$$\Delta P_{Dist} = (p_W - p_{atm}) - \rho_F g L_c - \Delta P_1 - \Delta P_2 \tag{3.19}$$

$$\Delta P_1 = (\rho_P - \rho_F)(1-\varepsilon_1)(L_1 - L_2) g \tag{3.20}$$

$$\Delta P_2 = f(U_{dis}) \tag{3.21}$$

2-valve configuration

$$\frac{dL_1}{dt} = \pm U_{dis} - U_d \tag{3.22}$$

$$\frac{dL_2}{dt} = \frac{(1-\varepsilon_1)(U_{dis} \pm U_d)}{(\varepsilon_1 - \varepsilon_2)} \tag{3.23}$$

$$-\frac{dp_W}{dt} = \frac{p_W}{V_W} (\pm U_{dis} Area + Q_V) \tag{3.24}$$

$$\Delta P_{Dist} = (p_W - p_{atm}) - \rho_F g L_c - \Delta P_1 \pm \Delta P_2 \tag{3.25}$$

The solution of the model equations requires the knowledge of the discharge valve pressure drop. A positive sign in Eqs. (3.22) – (3.25) applies when the gas is flowing from the windbox to the particle bed.

3.2.2 Bubble escape stage

1-valve configuration

The properties in the bubbling zone are assumed to be similar to those in the steady state bubbling fluidized bed.

$$\frac{dL_o}{dt} = U_{dis} - U_o \tag{3.26}$$

$$\Delta P_{Dist} = (p_w - p_{atm}) - \rho_F g L_c - \Delta P_o - \Delta P_1 - \Delta P_2 \tag{3.27}$$

$$\Delta P_o = (\rho_P - \rho_F)(1 - \varepsilon_o)(L_o - L_1)g \tag{3.28}$$

Eq. (3.26) has to be integrated simultaneously with Eqs. (3.16) – (3.18). U_{dis} can be calculated using Eq. (3.27). The initial condition for L_2 and L_1 is zero.

2-valve configuration

A criterion to specify the different bed collapse structures during the bubble escape stage has been added, due to the possibility of the flow reversal of the gas generated at the interface L_2. The first possible structure is as shown in Fig. 3.2(a), when zone 1 can exist. Another possible structure is when zone 1 cannot exist. To determine whether zone 1 can exist, U_1 is calculated based firstly on the assumption that zone 1 can exist using Eq. (3.29)

$$U_1 = \varepsilon_1(\pm U_{dis}) + (1 - \varepsilon_1)U_d \tag{3.29}$$

If U_1 is greater than zero, then zone 1 can exist. And, the bed collapse rate can be expressed as follows;

$$\frac{dL_o}{dt} = U_{dis} - U_o \tag{3.30}$$

$$\Delta P_{Dist} = (p_w - p_{atm}) - \rho_f g L_c - \Delta P_o - \Delta P_1 \pm \Delta P_2 \tag{3.31}$$

Eq. (3.30) has to be integrated simultaneously with Eqs. (3.22) – (3.24).

If U_1 is less than zero, the zone 1 cannot exist. In this case Eq. (3.30) has to be integrated with Eqs. (3.22), (3.24) and (3.32).

$$\frac{dL_2}{dt} = \frac{(1-\varepsilon_o)(U_o - U_{dis})}{(\varepsilon_o - \varepsilon_2)} \quad (3.32)$$

3.3 Prediction of dense phase properties using bed collapse model

System configuration information and model parameters, as the required inputs for the bed collapse model, are listed in Table 3.1.

Table 3.1 Model input information

System configurations	Parameters
Windbox volume Distributor pressure drop Discharge valve pressure drop	Fixed bed pressure drop Bed voidage, ε_o Dense phase voidage, ε_d Fixed bed voidage, ε_2 Inlet superficial velocity, U_o Dense phase superficial velocity, U_d

All parameters can be achieved independently, except the dense phase voidage and the dense phase superficial velocity, which have to be obtained from the interpretation of the experimental bed collapse curves following the method outlined bellows;

For a homogeneous expanded bed:

- Introducing the system configuration, fixed bed pressure drop, ε_o, ε_2 and U_o
- Initial estimate of ε_d
  - $\Delta P_{Dist}/\Delta P_{Bed}<1$, y-intercept of 1-valve sedimentation curve gives the correct ε_d.
  - $\Delta P_{Dist}/\Delta P_{Bed}>1$, y-intercept of 2-valve sedimentation curve gives the correct ε_d.
- Evaluation of U_d

- $\Delta P_{Dist}/\Delta P_{Bed}<1$, the correct U_d is selected iteratively until the experimental 1-valve sedimentation curve is fitted with the model prediction.
- $\Delta P_{Dist}/\Delta P_{Bed}>1$, the correct U_d is selected iteratively until the experimental 2-valve sedimentation curve is fitted with the model prediction.

- Re-validation of ε_d and U_d

ε_d and U_d from the 1-valve collapse curve ($\Delta P_{Dist}/\Delta P_{Bed}<1$) are used to predict the entire experimental 2-valve sedimentation collapse curve to validate the values obtained. On the contrary, for ε_d and U_d obtained from the 2-valve collapse curve ($\Delta P_{Dist}/\Delta P_{Bed}>1$), the 1-valve sedimentation collapse curve was used to validate the values.

For a bubbling bed, the same procedure can be applied except for ε_o interpretation. ε_o was selected to fit the bubble escape time of the 1-valve collapse curve ($\Delta P_{Dist}/\Delta P_{Bed}<1$). The ε_o, ε_d and U_d from the 1-valve collapse curve were validated by comparing the predictions for the 2-valve collapse curve with the experimental results. On the other hand, ε_o selected from the 2-valve collapse curve for $\Delta P_{Dist}/\Delta P_{Bed}>1$, the ε_o, ε_d and U_d from the 2-valve collapse curve were validated by comparing the predictions for the 1-valve collapse curve with the experimental results.

CHAPTER 4:MATERIAL AND METHODS

4.1 Experimental setup

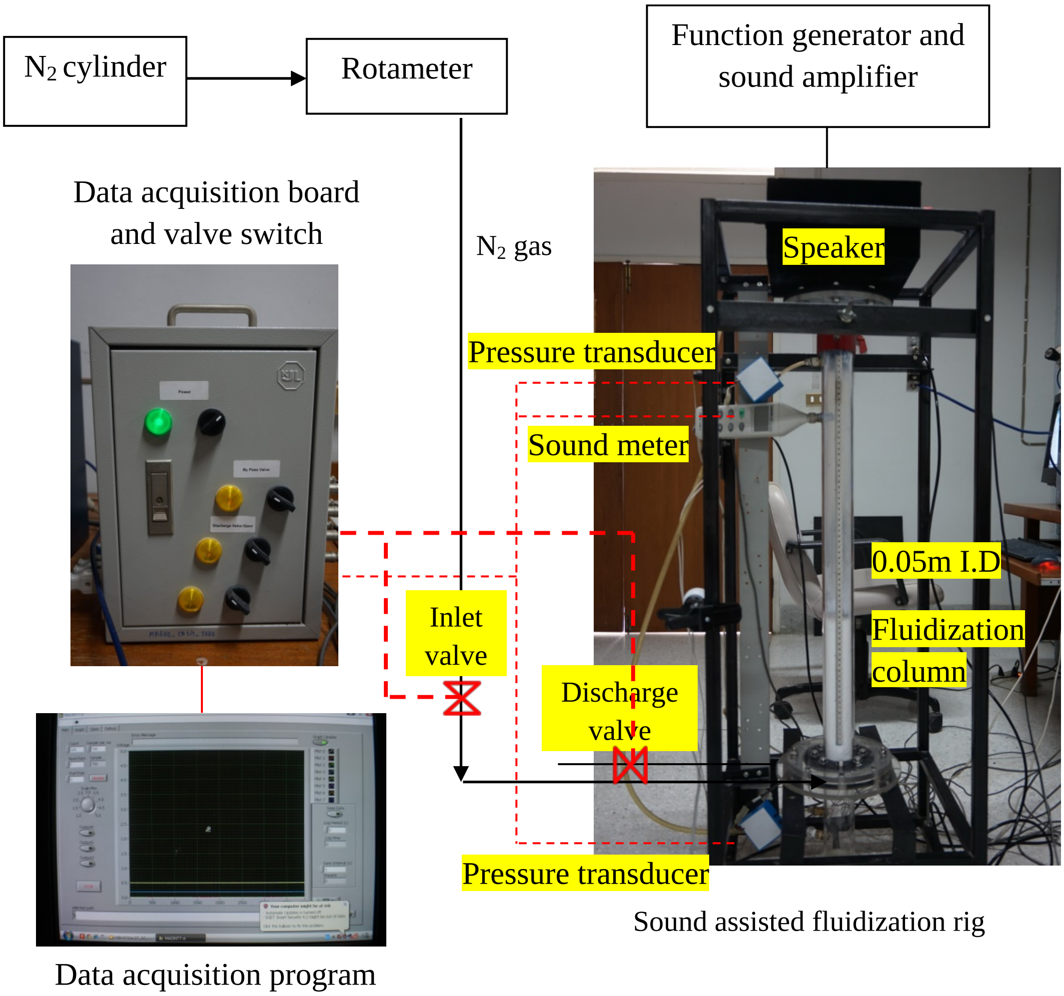

Fig. 4.1 The sound-assisted fluidization setup for the 0.10 m ID fluidization column

The sound-assisted fluidization setup (Fig.4.1) consisted of 99.99% pure nitrogen gas connected to a rotameter. After metering the gas flow rate, the nitrogen gas line was connected to a 0.10 m ID or 0.05 m ID fluidization column. The column was equipped with a gas distributor, pressure transducers, a sound level meter, and a speaker on top of the column. The pressure transducers and the sound meter were connected to a data acquisition board and, then, to a data acquisition program. To carry out 2-valve bed collapse experiment, the discharge valve, attached at the windbox, is synchronized with the inlet valve. These two valves are controlled using a valve switch. A flow range for this setup is from 0-30 L/min. A sound pressure level was fixed at 80 dB and a sound frequency is ranged from 0-500 Hz. A data acquisition rate is 100 data point per second. Finally, a measuring range of a pressure transducer is at 0-5 psi.

Empirical correlations of the distributor pressure drop and the discharge valve pressure drop are presented in Eqs. (4.1) and (4.2), respectively

$$\Delta P_{Dist}\,(kPa) = 2.28Q_{Windbox} \tag{4.1}$$

$$\Delta P_{V}\,(kPa) = 0.0008Q_{Windbox}^{2} + 0.0046Q_{Windbox} \tag{4.2}$$

4.2Material

The powder used was glass ballotini. In this work, the particle density was measured using pycnometer and the laser light scattering method was used for the measurement of the particle size and the particle size distribution. The particle properties are presented in Table 4.1and the particle size distribution is illustrated in Fig.4.2. The particle loading was 0.8509 kg.

Table 4.1 Particle Density and Average Particle Size

Material	Apparent density (kg/m^3)	Average particle diameter (μm)
Glass ballotini	2,432	32.61

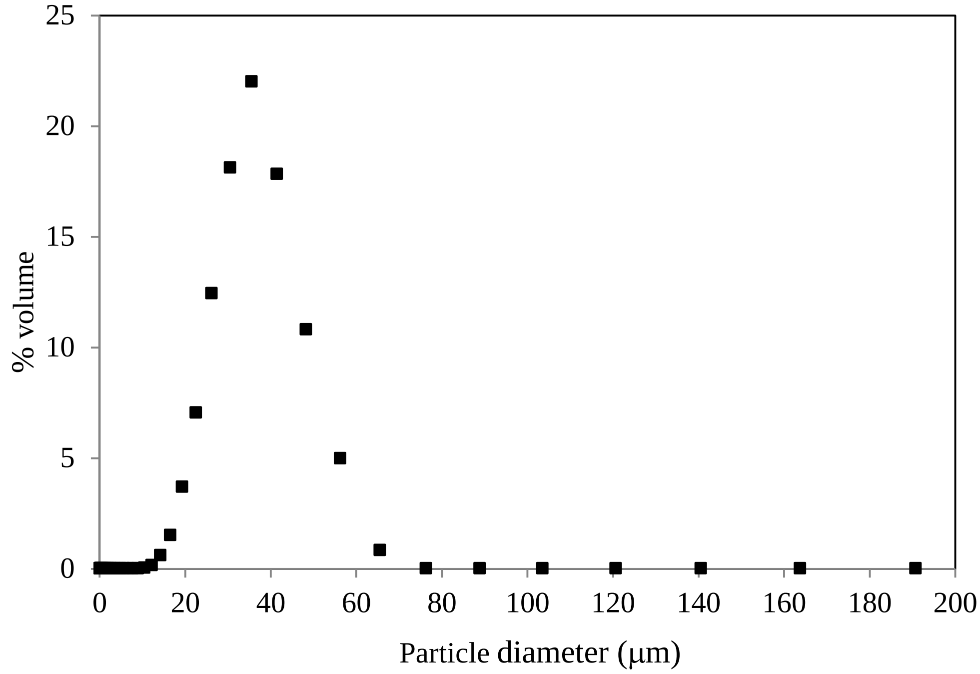

Fig. 4.2 The particle size distribution of glass ballotini

4.3Experimental methods

Fluidization experiment was performed by increasing the inlet superficial gas velocity and measuring the bed pressure drop at each gas velocity. On the other hand, defluidization experiment was carried out by decreasing the inlet superficial gas velocity and, likewise, measuring the bed pressure drop at each velocity. Table 4.2 presents the summary of the experimental conditions used in this work.

1-valve bed collapse experimental was carried out by energizing the inlet valve to close while the discharge valve remained closed. For the 2-valve bed collapse experiment, the inlet valve was synchronized to close, with the opening of the discharge valve to release the gas.Then, the particle bed collapsed. A digital camera was used to record the bed surface during the bed collapse process.

Table 4.2 Summary of Experimental Conditions

Experimental conditions	Inlet superficial velocity (mm/s)	Sound pressure level (dB)	Sound frequency (Hz)
	0–15	0	0
	0–15	80	50,80,100,300,500

CHAPTER 5:RESULTS AND DISCUSSION

5.1 Total bed pressure drop in sound-assisted fluidization

5.1.1 Total bed pressure drop in sound assisted fluidization

Fig. 5.1 presents the total bed pressure drop of both conventional fluidization (Fig. 5.1 (a)) and sound-assisted fluidization at a sound pressure level of 80 dB and a sound frequency of 50 Hz (Fig. 5.1 (b)). It was found that if the particle bed is fully fluidized, the total bed pressure drop can reach the maximum point in both the cases where the total bed pressure drop values were equal to the weight of the bed per cross section area. In addition, it needs to be pointed out that with the application of sound, the flow resistance in the fixed bed was observed to have increased.

5.1.2 Fixed bed pressure drop

Fig. 5.2 presents the fixed bed pressure drop of the sound-assisted fluidized bed in comparison with the fixed bed pressure drop of the conventional fluidized bed from the fluidization and the defluidization experiments. It can be seen that the increase in the sound frequency resulted in an increase in the fixed bed pressure drop, also reported byXu et al. (2006). Besides, there was linear relation between the sound frequency and the fixed bed pressure drop resistance, as illustrated in Fig. 5.3. This can be explained by the fact that gas oscillation velocity due to propagation of sound wavescauses higher pressure drop in the fixed bed.

5.2 Transition from fixed bed to fluidized bed

5.2.1 Incipient and complete fluidization

The transition point from the fixed bed to the fluidized bed for the sound-assisted fluidized bed can be observed as a range from the incipient and the complete fluidization points (Fig. 5.4), also reported by Xu et al. (2006). The incipient fluidization point was defined at the inlet superficial velocity where the fixed bed pressure drop implicitly deviated from the linear trend of the fixed bed pressure drop but was still less than the desired maximum value. As for the complete fluidization point, the value was defined at the first inlet superficial velocity where the total bed pressure reached the maximum value. And, the complete fluidization point is also specified as the minimum fluidization point.

5.2.2 Minimum fluidization point

It is obvious from Fig. 5.5 that with the application of sound, the particle bed can be fluidized at the lower inlet superficial velocity. The minimum value was found at the sound frequency of 50 Hz. After this, the minimum fluidization velocity increased again and was independent of sound frequency from sound frequency values of 100 Hz to 500 Hz. And, the common explanation for the minimum value found was the resonance behavior between the bed natural frequency and the sound frequency. However, this explanation can be misleading in that the possibility for the minimum value of the minimum fluidization can exist at only one value of the sound frequency. Based on a different point of view, the theory of the standing wave characteristics could claim a better explanation for the observed behavior. Hence, this will be expanded in the following section.

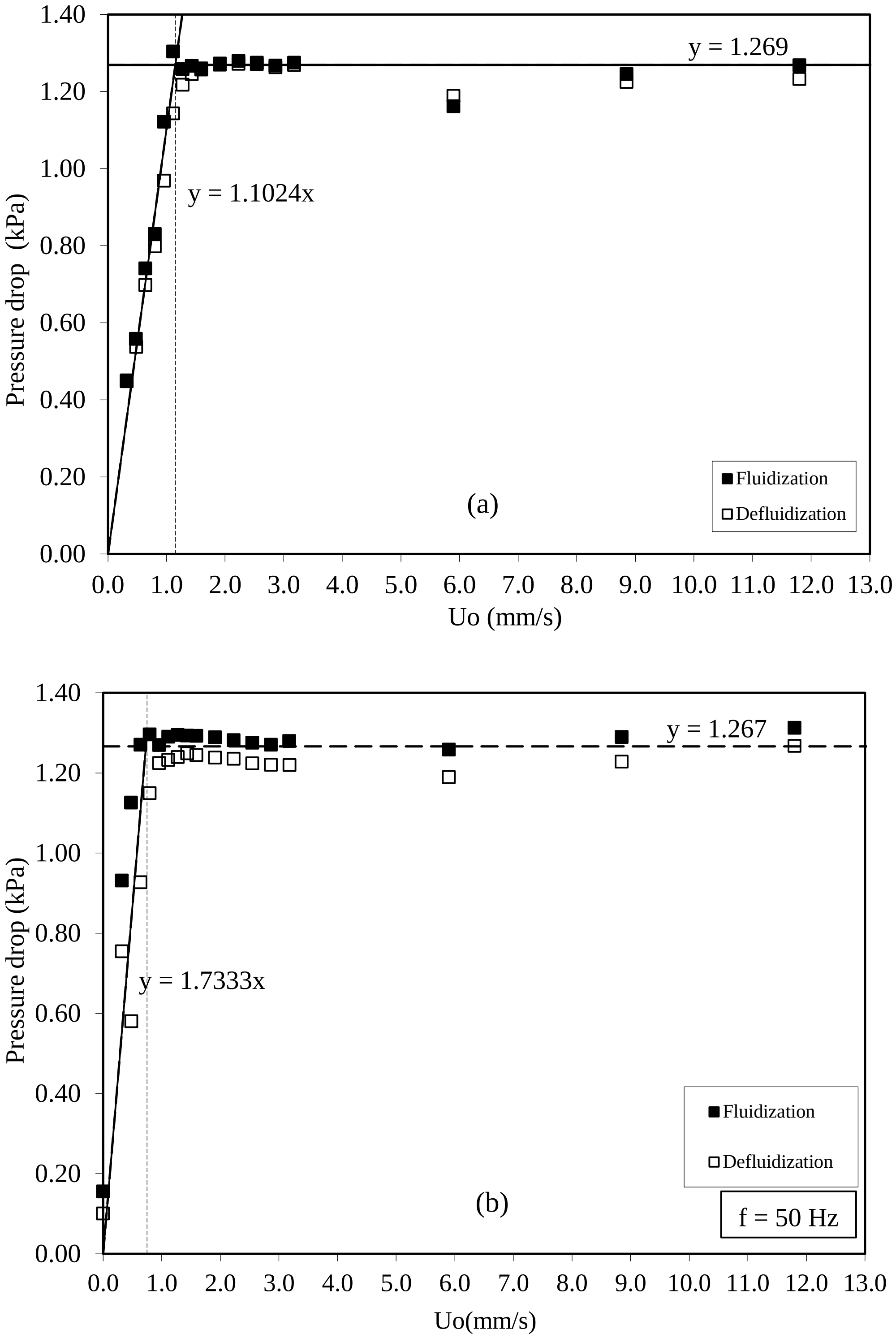

Fig. 5.1 Total bed pressure drop versus inlet superficial velocity for (a) conventional fluidization and (b) sound-assisted fluidization at sound pressure level = 80 dB and sound frequency = 50 Hz

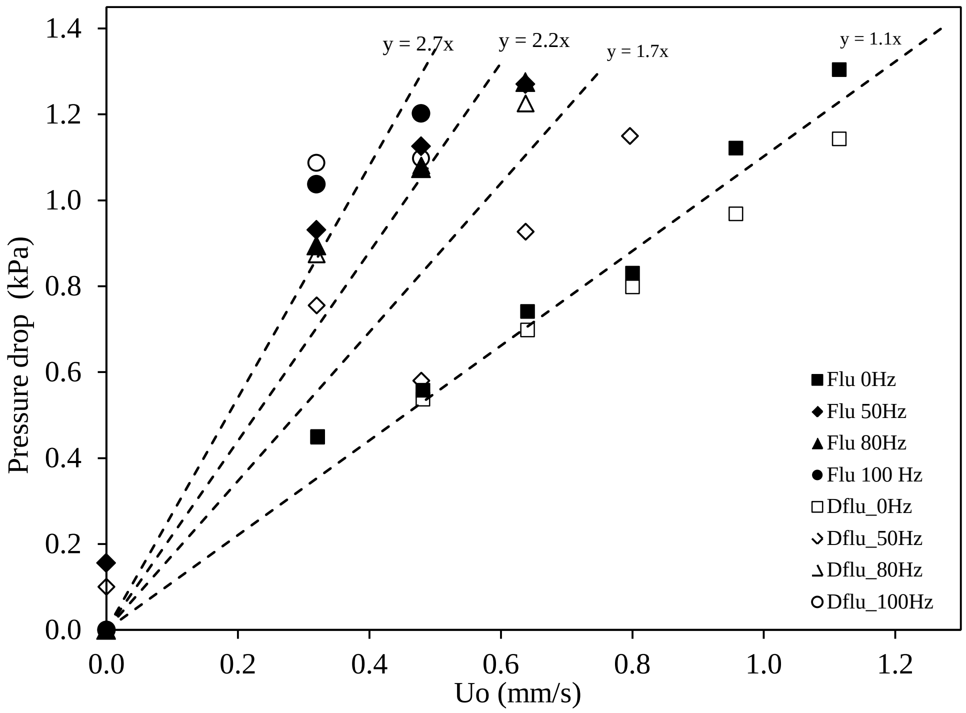

Fig. 5.2 Fixed bed pressure drop versus inlet superficial velocity of conventional and sound-assisted fluidized beds from the fluidization and the defluidization experiments

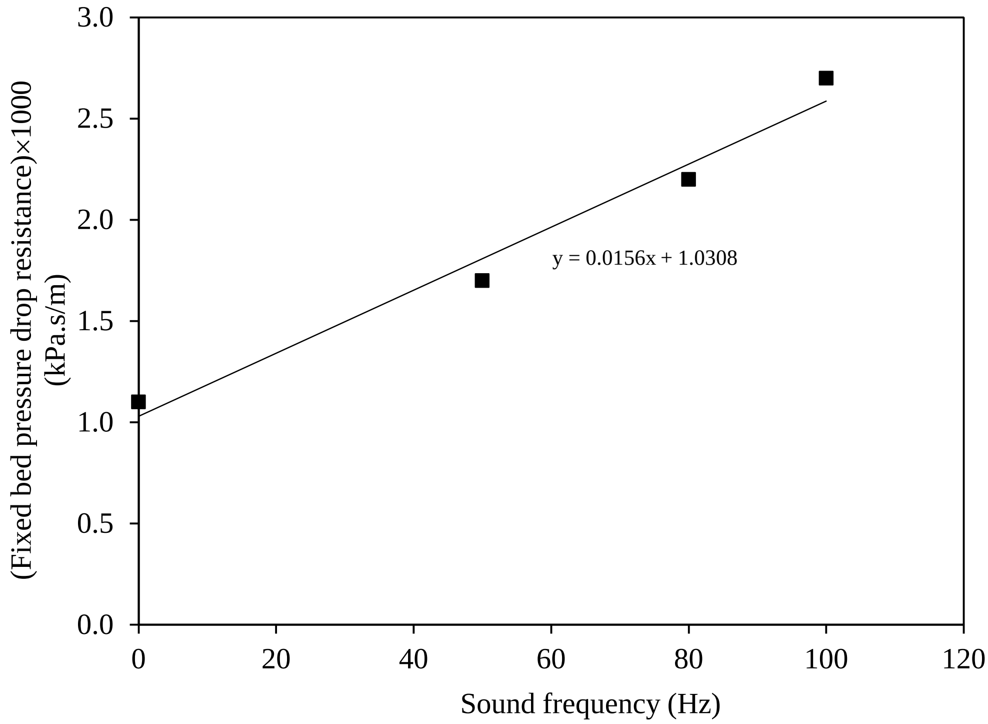

Fig. 5.3 Relation between sound frequency and fixed bed pressure drop resistance

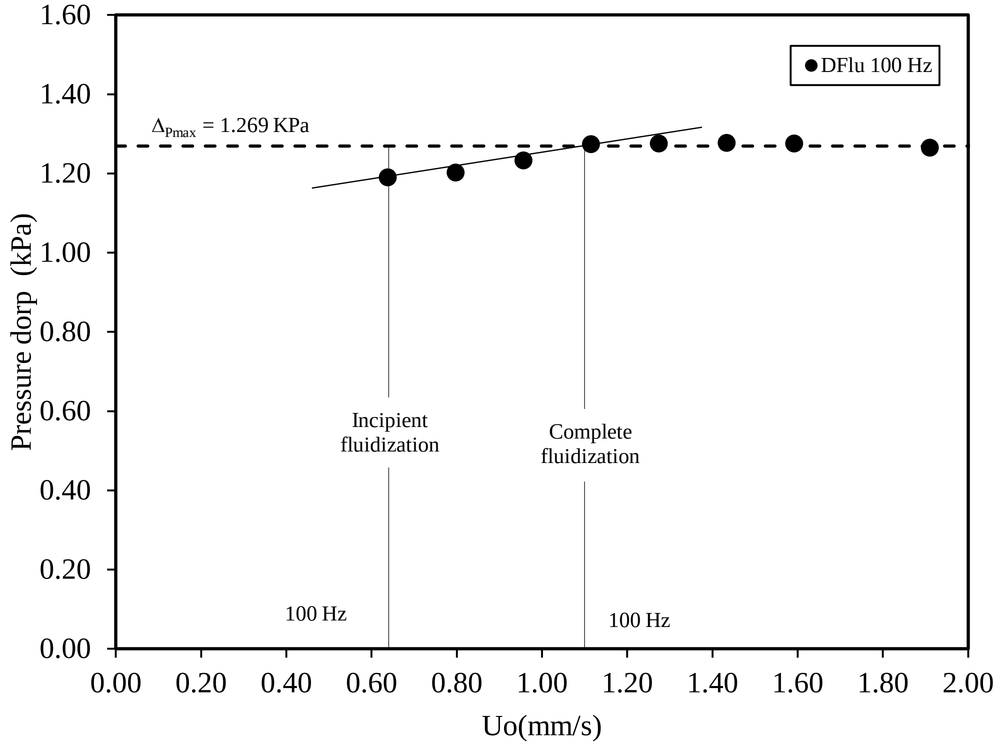

Fig. 5.4 Incipient and complete fluidization points of sound-assisted fluidization at sound pressure level = 80 dB and sound frequency = 100 Hz for the defluidization experiment

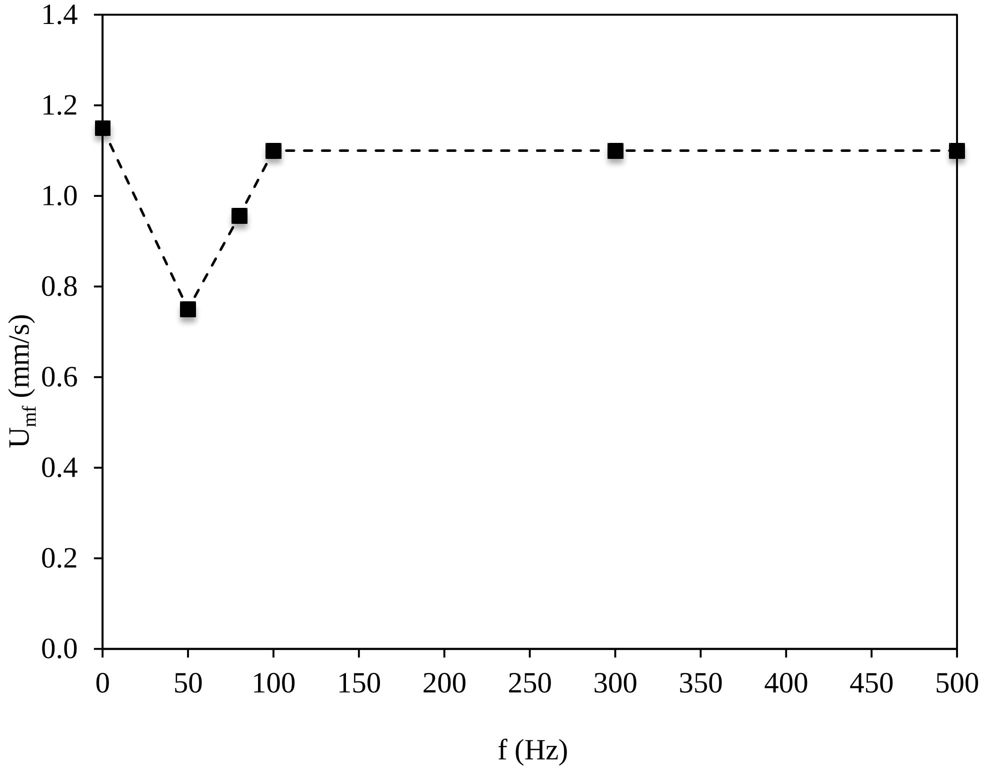

Fig. 5.5 Minimum fluidization point versus sound frequency for sound-assisted fluidization

5.3 Standing wave characteristics in sound-assisted fluidization

The standing wave characteristics implicitly influence the fluidization characteristics. In this part, the change in the standing wave characteristics in the fixed bed with the sound wave properties was declared, where the standing wave pattern in the fluidized bed in the form of SPL versus distance from the distributor (x) can be calculated using Eqs.(3.7), (3.8), and (3.10).

A variation in the wave number (kh)for the fixed bed, where h and bed voidage are constant, represents a variation in the sound wave frequency. Furthermore, the standing wave patterns with variation of kh from 0 to π/2 and kh from π/2 to π for the harmonic number (n) = 1 are shown in Fig. 5.6(a) and Fig. 5.6(b), respectively. It can be seen from Fig. 5.6(a) that at x= h, or at the bed surface, the SPL was always at 80 dB. With increase in the distance down to the distributor, the SPL increased, and the maximum SPL was at x=0. From Fig. 5.6(a), it is evident that there is no trough for kh from 0 to $\pi/2$. In addition, it has been illustrated that SPL increases with kh. Besides, when kh approached $\pi/2$, there appeared to be a rapid increase in the SPL, and the maximum SPL was found at kh = $0.99\pi/2$. In contrast, for kh from $\pi/2$ to π (Fig. 5.6(b)), there appeared to be one trough for kh $>\pi/2$, but there was no trough at kh = $\pi/2$. With increasing kh, the trough tends to move toward the distributor. In addition, at kh=$\pi/2$, the SPL is substantially high in comparison with the SPL for other kh values. This kh value was found to correspond to the critical kh calculated from Eq. (3.11). From Fig. 5.6(b), it is clear that for kh higher than the critical value, the SPL decreased implicitly and was distributed approximately over the same average value, even though the decrease with increasing kh can still be observed.

Fig. 5.7 presents the variation in SPL_o with kh: the figure illustrates that there was a critical kh value for each harmonic number that gave a high magnitude of SPL_o. For n=1 ($0<kh<\pi$), the critical kh is at $\pi/2$ and for n=2 ($\pi<kh<2\pi$), the critical kh is at $3\pi/2$, according to Eq. (3.11). In addition, for each harmonic number, SPL_o is observed to increase and decrease exponentially with kh for kh of less than the critical value and that of higher than the critical value, respectively. This explains the local minimum point of the minimum fluidization velocity at certain sound frequencies but approximately the same superficial velocity at other values of the sound frequency.

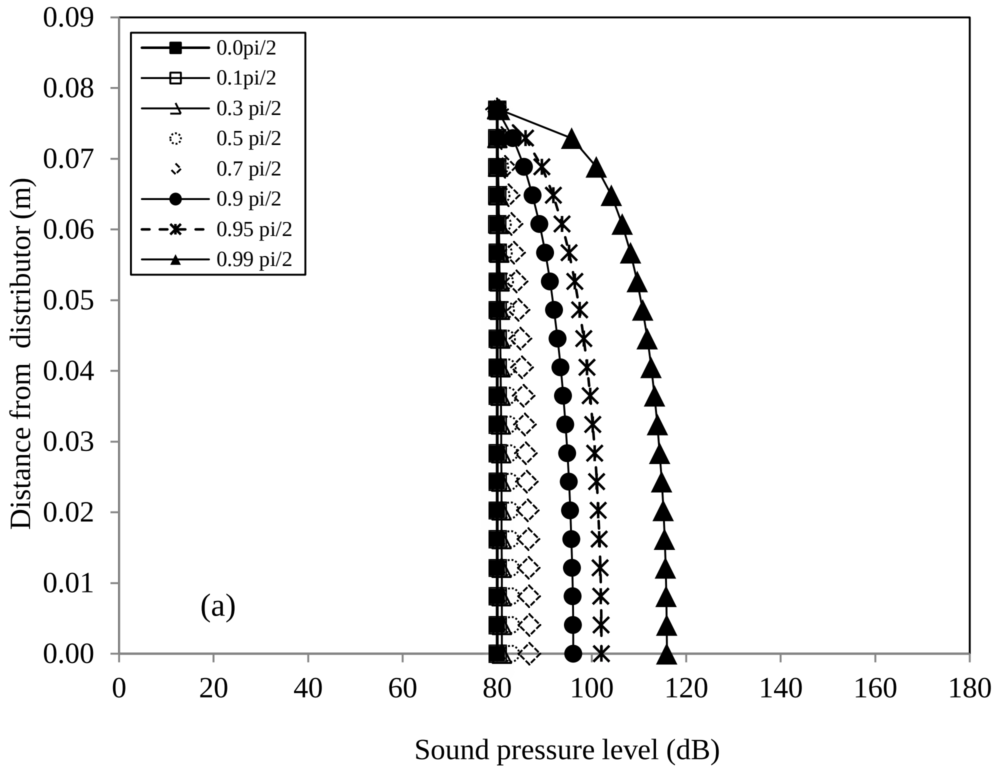

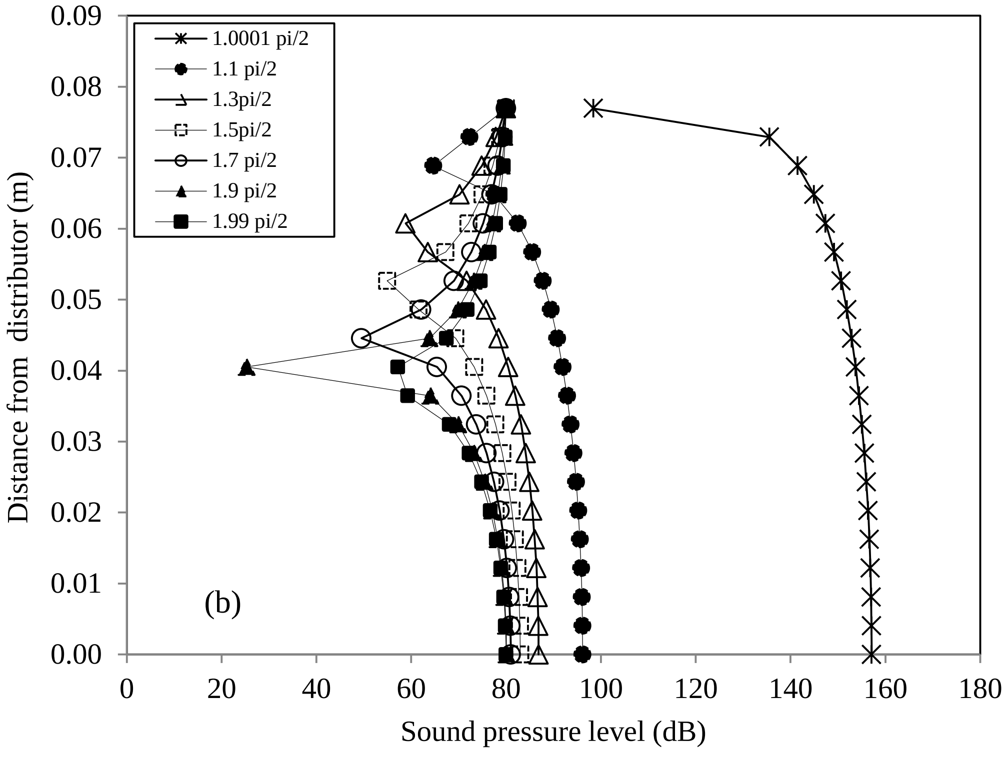

Fig. 5.6 Variation in the sound pressure level along the bed height (0<x<h): (a) 0<kh<π/2 and (b) π/2<kh<π for n = 1

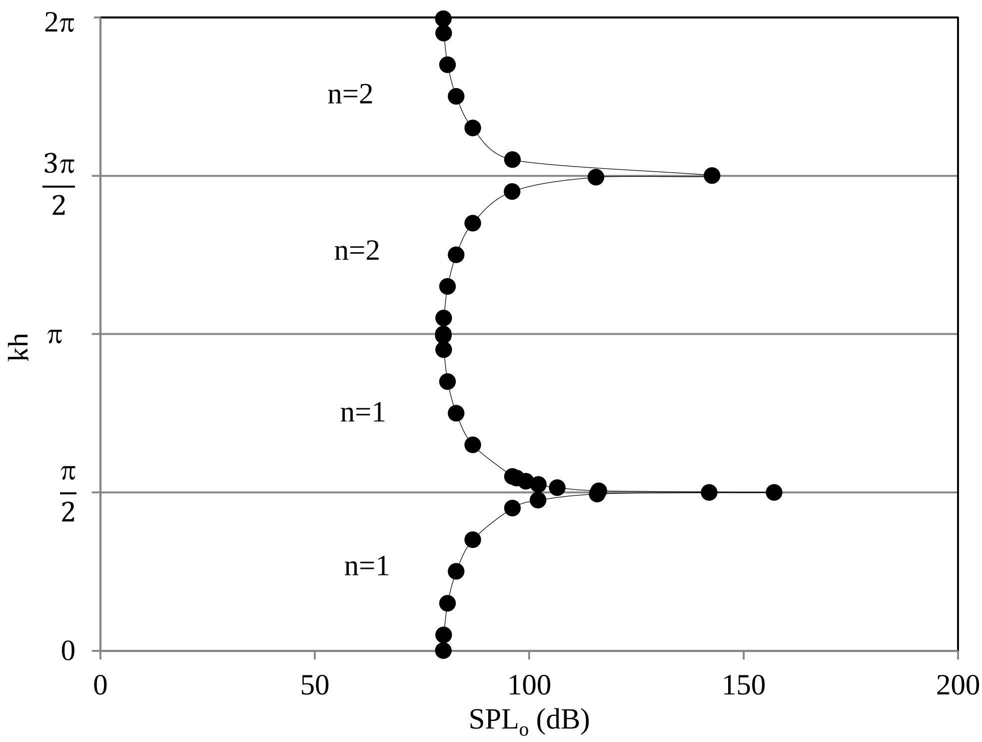

Fig. 5.7 Variation in SPL_o with kh for 0<kh<π, n = 1 and for π<kh<π/2, n = 2

5.4 Quantitative relation between minimum fluidization velocity and standing wave characteristics

The magnitude of the SPL along the distance x and the standing wave pattern imparted an effect on the gas oscillation strength and, certainly, the hydrodynamic properties. It can be seen from Fig. 5.5 that the minimum fluidization velocity decreased with the application of the sound wave and that the local minima was found at the sound frequency of 50 Hz. After this, the minimum fluidization velocity increased again and leveled off at sound frequencies higher than 100 Hz. The standing wave patterns obtained in this study at different sound frequencies are presented in Fig. 5.8. It can be seen that with the change in the sound frequency, the standing wave pattern and the SPL magnitude had changed in accordance with the explanation, as described above. At the sound frequency of 50 Hz, the SPL magnitude along the distance x of the standing wave was the highest in comparison with those of all the other sound frequencies as well as their average values (Table 5.1). This caused the minimum fluidization velocity to be the lowest at this particular sound frequency (Table 5.1). As for other sound frequency values, even though the standing wave patterns were different, the average value of the SPL, as demonstrated in Table 5.1, was found to be approximately the same and, hence, the minimum fluidization velocity.

The important conclusion from the use of the standing wave characteristics to explain the variation in the minimum fluidization velocity with the sound properties is that the point of local minima of the minimum fluidization velocity can be several points, that is, wherever the kh values hit the critical points, as calculated by Eq. (3.11). And, this is more pronounced than the explanation using the resonance behavior between the standing wave frequency and the bed natural frequency, where there existed only a single resonance point and only one value of the local minima of the minimum fluidization velocity was possible.

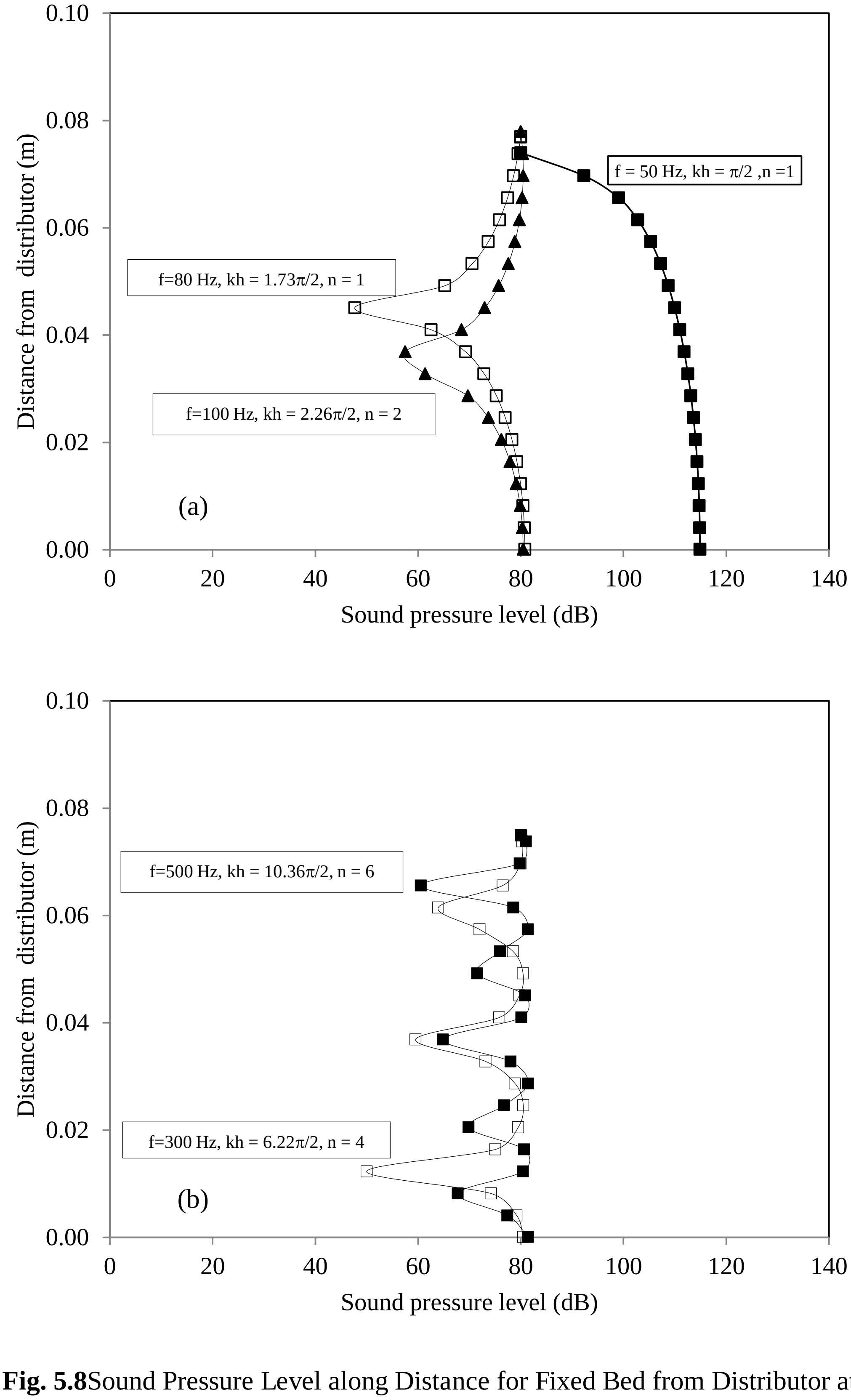

Fig. 5.8 Sound Pressure Level along Distance for Fixed Bed from Distributor at Different Sound Frequencies: (a) f = 50 Hz, 80 Hz, and 100 Hz; and (b) f = 300 Hz and 500 Hz

Table5.1 Summary of Standing Wave Properties and Corresponding Minimum Fluidization Velocities

Sound frequency (Hz)	kh	Harmonic number (n)	Average SPL (dB)	U_{mf} (mm/s)
50	$\pi/2$	1	108.15	0.750
80	$1.73\pi/2$	1	74.52	0.956
100	$2.26\pi/2$	2	76.02	1.100
300	$6.22\pi/2$	4	75.13	1.100
500	$10.36\pi/2$	6	76.59	1.100

5.5 Fixed bed pressure drop correlation for sound-assisted fluidization

The analysis was based on the force-balance principle, and Fig. 5.9 shows the schematic diagram of the forces asserted on the particle under the fluid flow and the sound wave pressure.

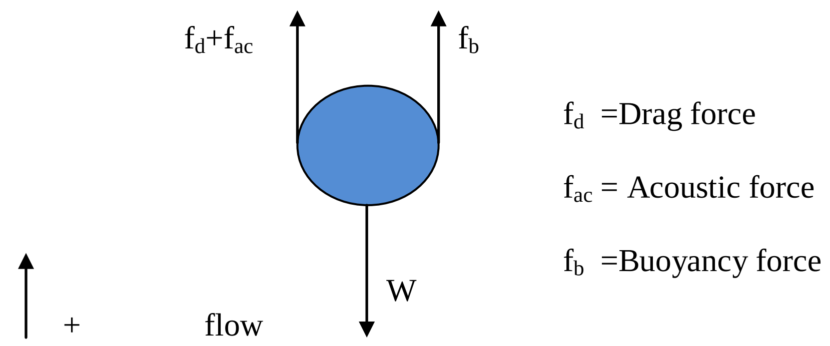

Fig. 5.9 The schematic diagram of the forces asserted on the particle under fluid flow and sound wave pressure

According to Fig. 5.9, the force-balance can be presented as given in Eq. (5.1)

$$f_d + f_{ac} + w_e = ma\ 16 \tag{5.1}$$

when

$$f_b + w = w_e . \tag{5.2}$$

For fixed bed, the pressure drop was contributed by the drag force due to the flowing of the fluid and the drag force due to the gas oscillation velocity (u_{ac}) on the sound wave field called "acoustic force." These two forces can be defined in terms of the pressure drop, using Eqs. (5.3) and (5.4).

$$f_d = \frac{\pi d_P^3 \varepsilon}{6L(1-\varepsilon)} \Delta P_d \tag{5.4}$$

and

$$f_{ac} = \frac{\pi d_P^3 \varepsilon}{6L(1-\varepsilon)} \Delta P_{ac} \tag{5.5}$$

Therefore, the fixed bed pressure drop can be written as follows:

$$\Delta P = \Delta P_d + \Delta P_{ac} \tag{5.6}$$

According to the drag force correlation purposed by Foscolo et al. (1983), who modified the Ergun equation (Ergun, 1952), the pressure drop correlation due to the drag force under the field of the flowing fluid and that under the gas oscillation velocity under the sound wave field for a distance Δx is as presented in Eq.(5.7).

$$\frac{\Delta P}{\Delta x} = \frac{\rho_F (1-\varepsilon)}{d_P} \left(\frac{17.3\mu_F ((U_o/\varepsilon) + \bar{u}_{ac_{i+1}})}{d_P \rho_F} + \frac{0.336((U_o/\varepsilon)^2 + \bar{u}^2_{ac_{i+1}})}{\varepsilon} \right) \varepsilon^{-3.8} \tag{5.7}$$

For an overall distance L, the fixed bed pressure correlation can be rewritten as follows:

$$\frac{\Delta P}{\Delta x}=\frac{\rho_F(1-\varepsilon)}{d_P}\left(\frac{17.3\mu_F(\sum_i(U_o/\varepsilon)_{i+1}+\sum_i\bar{u}_{ac_{i+1}})}{d_P\rho_F}+\frac{0.336(\sum_i(U_o/\varepsilon)^2_{i+1}+\sum_i\bar{u}^2_{ac_{i+1}})}{\varepsilon}\right)\varepsilon^{-3.8}$$

(5.8)

The Ergun equation can also be used to represent the pressure drop in the fixed bed for the sound-assisted fluidized bed, which is as presented in Eq. (5.9) for a distance Δx.

$$\frac{\Delta P}{\Delta x}=\frac{150((U_o/\varepsilon)+\bar{u}_{ac_{i+1}})\mu_F}{g_c\phi_S^2 d_P^2}\frac{(1-\varepsilon)^2}{\varepsilon^2}+\frac{1.75\rho_F((U_o/\varepsilon)^2+\bar{u}^2_{ac_{i+1}})}{g_c\phi_S d_P}\frac{(1-\varepsilon)}{\varepsilon} \quad (5.9)$$

For the overall distance L, the fixed bed pressure drop correlation based on the Ergun equation can be written as follows:

$$\frac{\Delta P}{\Delta x}=\frac{150(\sum_i(U_o/\varepsilon)_{i+1}+\sum_i\bar{u}_{ac_{i+1}})\mu_f}{g_c\phi_S^2 d_P^2}\frac{(1-\varepsilon)^2}{\varepsilon^2}+\frac{1.75\rho_f(\sum_i(U_o/\varepsilon)^2_{i+1}+\sum_i\bar{u}^2_{ac_{i+1}})}{g_c\phi_S d_P}\frac{(1-\varepsilon)}{\varepsilon}$$

(5.10)

The gas oscillation velocity ($u_{ac}(x,t)$) at distance x along the bed height can be calculated according to Eq. (5.11):

$$u_{ac}(x,t)=U_A\sin(2\pi ft) \quad (5.11)$$

And,

$$SPL=20\log\left[\frac{U_A}{\sqrt{2}U_{ref}}\right] \quad (5.12)$$

The average gas oscillation velocity ($\bar{u}_{ac_{i+1}}$) over the distance Δx can be calculated as

$$\bar{u}_{ac_{i+1}}=\frac{u_{ac}(x,t)_i+u_{ac}(x,t)_{i+1}}{2} \quad (5.13)$$

5.6 Prediction ability of pressure drop correlations

The revised Ergun equation and the Ergun equation were used, firstly, for the prediction of the fixed bed pressure drop for the conventional fluidized bed. It can be seen from Fig. 5.10(a) for the revised Ergun equation (Eq. (5.8)) and Fig. 5.10(b) for the Ergun equation (Eq. (5.10)) that without the sound vibration, these two original equations can predict perfectly the relation between the fixed bed pressure drop and the inlet superficial velocity. However, when the same correlations were used for sound-assisted fluidization with a sound pressure level of 80 dB and a sound frequency of 80 Hz, deviations between the experimental results and the theoretical prediction were found even though the gas oscillation velocity was taken into account in the correlations, as presented in Fig. 5.11(a) for the revised Ergun equation (Eq. (5.8)) and Fig. 5.11(b) for the Ergun equation (Eq. (5.10)). Therefore, in order to develop the fixed bed pressure drop correlations appropriately for sound-assisted fluidization, adjustment of the empirical factor of both the correlations is also needed. For the revised Ergun equation, the empirical exponential factor should be modified and for the Ergun equation, the empirical multiplication factor should be modified. Hence, a general form of the correlation should be drawn, as shown in Eq. (5.14) and Eq. (5.15), for the revised Ergun equation and the Ergun equation, respectively.

$$\frac{\Delta P}{\Delta x}=\frac{\rho_F(1-\varepsilon)}{d_P}\left(\frac{17.3\mu_F\left(\sum_i (U_o/\varepsilon)_{i+1}+\sum_i \bar{u}_{ac_{i+1}}\right)}{d_P\rho_F}+\frac{0.336\left(\sum_i (U_o/\varepsilon)^2_{i+1}+\sum_i \bar{u}^2_{ac_{i+1}}\right)}{\varepsilon}\right)\varepsilon^{-\beta} \tag{5.14}$$

$$\frac{\Delta P}{\Delta x}=\frac{X\left(\sum_i (U_o/\varepsilon)_{i+1}+\sum_i \bar{u}_{ac_{i+1}}\right)\mu_F}{g_c\phi_S^2 d_P^2}\frac{(1-\varepsilon)^2}{\varepsilon^2}+\frac{1.75\rho_F\left(\sum_i (U_o/\varepsilon)^2_{i+1}+\sum_i \bar{u}^2_{ac_{i+1}}\right)}{g_c\phi_S d_P}\frac{(1-\varepsilon)}{\varepsilon} \tag{5.15}$$

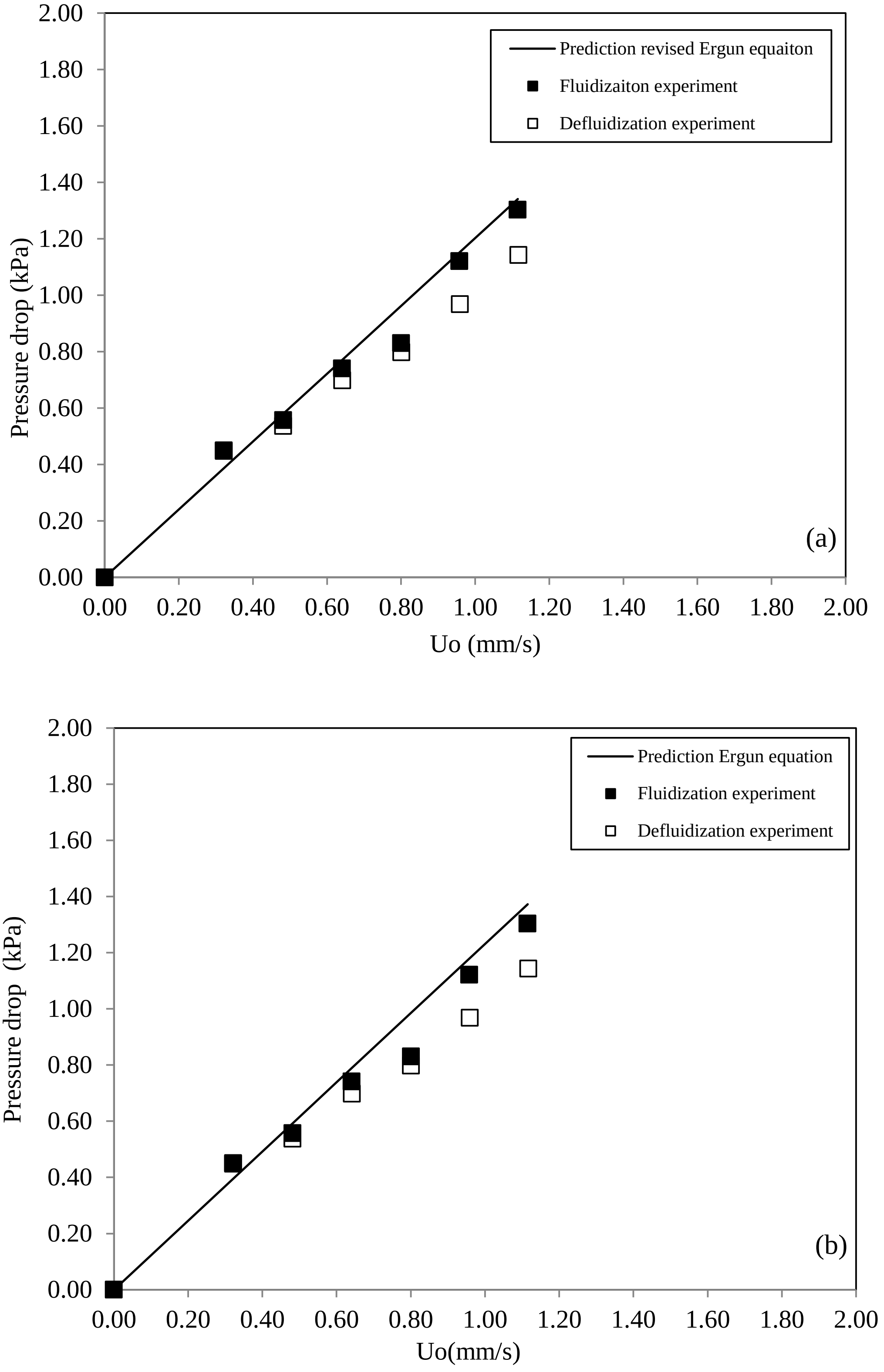

Fig. 5.10 Comparison between the experimental fixed bed pressure drop from conventional fluidized bed and that from (a) revised Ergun equation prediction and (b) Ergun equation prediction

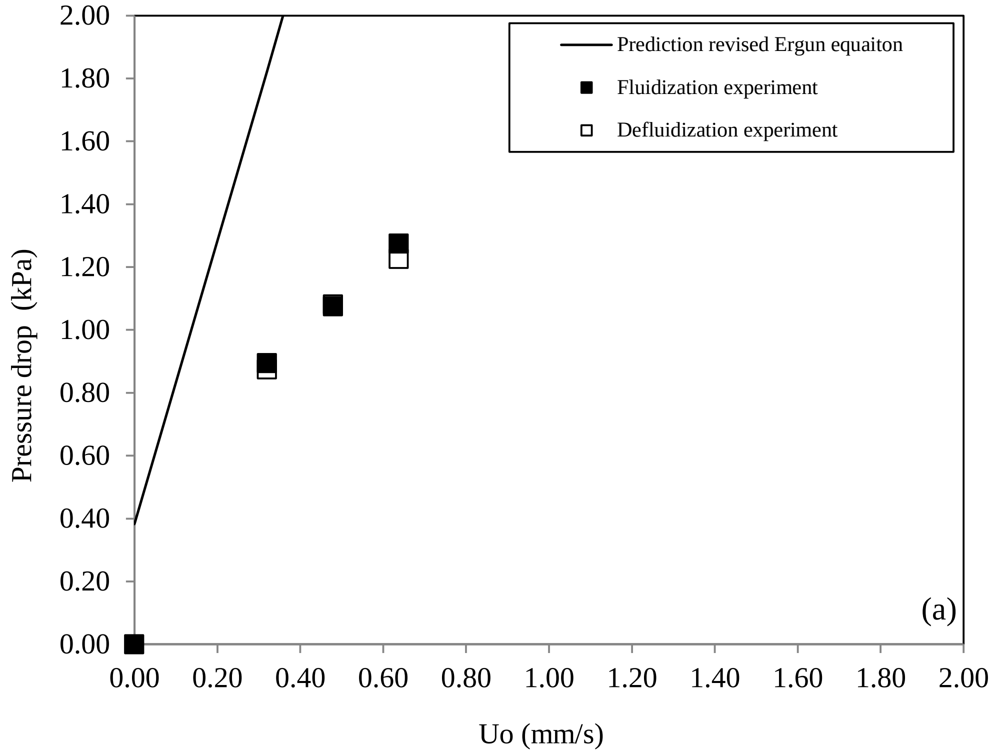

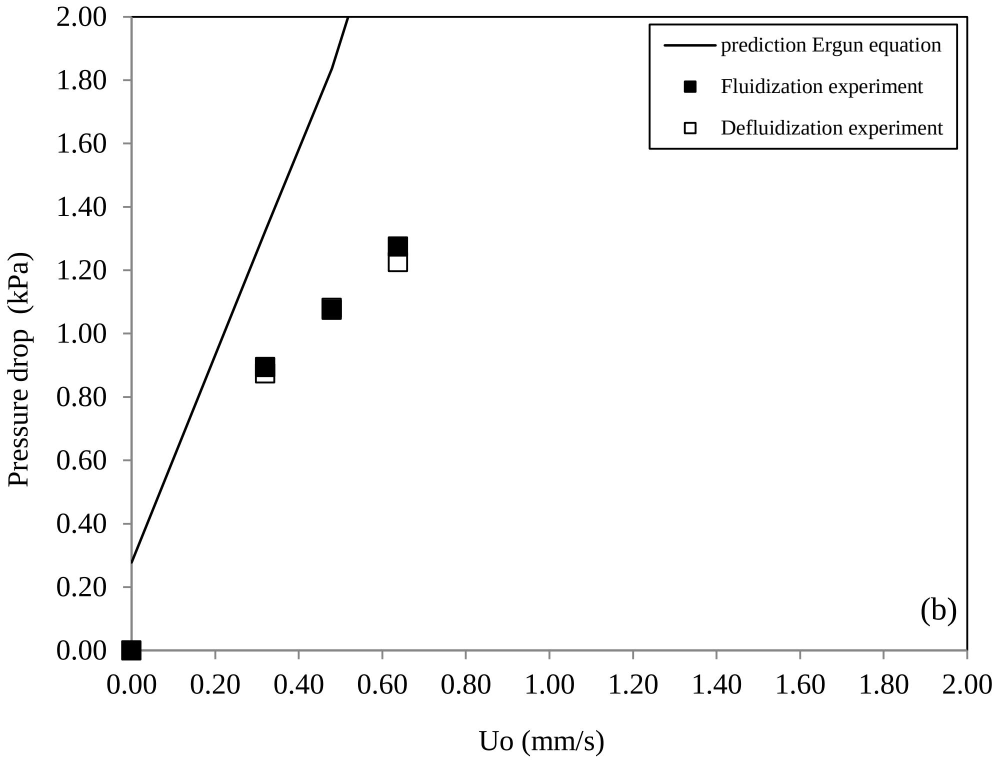

Fig. 5.11 Comparison between the experimental fixed bed pressure drop from sound-assisted fluidized bed (SPL = 80 dB and f = 80 Hz) and that from (a) the revised Ergun equation prediction and (b) the Ergun equation prediction

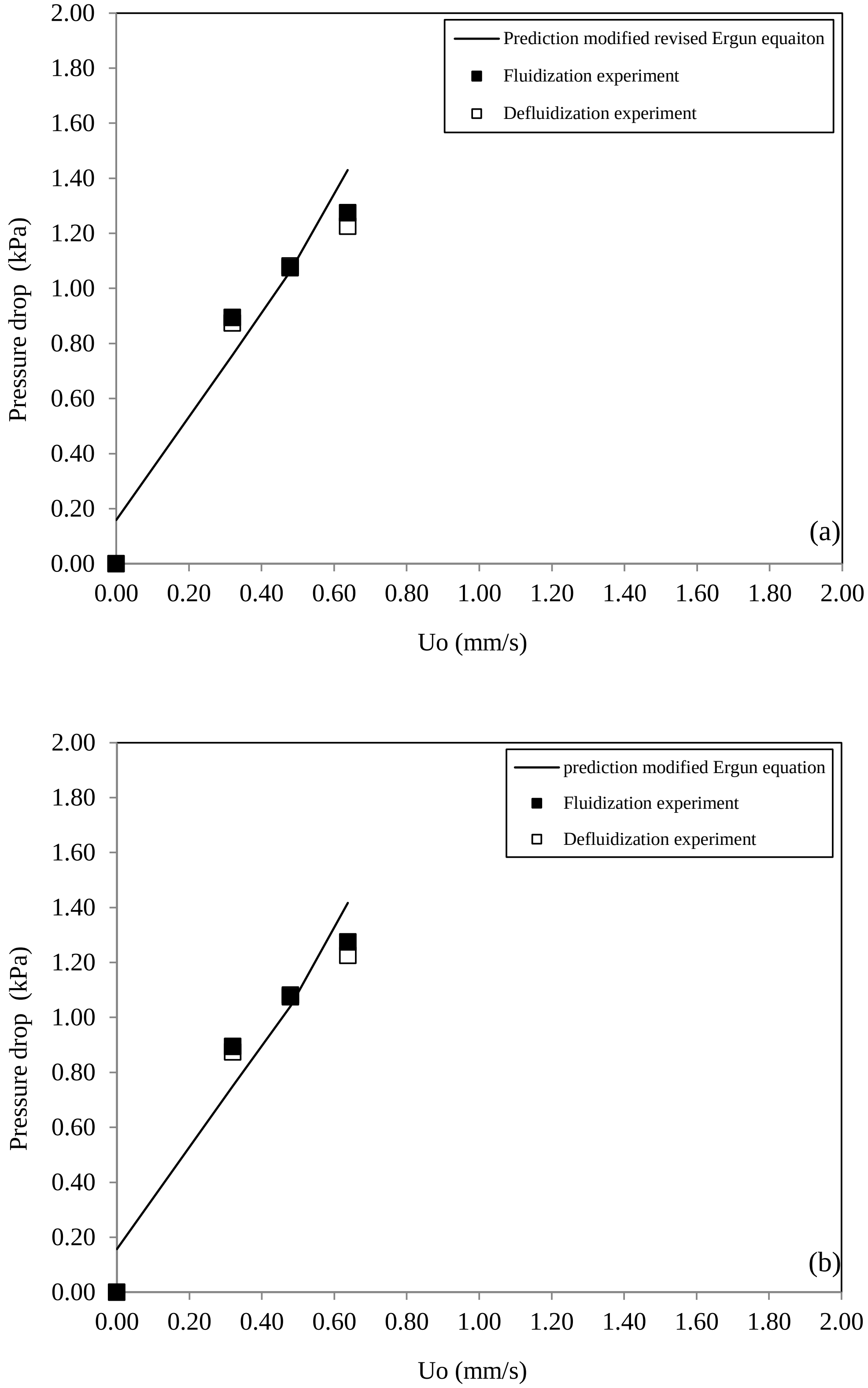

Fig. 5.12 Comparison between the experimental fixed bed pressure drop from sound-assisted fluidized bed and (a) the modified revised Ergun equation prediction (β = 3.05) and (b) the modified Ergun equation prediction (X = 85)

Fig. 5.12(a) and (b) present the experimental fixed bed pressure drop under the sound pressure level of 80 dB and sound frequency of 80 Hz from the fluidization and the defluidization experiments in comparison with the theoretical predictions from the modified revised Ergun equation (Eq. (5.14)) and the modified Ergun equation (Eq. (5.15)), respectively, when the empirical factors were used. It is obvious that the experimental fixed bed pressure drop was coinciding more with its corresponding theoretical predictions. Besides, it was also found that the empirical values varied with the sound frequency, as shown in Figs.5.13and 5.14. Fig. 5.13shows the variation in the empirical exponential factor (β) for the modified revised Ergun equation (Eq. (5.14)). Fig. 5.14shows the variation in the empirical multiplication factor for the modified Ergun equation (Eq. (5.15)).

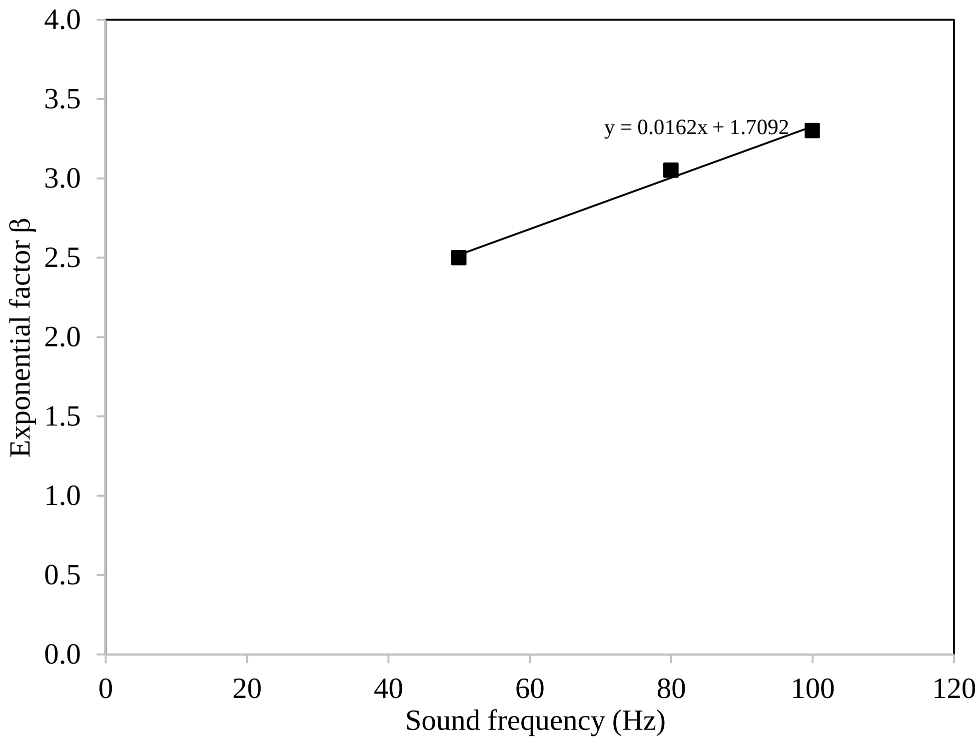

Fig. 5.13 Variation in the empirical exponential factor (β) for the modified revised Ergun equation (Eq. (28))

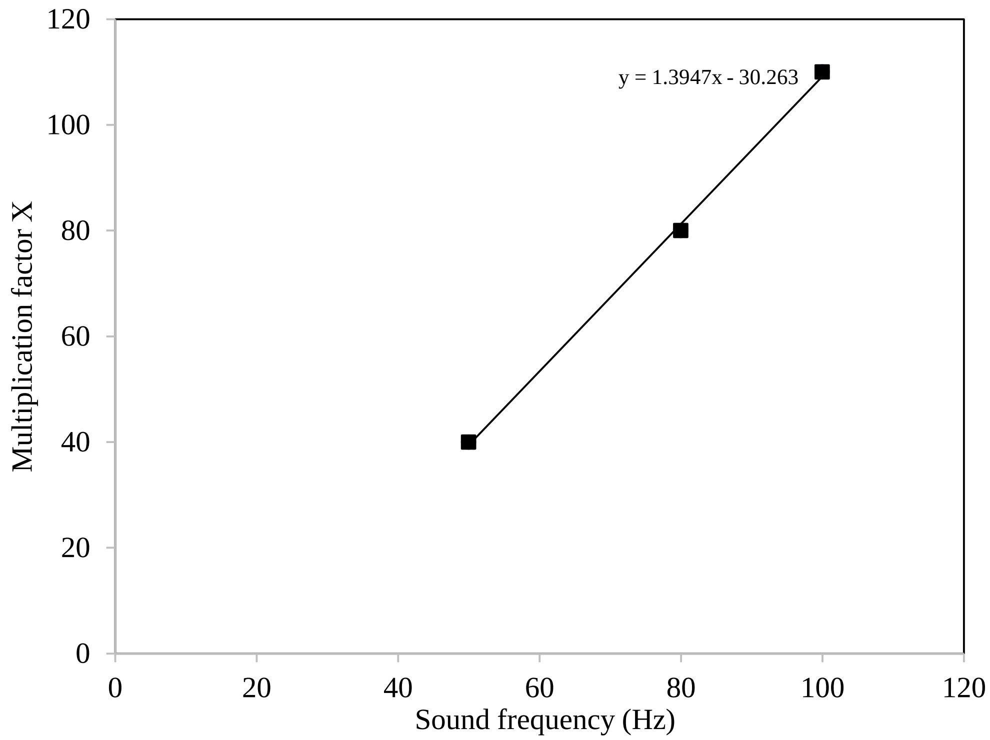

Fig. 5.14 Variation in the empirical multiplication factor for the modified Ergun equation (Eq. (29))

For both cases, the linear relation between the factor and the sound frequency were found. Additionally, the closure equations were purposed in Eq. (5.16) and (Eq. (5.17).

The closure equation for the modified revised Ergun equation is as follows:

$$\beta = 0.0162(f) + 1.7092\,. \tag{5.16}$$

And, the closure equation for the modified Ergun equation is as follows:

$$X = 1.3974(f) - 30.263\,. \tag{5.17}$$

5.7 Prediction of total bed voidage and dense phase properties using bed collapse model

An interpretation of ε_o, ε_d and U_d from 1-valve and 2-valve bed collapse curves for a homogeneous expanded bed and a bubbling bed has been explained thoroughly in Cherntongchai and Brandani (2005).

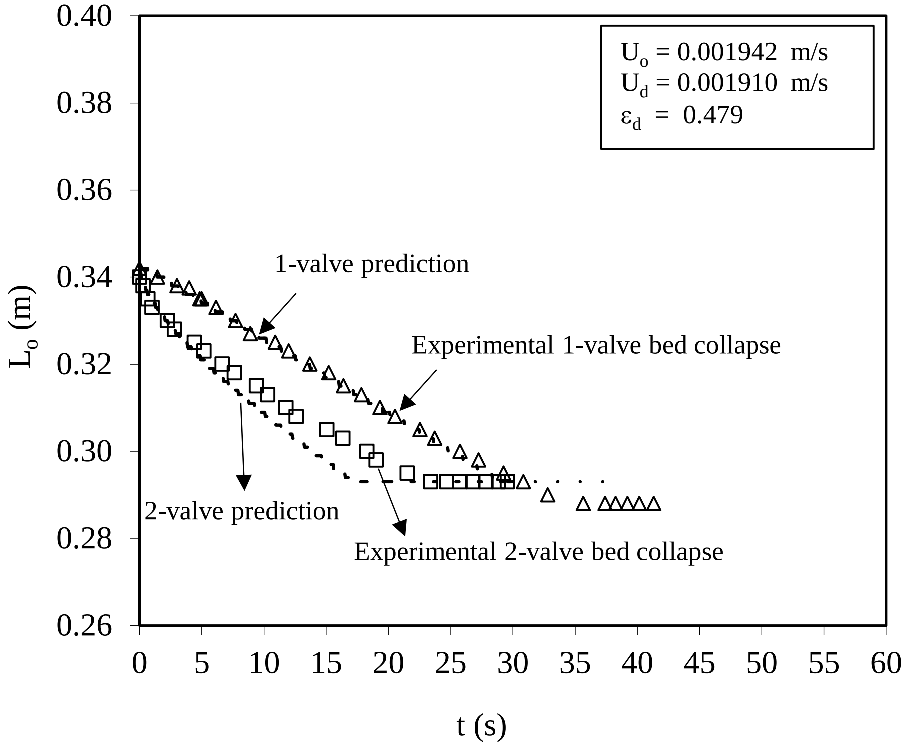

Fig. 5.151-valve and 2-valved bed collapse curves and model predictions for homogenous expanded bed in sound assisted fluidized bed at SPL = 80 dB and f = 100 Hz

Fig. 5.15 was the bed collapse curves for the homogeneous expanded bed where there is no bubble escape stage. And, the y-intercept from the 1-valve bed collapse curve was used to determine the correct ε_d. Then, U_d, equivalent to U_o, was used to predict correctly the entire 1-valve collapse curve. The 2-valve collapse curve was fully predicted using ε_d and U_d obtained from the 1-valve bed collapse curve. By this way, the set of ε_d and U_d was re-validated.

The bubbling bed collapse curves were presented in Fig. 5.16. ε_o was selected to match with the bubble escape time. ε_d was acquired from the y-intercept of the 1-valve sedimentation state linear extrapolation and U_d was iterated to match the predicted 1-valve sedimentation curve with the experimental curve. As for the homogeneous bed, the entire 2-valve collapse curve was predicted using the same set of ε_o, ε_d and U_d.

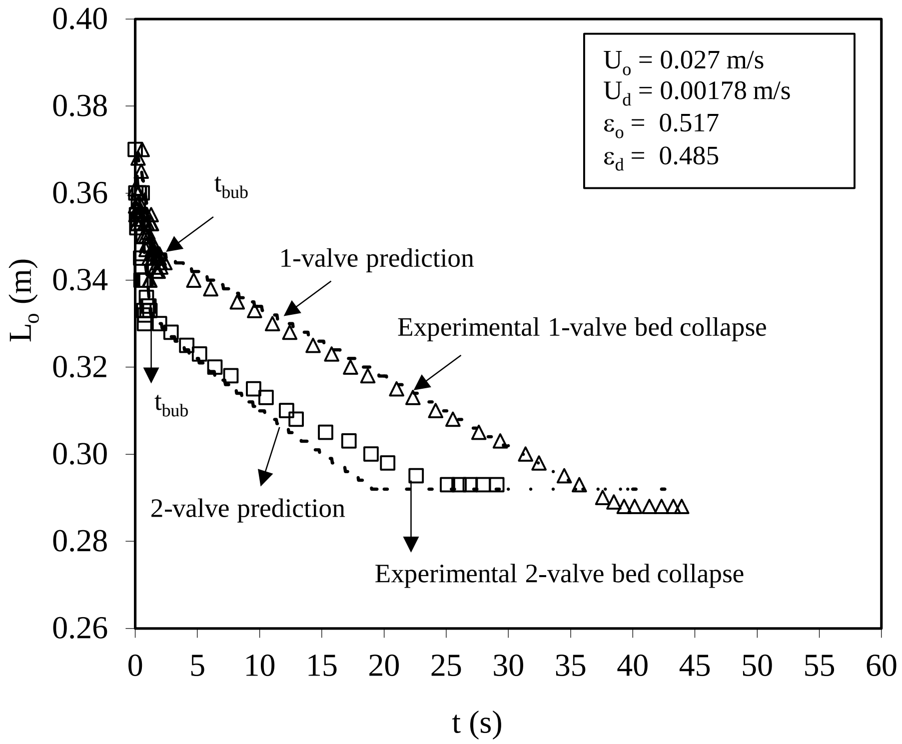

Fig. 5.161-valve and 2-valved bed collapse curves and model predictions for bubbling bed in sound assisted fluidized bed at SPL = 80 dB and f = 100 Hz

5.8 Total bed voidage and dense phase properties

An aspect of the bed expansion in the sound assisted fluidization has been published by some previous works using the visual observation (Russo et al., 1995; Herrera and Levy, 2001; Zhu et al., 2004; Ammendola and Chirone, 2010; Ammendola et al., 2011; Kaliyaperumal et al., 2011; Langde and Sonolikar, 2011; Raganati et al., 2014). The previous works(Russo et al., 1995; Langde and Sonolikar, 2011) stated that there was a non-monotonically increase with the inlet superficial velocity of the overall bed voidage or the bed expansion ratio obtained visually. And, there was the increase of the bed expansion ratio in the sound assisted fluidization, in comparison with the conventional fluidization. In addition, based on the expansion ratio, the other works reported the existing of the maximum bed expansion at the resonance frequency, usually at 120 Hz. (Ammendola and Chirone, 2010; Kaliyaperumal et al., 2011; Langde and Sonolikar, 2011)

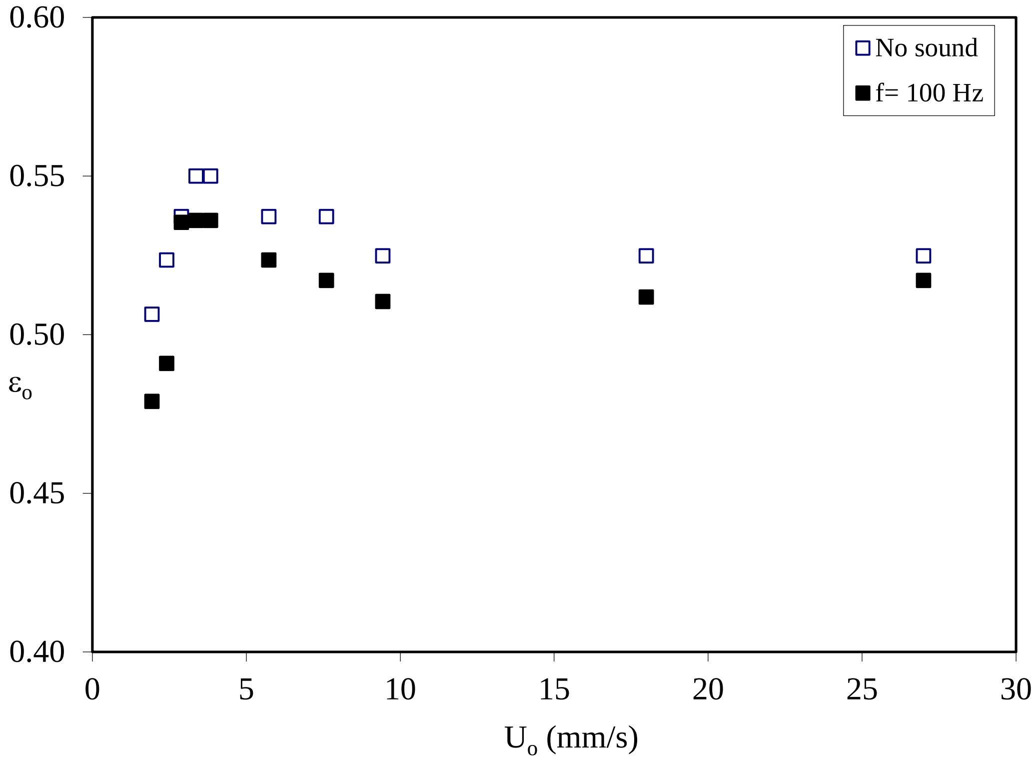

Fig. 5.17 Total bed voidage and inlet superficial velocity relation for conventional fluidization and sound assisted fluidization at SPL = 80 dB and sound frequency = 100 Hz

Our work using the more accurate method on defining the bed expansion characteristics, as mentioned above. We have found in contrary, for the sound assisted fluidization and the conventional fluidization that the total bed voidage increased with the inlet superficial velocity in the homogeneous expanded bed(Fig. 5.17). After the minimum bubbling point, where the dense phase voidage is the highest, the total bed voidage decrease with increasing the inlet superficial velocity. At a certain inlet superficial velocity, the total bed voidage reached the minimum and, then, started to increase again. And, this same pattern of variation was also found for the relation between the dense phase voidage and the inlet superficial velocity for both the conventional and the sound assisted fluidization of different sound found frequency (Figs.5.18 and 5.19).

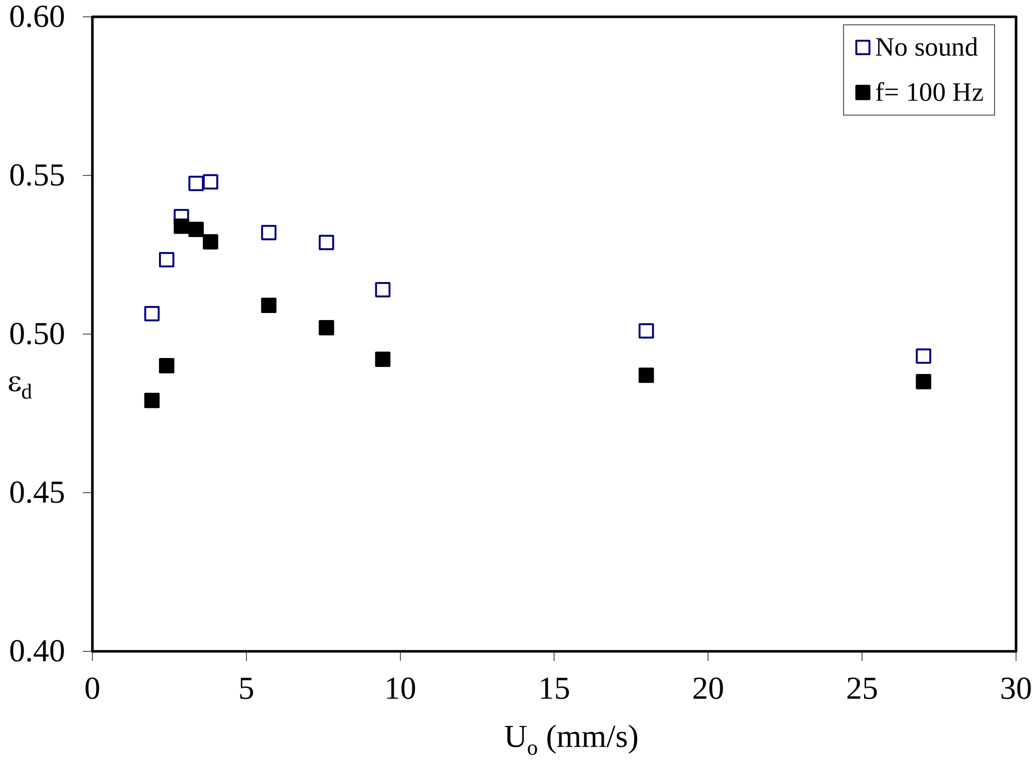

Fig. 5.18 Dense phase voidage and inlet superficial velocity relation for conventional fluidization and sound assisted fluidization at SPL = 80 db and sound frequency = 100 Hz

It was also proved in our work that the application of the sound vibrational force reduced the dense voidage, as well as the total bed voidage, in comparison with those of the conventional fluidization (Figs.5.17,5.18 and5.19). Besides, under the variation of the sound frequency, the dense phase voidage with respect to the inlet superficial velocity were considered to be randomly distributed over approximately the same values (Fig. 5.19).

Fig. 5.20 presented the relation between the dense phase voidage and the dense phase superficial velocity. It was found to be failed on the same trend for both the conventional and the sound assisted fluidization. Even, the dense phase voidage with respect to the inlet superficial velocity (Fig. 5.18 and Fig. 5.19) were different, including those for the homogeneous expanded bed.

An explanation of the change of the total bed voidage and the dense phase voidage under the sound vibrational force field was similar to many other reports due to the rearrangement of the bed structure. However, from our results, it was possible to further explain that the gas oscillation under the sound vibrational induced more cavities or bubble phase in the fluidizing bed, and the structure of the dense phase was remained. Therefore, the same force equilibrium relation existed for both systems of fluidization.

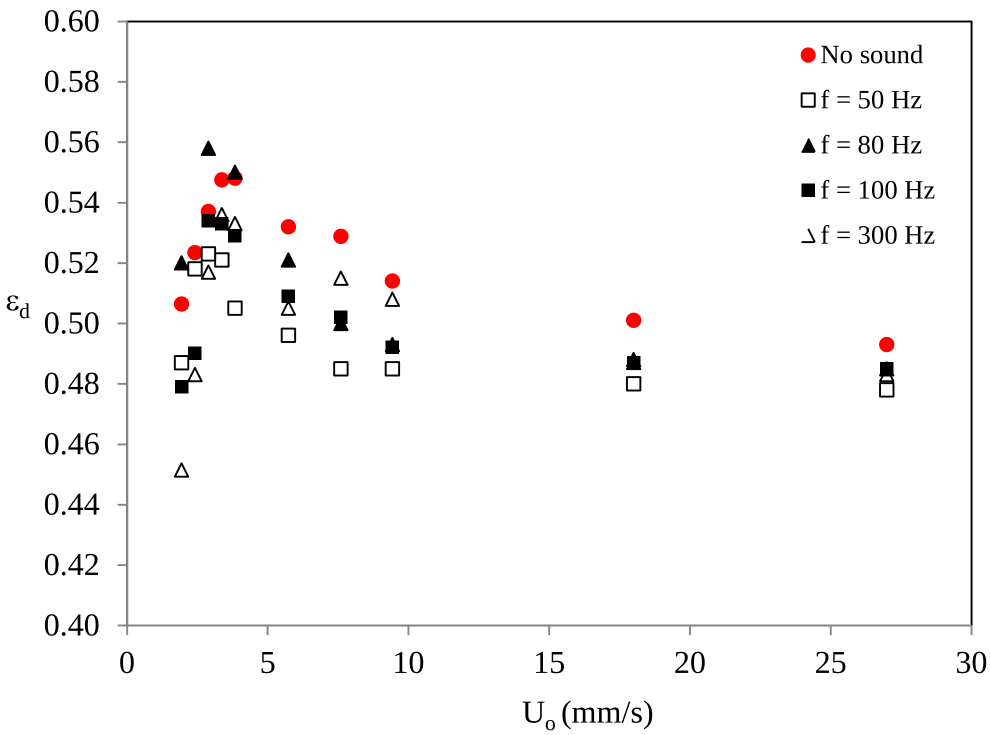

Fig. 5.19 Dense phase voidage and inlet superficial velocity relation for conventional fluidization and sound assisted fluidization at SPL = 80 dB and sound frequency = 50 Hz, 80 Hz, 100 Hz and 300 Hz

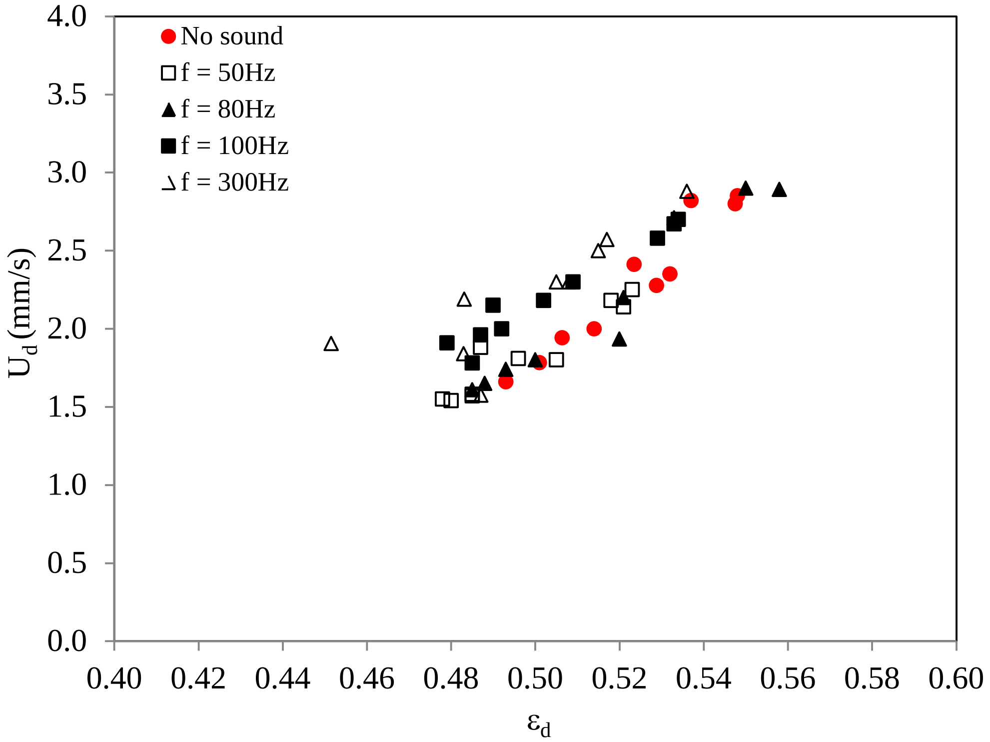

Fig. 5.20 Dense phase voidage and inlet superficial velocity relation for sound assisted fluidization at SPL = 80 dB and sound frequency = 50 Hz, 80 Hz, 100 Hz and 300 Hz

5.9 Validation of drag force correlation

It is well known that the drag force is the key component on describing the fluidization characteristics. One of which is the revised Ergun drag force correlation (Foscolo et al., 1983) This correlation was applicable for the fixed bed to the fluidized bed for an entire range of flow regime. And, it was proved by Cherntongchai and Brandani (2013) that to apply this correlation more accurately the empirical β should be applied. Therefore, they proposed the modified revised Ergun equation, as presented in Eq. (5.18) and suggested β value from this work was 4.21 for the conventional fluidization. At equilibrium condition, this drag force correlation is equaled to an effective weight (Eq. (5.19)). Hence, the relation between the dense phase voidage and its superficial velocity can be described.

$$F_D = \frac{4}{3}\frac{\rho_F}{d_P}C_D U^2 (1-\varepsilon)\varepsilon^{-\beta} \tag{5.18}$$

At equilibrium, Eq. (20) is equaled to Eq. (21)

$$F_D = \varepsilon(\rho_P - \rho_F)(1-\varepsilon)g \tag{5.19}$$

Richardzon and Zaki expansion law (Richardson and Zaki, 1954) (Eq. (5.20)) is also a basic correlation used to describe the relation between the dense phase voidage and its superficial velocity.

$$\frac{U_d}{U_t} = \varepsilon_d^{n'} \tag{5.20}$$

And, the empirical Richardson and Zaki index (n') was recommended, especially for gas fluidization. For a sound assisted fluidization, Ammendola et al. (2011) worked with the homogeneous bed expansion data and gave the suggested value at approximately 5. While n index will be experimentally defined, terminal falling velocity (U_t) can be calculated from Eq. (5.21). (Dallavalle, 1948).

$$U_t = \left(-3.809 + \sqrt{3.809^2 + 1.832\sqrt{Ar}}\right)^2 \frac{\mu_F}{\rho_F d_P} \tag{5.21}$$

Where;

$$Ar = g d_P^3 \rho_F \frac{\rho_P - \rho_F}{\mu_F^2} \tag{5.22}$$

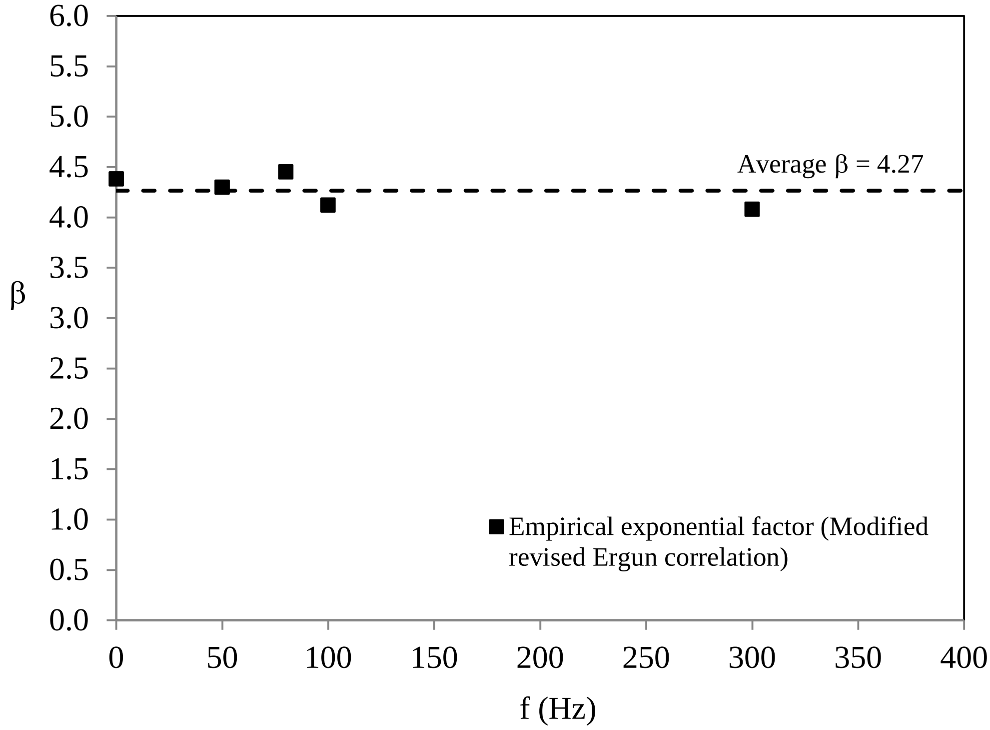

Fig. 5.21 Empirical exponential factor of revised Ergun correlation for conventional fluidization and sound assisted fluidization at various sound frequency and SPL = 80 dB

Fig. 5.21 showed that the empirical β values of the revised Ergun correlation for the conventional fluidization and the sound assisted fluidization at different sound frequency were distributed over the same average value (β = 4.27). This was considerably very close to the value suggested by Cherntongchai and Brandani (2013) (β=4.21).

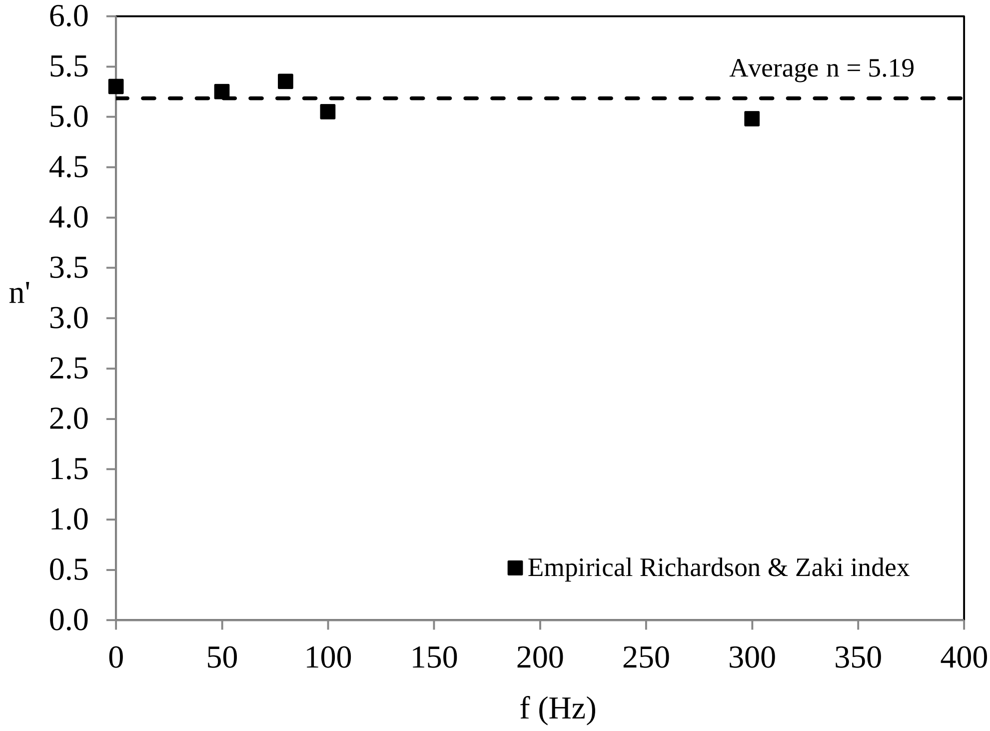

Fig. 5.22 Empirical Richardson and Zaki index (n') for conventional fluidization and sound assisted fluidization at various sound frequency and SPL = 80 dB

Fig. 5.22 presented empirical n index for the Richardson and Zaki expansion law. As for the drag force correlation, the n index of the conventional fluidization and those of the sound assisted fluidization at different sound frequency were failed on the same average value (n' = 5.19)

Fig. 5.23 showed a good agreement between the prediction by the modified revised Ergun correlation (β = 4.27) and the empirical Richardson and Zaki correlation (n' = 5.17) for the conventional fluidization and the sound assisted fluidization at sound pressure level of 80 dB and sound frequency of 50-300 Hz.

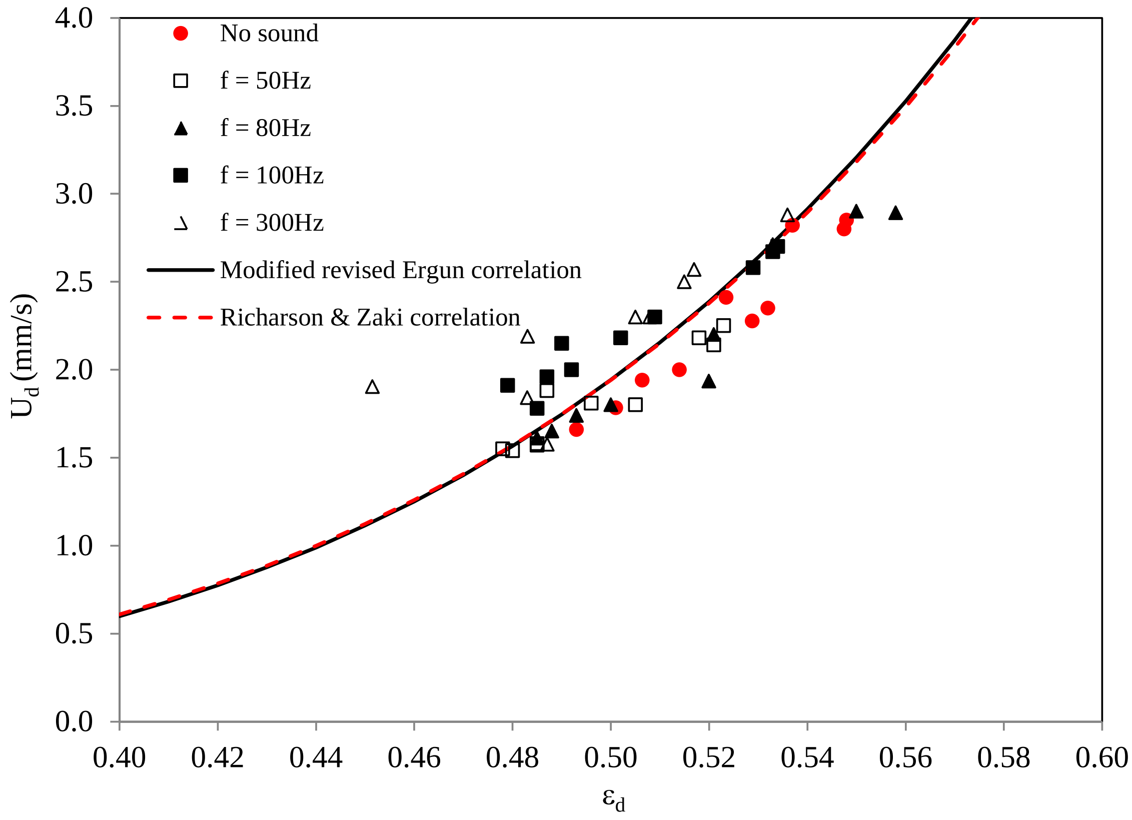

Fig. 5.23 Predictability of modified revised Ergun correlation and Richardson and Zaki correlation using empirical Richardson and Zaki index for conventional fluidization and sound assisted fluidization at various sound frequency and SPL = 80 dB

It is enable us to conclude that the sound vibration force tended to initiate the cavity or the bubble in the sound assisted fluidized bed rather than causing the change in the dense phase voidage and its superficial velocity relation. Hence, the force equilibrium in the dense phase for the sound assisted fluidized bed is remained as that for the conventional fluidization and the same drag force correlation or the bed expansion law can be applied.

5.10 Minimum bubbling point

A visual observation is the most common method used for an identification of a minimum bubbling point. However, it has been generally known that this method gives a very degree of uncertainty. By definition, the minimum bubbling point is the point where the very first bubble appears in the particle bed and the dense phase expansion is the highest. To define the minimum bubbling point, it was recommended to use the plot between the dense phase voidage and its superficial velocity (Cherntongchai and Brandani, 2013) and the minimum bubbling point was defined at the maximum dense phase expansion point (Fig. 5.24).

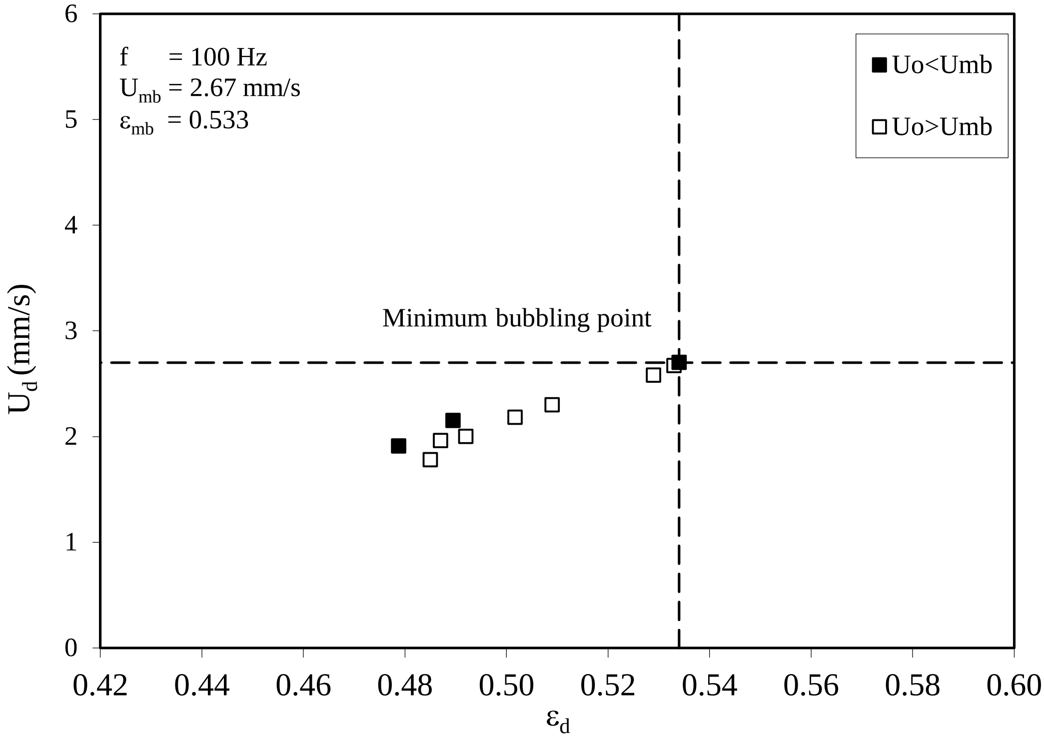

Fig. 5.24 Minimum bubbling point identification for the sound assisted fluidization at sound pressure level = 80 dB and sound frequency = 100 Hz

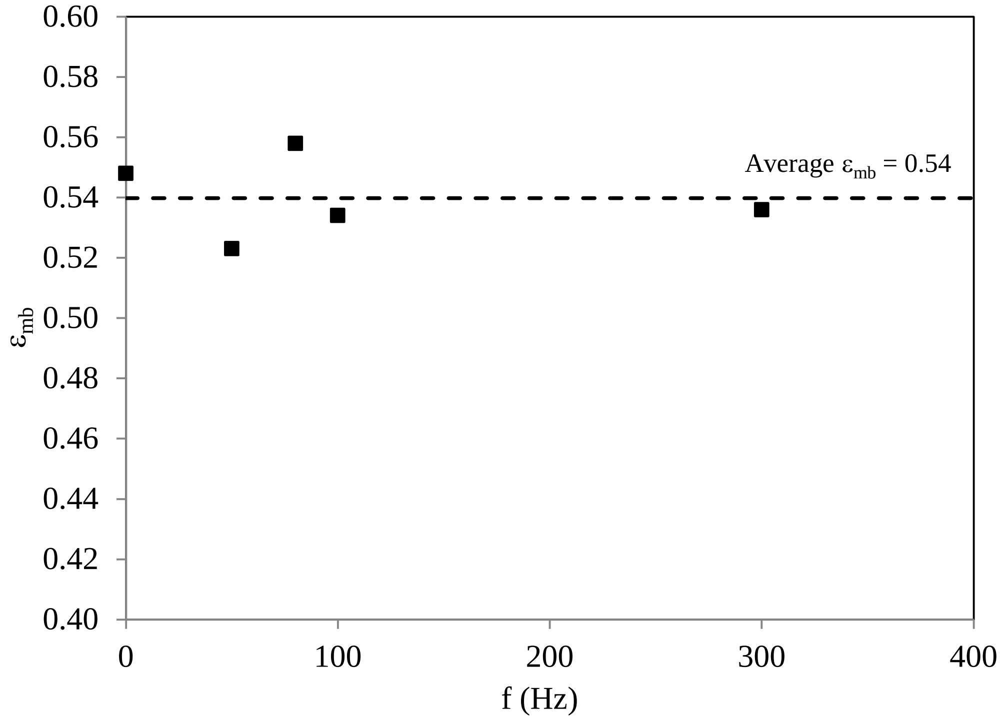

Fig. 5.25 Minimum bubbling voidage for conventional fluidization and sound assisted fluidization at various sound frequency and SPL = 80 dB

Fig. 5.25 showed that the minimum bubbling voidages (ε_{mb}) of the conventional fluidization (f = 0 Hz) and the sound assisted fluidization (f = 50-300 Hz) were distributed on the same average value (ε_{mb}=0.54). Accordingly, their minimum bubbling velocities (Fig. 5.26) was distributed on the average value (U_{mb} = 2.714 mm/s). This means the sound vibrational force within the range of our study does not affect the bed stability. It rather imparts the effect of creating a premature bubbling in the homogeneous expanded bed or a more bubble fraction in the bubbling bed.

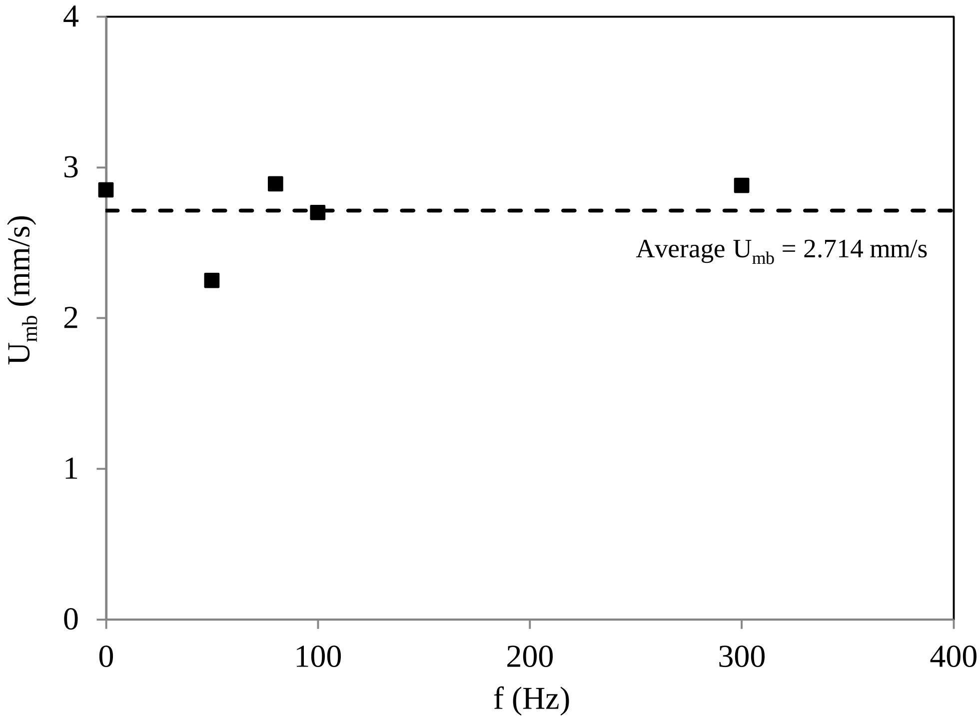

Fig. 5.26 Minimum bubbling velocity for conventional fluidization and sound assisted fluidization at various sound frequency and SPL = 80 dB

5.11 Prediction of minimum bubbling point for sound assisted fluidization

The transition from the particulate to the bubbling beds is considered to be an instability problem. The stability criterion developed by Brandani and Zhang (2006)required a correct knowledge of the characteristic length and the drag force correlation. By Cherntongchai and Brandani (2013), the modified revised Ergun drag force correlation was recommended and the characteristic length (δ/d_p) as a function of a voidage was purposed. In this work, the stability criterion of Brandani and Zhang (2006), with a combination the modified revised Ergun drag force correlation and a voidage dependency of the characteristic (δ/d_p) will be used for a prediction of the minimum bubbling point in a system of the sound assisted fluidization.

The stability criterion can be summarized as follows(Cherntongchai and Brandani, 2013);

$$U_\varepsilon = U_D \tag{5.23}$$

$$U_\varepsilon = (1-\varepsilon)\left(\frac{\partial U}{\partial \varepsilon}\right)_{Equil} = \frac{1-\varepsilon}{\varepsilon}.\frac{(\beta+1)U}{2+\frac{dC_D}{d\,Re_P}\frac{Re_P}{C_D}} \tag{5.24}$$

$$U_D = \sqrt{V^2 - G} + V \tag{5.25}$$

Where β = 4.27 and the Dallavalle equation (Dallavalle, 1948) is used for the drag coefficient.

$$C_D = \left(0.63 + \frac{4.8}{\sqrt{Re_P}}\right)^2 \tag{5.26}$$

$$V = \frac{1-\varepsilon}{\varepsilon}\frac{\rho_F U}{\varepsilon\rho_P + (1-\varepsilon)\rho_F} \tag{5.27}$$

$$G = \frac{\frac{1-\varepsilon}{\varepsilon^2}\rho_F U^2 - \delta\left[(1-\varepsilon)\rho_P + \varepsilon\rho_F\right]g}{\varepsilon\rho_P + (1-\varepsilon)\rho_F} \tag{5.28}$$

The empirical correlation for the characteristic length (δ/d_P) as function of the voidage is;

$$\frac{\delta}{d_P} = 0.55 + 3.0\left[\exp^{-42(\varepsilon-\varepsilon_{mf})}\right] \tag{5.29}$$

Table 5.2 Comparison between model prediction and experimental minimum bubbling point for sound assisted fluidization at various sound frequency and SPL = 80 dB

Sound pressure level (dB)	Sound frequency (Hz)	Experimental average values		Model prediction	
		ε_{mb}	U_{mb} (mm/s)	ε_{mb}	U_{mb} (mm/s)
80	50-300	0.54	2.714	0.53	2.671

It was presented in Table 5.2. that the new stability purposed by Cherntongchai and Brandani (2013) can be predicted excellently the minimum bubbling point of Geldart's group A powder in the sound assisted fluidization.

CHAPTER 6:CONCLUSIONS

Hydrodynamics behaviors of a sound-assisted fluidization of fine powder (Geldart's group A powder) under effects sound wave properties were investigated. And, standing wave characteristics were employed to explain the hydrodynamic behavior of sound-assisted fluidization of the fine powder under different inlet superficial velocities and sound frequencies ranging from 0 Hz to 500 Hz at a fixed sound pressure level of 80 dB.

It can be concluded that due to the exponential and periodic variation of the vibration strength of the standing wave with the sound properties, the minimum fluidization velocity was varied in the same manner. Besides, it can be pointed out that the local minima of the minimum fluidization velocities were, thus, multiple values rather than a single value. To this end, fixed bed pressure drop correlations, based on the revised Ergun equation and the Ergun equation, for sound-assisted fluidization were purposed, where the gas oscillation velocity, calculated using the standing wave theory, was taken into account. It was found that even when the gas oscillation velocity is included, the original revised Ergun equation and the original Ergun equation cannot be used to describe the fixed bed pressure drop in a sound-assisted fluidized bed unless the empirical exponential factor for the revised Ergun equation and the empirical multiplication factor for the Ergun equation are used. In addition, it was observed that these two empirical factors were not a constant value but varied linearly with the sound frequency. Hence, the purposed correlations and their corresponding empirical closure equations can be concluded as follows:

1. Modified revised Ergun equation for the fixed bed pressure drop in sound-assisted fluidization:

$$\frac{\Delta P}{\Delta x}=\frac{\rho_f(1-\varepsilon)}{d_p}\left(\frac{17.3\mu_f(\sum_i(U_o/\varepsilon)_{i+1}+\sum_i\bar{u}_{ac_{i+1}})}{d_p\rho_f}+\frac{0.336(\sum_i(U_o/\varepsilon)^2_{i+1}+\sum_i\bar{u}^2_{ac_{i+1}})}{\varepsilon}\right)\varepsilon^{-\beta},$$

where

$$\beta=0.0162(f)+1.7092$$

2. Modified Ergun equation for the fixed bed pressure drop in sound-assisted fluidization:

$$\frac{\Delta P}{\Delta x}=\frac{X(\sum_i(U_o/\varepsilon)_{i+1}+\sum_i\bar{u}_{ac_{i+1}})\mu_f}{g_c\phi_S^2 d_P^2}\frac{(1-\varepsilon)^2}{\varepsilon^2}+\frac{1.75\rho_f(\sum_i(U_o/\varepsilon)^2_{i+1}+\sum_i\bar{u}^2_{ac_{i+1}})}{g_c\phi_S d_P}\frac{(1-\varepsilon)}{\varepsilon},$$

where

$$X=1.3974(f)-30.263.$$

Intrinsic bed expansion characteristics of Geldart's group A powder in the sound assisted fluidization of a fixed sound pressure level and a varied sound frequency was also investigated. To obtain an accurate bed expansion data, the 1-valve and 2-valve bed collapse experiment was carried out and the bed collapse model was used to interpret correctly the bed collapse curves. The bed expansion characteristics were found differently from previous reports. And, the following points can be concluded;

1. A total bed voidage and a bed voidage for the sound assisted fluidization were varied with an inlet superficial velocity in the same fashion as those for a conventional fluidization.

2. The voidage with respect to the inlet superficial velocity of the sound assisted fluidization was found to be lower than that of the conventional fluidization.
3. A dense phase voidage and its superficial velocity relations of the sound assisted fluidization at different sound frequency were found to be approximately on the same trend as that for the conventional fluidization.
4. A minimum bubbling point, defined using the dense phase voidage and dense phase superficial velocity characteristic curve, was also unaffected by the sound vibration force.

This suggested that an addition of sound vibrational force tended to create more cavity or bubble phase in the fluidized bed, rather than changing a hydrodynamics relation in the dense phase. Therefore, the same equilibrium of force can still be used to describe both systems of fluidization. Besides, the stability criteria can be applied for both systems. Finally, it was proved that the modified revised Ergun drag force correlation can describe well the dense phase voidage and the dense phase superficial velocity characteristic curves. And, the stability criterion purposed by Cherntongchai and Brandani (2013) can predict excellently the minimum bubbling points.

REFERENCES

Ammendola P., Chirone R., Aeration and mixing behaviours of nano-sized powders under sound vibration, Powder Technology 201(2010) 49-56.

Ammendola P., Chirone R., Raganati F., Fluidization of binary mixtures of nanoparticles under the effect of acoustic fields, Advanced Powder Technology 22 (2011) 174-183.

Brandani S., Zhang K., A new model for the prediction of the behaviour of fluidized beds, Powder Technology, 163(1-2) (2006) 80-87.

Cherntongchai P., Brandani S., A model for the interpretation of the bed collapse experiment, Powder Technology, 151 (2005) 37-48.

Cherntongchai P., Brandani S., Prediction ability of a new minimum bubbling criterion, Advanced Powder Technology, 24 (2013) 1-13.

Cherntongchai P., Innan T., Brandani S., Mathematical description of pressure drop profile for the 1-valve and 2-valve bed collapse experiment, Chemical Engineering Science, 66 (2011) 973-981.

Dallavalle J. M., Micromeritics, Pitman, New York, 1948

Ergun S., Fluid flow through packed columns, Chemical Engineering Progress 48 (2) (1952) 89– 94.

Escudero D., Heindel T. J., Minimum fluidization velocity in a 3D fluidized bed modified with an acoustic field, Chemical Engineering Journal 213 (2013) 68-75.

Foscolo P.U., Gibilaro L.G., Waldram S.P., A unified model for particulate expansion of fluidised beds and flow in fixed porous media, Chemical Engineering Science 38 (8) (1983) 1251–1260.

Guo Q., Li Y., Wang M., Shen W., Yang C., Fluidization characteristics of SiO_2 nanoparticles in an acoustic fluidized bed, Chemical Engineering Technology 26 (1) (2006) 78-86.

Guo Q., Wang M., Li Y., Yang C., Fluidization of ultrafine particles in a bubbling fluidized bed with sound assistance, Chemical Engineering Technology 28 (10) (2005) 1117-1124.

Herrera C.A., Levy E.K., Ochs J., Characteristics of acoustic standing waves in fluidized beds, AIChE Journal 48 (3) (2002) 503–513.

Kaliyaperumal S., Barghi S., Zhu J., Briens L., Rohani S., Effects of acoustic vibration on nano and sub-micron powders fluidization, Powder Technology 210 (2011) 143-149.

Langde M. L., Sonolikar R. L., Dharmaraj J. T., The influence of acoustic field and frequency on hydrodynamics of group B particles, Thermal Science 15(1) (2011) 159-169.

Liu H., Guo Q., Chen S., Sound-assisted fluidization of SiO2 nanoparticles with different surface properties, Industrial & Engineering Chemistry Research 46 (2007) 1345-1349.

Leu L., Li J., Chen C., Fluidization of group B particles in an acoustic field, Powder Technology 94 (1997) 23-28.

Morse R. D., Sonic energy in granular solid fluidization, Industrial & Engineering Chemistry Research 47 (1955) 1170-1175.

Raganati F., Ammendola P., Chirone R., CO_2 adsorption on fine activated carbon in a sound assisted fluidized bed: Effect of sound intensity and frequency, CO_2 partial pressure and fluidization velocity, Applied Energy 113 (2014) 1269-1282.

Richardson J.F., Zaki W.N., The sedimentation of a suspension of uniform spheres under conditions of viscous flow, Chemical Engineering Science 3 (1954) 65-73.

Russo P., Chirone R., MassimillaL., Russo S., The influence of the frequency of acoustic waves on sound-assisted fluidization of beds of fine particles, Powder Technology 82 (1995) 219-230.

Si C., Guo Q., Fluidization characteristics of binary mixtures of biomass and quartz sand in an acoustic fluidized bed, Industrial & Engineering Chemistry Research 47 (2008) 9773-9782.

Si C., Wu J., Wang Y., Zhang Y., Liu G., Effect of acoustic filed on minimum fluidization velocity and drying characteristics of lignite in a fluidized bed, Fuel Processing Technology 135 (2015) 112-118.

Urciuolo M., Salatino P., Cammarota A., Chirone R., Development of a sound-assisted fluidized bed filter/afterburner for particle-laden gas clean-up, Powder Technology 180 (2008) 102–108.

Wang S., Li X., Lu H., Liu G., Wang J., Xu P., Simulation of cohesive particle motion in a sound-assisted fluidized bed, Powder Technology 207 (2011) 65–77.

Xu C., Cheng Y., Zhu J., Fluidization of fine particles in a sound field and identification of group C/A particles using acoustic waves, Powder Technology 161 (2006) 227-234.

Zhu G., Liu Q., Yu Q., Pfeffer R., Dave R.N., Nam C.H., Sound assisted fluidization of nanoparticle agglomerates, Powder Technology 141 (2004) 119-123.Zhu et al., (2004)

OUTPUTS

1. International conference

- Cherntongchai, P., Hydrodynamics of Sound Assisted Fluidization of Rigid-microsized Powder, 2017AIChE Annual Meeting, October 29 - November 3, 2017, Minneapolis, MN, USA.(Oral presentation)

2. International publications

- Cherntongchai P., Chaiwattana S., Leruk R., Panyaruean J., Sriboonnak S., Influence of Standing Wave Characteristics on Hydrodynamics Behaviors in Sound Assisted Fluidization of Geldart's Group A Powder, Chemical Engineering Science. (Submitted).
- Cherntongchai P., Chaiwattana S., Leruk R., Bed expansion characteristics in Sound Assisted Fluidization of Geldart's Group A powder, Chemical Engineering Science. (Submitted).

APPENDIXA: INTERNATIONAL CONFERENCE

AIChE
The Global Home of Chemical Engineers

AMERICAN INSTITUTE OF CHEMICAL ENGINEERS
120 WALL STREET
NEW YORK, NY 10005
TEL 646.495.1300
www.aiche.org

Dear Parimanan Cherntongchai,

The American Institute of Chemical Engineers (AIChE) with more than 50,000 members from over 100 countries is the premiere professional society for chemical engineering. AIChE would like to thank you for attending the 2017 Annual Meeting, held at the Minneapolis Convention Center and Hilton Minneapolis in Minneapolis, Minnesota, USA. The conference formally ran from October 29 – November 3, 2017 with some technical activities taking place before and after the conference.

This letter confirms that Parimanan Cherntongchai attended the 2017 Annual Meeting in Minneapolis, MN on October 29 – November 3, 2017.

The technical program, containing all papers presented, can be found at the following page: https://aiche.confex.com/aiche/2017/meetingapp.cgi

The AIChE Annual Meeting is accomplished by participation of all who attend the conference. The above participations were beneficial and invaluable to the meeting and the dissemination of knowledge. We are pleased that you have joined us. Should you require additional information, please do not hesitate to contact me.

Thank you very much.

Regards,

Stéphanie Orvoine-Couvrette
B.S. Chemical Engineering
Senior Engineering Specialist, Program Development
AIChE Global Home Office
120 Wall Street, New York, NY 10005
programming@aiche.org

Hydrodynamics of Sound Assisted Fluidization of Rigid-microsized Powder

Cherntongchai, P.*

Department of Industrial Chemistry, Faculty of Science, Chiang Mai University, Chiang Mai, Thailand

Abstract

An objective of this work was to investigate hydrodynamic behaviors of sound-assisted fluidization of rigid-microsized powder under different inlet superficial velocity and sound frequency ranging from 0-500 Hz at a fixed sound pressure level of 80 dB. The hydrodynamics behaviors were observed such as a fixed bed pressure drop, a total bed pressure drop, an incipient fluidization velocity and a complete fluidization velocity (a minimum fluidization velocity). It was found that the fixed bed pressure drop increased with sound frequency, in comparison with a normal fluidization. The complete fluidization velocity was significantly decreased with increasing sound frequency and the minimum value was found at sound critical frequency of 80 Hz. Then, the values were increased again and leveled off. This pattern of variation was found to be according to a standing wave sound pressure level characteristic in fluidization medium, when the magnitude of the sound pressure level changed exponentially and periodically with the standing wave properties.

Keywords: Fluidization, Hydrodynamic, Bed collapse, Sound assisted, Rigid-microsized powder

*Corresponding author.
Tel.:0-5394-3401; Fax: 0-5389-2262
E-mail: parimanan@gmail.com

Hydrodynamics of Sound Assisted Fluidization of Rigid-microsized Powder

Cherntongchai, P.*

Department of Industrial Chemistry, Faculty of Science, Chiang Mai University, Chiang Mai, Thailand

Email: Parimanan@gmail.com

Outline:

Introduction: Sound assisted fluidization

modification of conventional fluidization by sound vibrational force

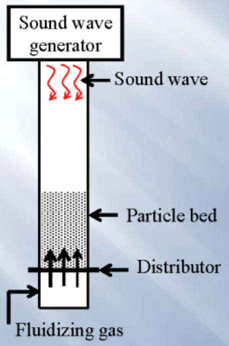

Effects:

- Better fluidization quality
- Smaller agglomerate size
- Particle elutriation reduction
- Hydrodynamics behaviors

Theory:

- Standing wave characteristics
- Force balance principle

Objectives:

- To investigate and explain influence of sound frequency on minimum fluidization velocity of Geldart's group A powder, using standing wave characteristics.

Research novelty:

- Rationale for the influence of sound frequency on fluidization hydrodynamics of Geldart's group A powder, using tanding wave characteristics.

Theory: Standing wave characteristics [1]

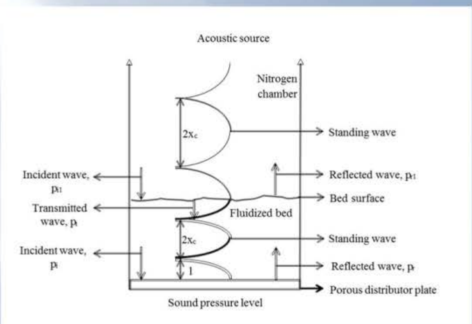

Figure 1 Standing wave pattern in fluidization media

Theory: Standing wave characteristics [1]

- Sound propagation was an adiabatic one-dimensional process and a wave equation in terms of pressure is;

$$\frac{\partial^2 p}{\partial x^2} = \frac{1}{\varepsilon^2}\frac{\partial^2 p}{\partial t^2} \qquad (1)$$

- A solution of Eq. (1) is;

$$p(x,t) = Ae^{-j(\omega t - kx)} \qquad (2)$$

- A Sum of incident and reflected waves within the fluidized bed in form of total pressure.

$$p(x,t) = Ae^{-j(\omega t - kx)} + Be^{-j(\omega t - kx + \theta)} \qquad (3)$$

- Pressure distribution becomes;

$$|p(x,t)| = P_{fs}\sqrt{\frac{\cos^2 kx}{\cos^2 kh}} \qquad (4)$$

Theory: Standing wave characteristics [1]

- At critical state, $|p(x,t)|$ was very large which occurred at;

$$kh = (2n-1)\frac{\pi}{2}, \text{for } n = 1,2... \quad (5)$$

- Value of $|p(x,t)|$ can be interchanged using Eqs. (6) and (7).

$$P_{rms} = \frac{|p(x,t)|}{\sqrt{2}} = \frac{P}{\sqrt{2}} \quad (6)$$

$$SPL = -20\log\left[\frac{Prms}{Pref}\right] \quad (7)$$

Experiments: Experimental setup

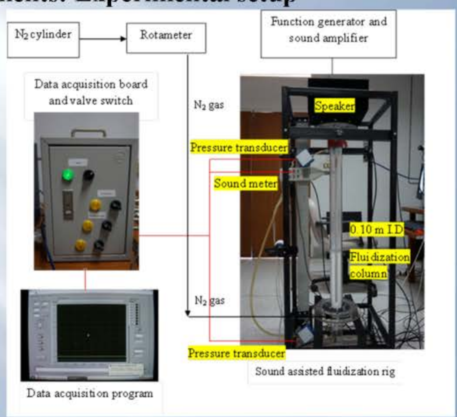

Figure 2 Sound assisted fluidization setup for 0.10 m ID fluidization column

4

Experiments: Materials

Table 1 Particle density and average particle size

Material	Apparent density (kg/m³)	Average particle diameter (mm)
Glass ballotini	2,432	32.61

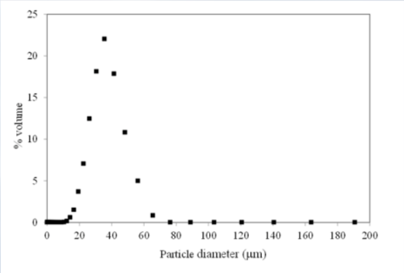

Figure 3 Particle size distribution of glass ballotini

Experiments: Methodology

- Fluidization experiment was performed by increasing inlet superficial gas velocity and measuring bed pressure drop at each gas velocity.
- Defluidization experiment was, on the other hand, by decreasing inlet superficial gas velocity.

Experiments: Experimental conditions

Table 2. Summary of experimental conditions

Experimental conditions	Inlet superficial velocity (mm/s)	Sound pressure level (dB)	Sound frequency (hz)
	0-15	0	0
	0-15	80	50,80,100,300,500

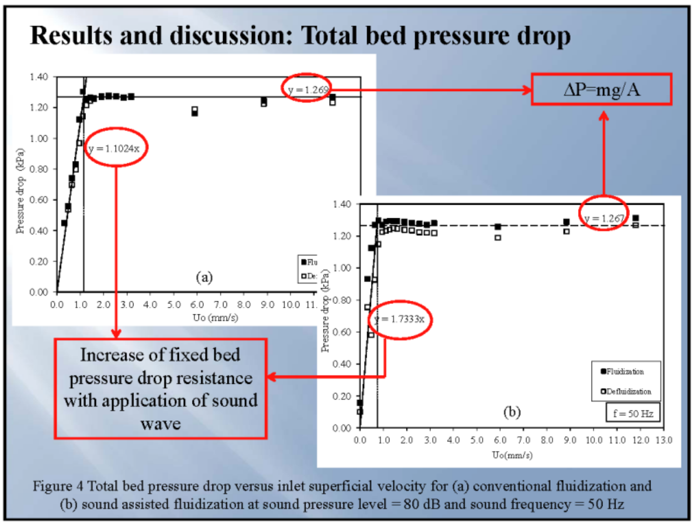

Figure 4 Total bed pressure drop versus inlet superficial velocity for (a) conventional fluidization and (b) sound assisted fluidization at sound pressure level = 80 dB and sound frequency = 50 Hz

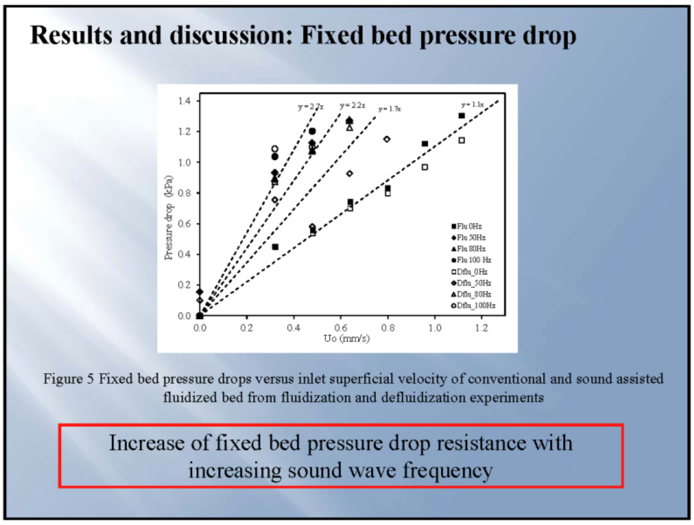

Figure 5 Fixed bed pressure drops versus inlet superficial velocity of conventional and sound assisted fluidized bed from fluidization and defluidization experiments

Results and discussion: Fixed bed pressure drop

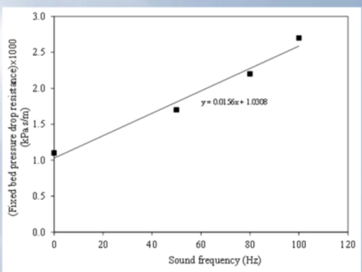

Figure 6 Relation between sound frequency and fixed bed pressure drop resistance

Linear increase of fixed bed pressure drop resistance with sound wave frequency

Results and discussion: Incipient and complete fluidization

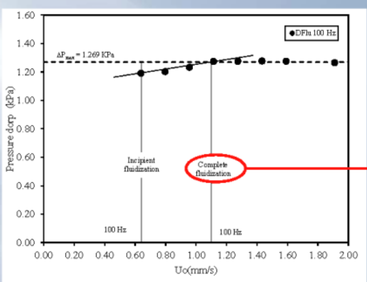

Minimum fluidization velocity

Figure 7 Incipient fluidization point and complete fluidization point

Range from incipient and complete fluidization points for transition from fixed bed to fluidized bed

Results and discussion: Minimum fluidization point

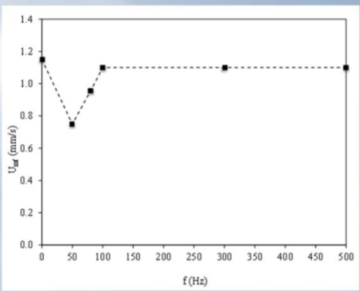

Figure 8 Relation between sound frequency and minimum fluidization velocity

- With application of sound, particle bed fluidized at lower inlet superficial velocity.
- Minimum value of minimum fluidization velocity found at sound frequency of 50 Hz.

Results and discussion: Standing wave characteristics

- x= h or at bed surface, SPL =80 dB.
- With increasing distance down to distributor, SPL increased and maximum SPL was at x=0. .

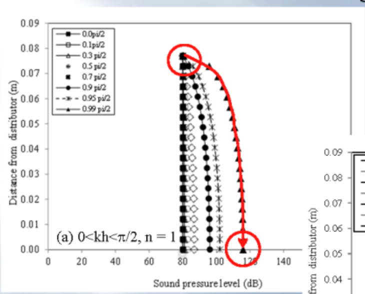

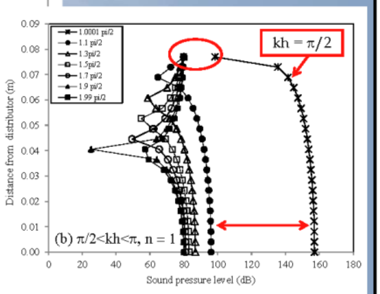

- Rapid increase in SPL when kh approached π/2.
- Maximum SPL found at kh = π/2.

Figure 9 Variation of sound pressure level along bed height (0<x<h) for n = 1

Results and discussion: Standing wave characteristics

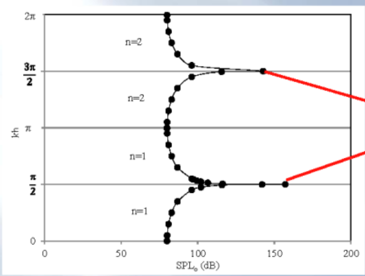

Critical kh value for each harmonic number giving high magnitude of SPL_o

Figure 10 Variation of SPL_o with kh for $0<kh<\pi$, n = 1 and for $\pi<kh<\pi/2$, n = 2

- Exponential increase and decrease of SPL_o with kh for kh of less than critical value and that of higher than critical value, respectively.
- Explanation of local minimum of minimum fluidization velocity at certain sound frequency.
- Possibility of several local minima of minimum fluidization velocity, at critical kh values.

Results and discussion: Minimum fluidization velocity in relation to standing wave characteristic

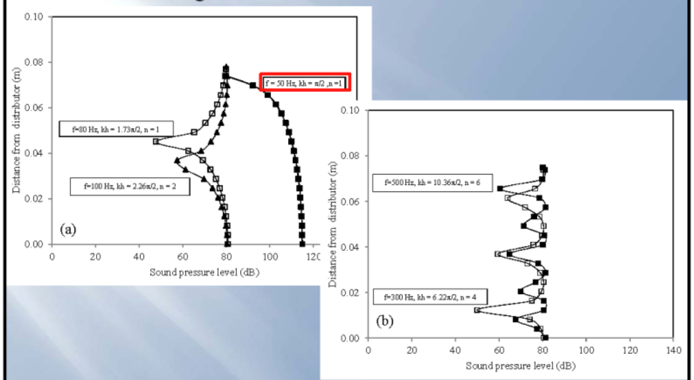

Figure 11 Sound pressure level along distance for fixed bed from distributor at different sound frequency (a) f = 50, 80, and 100 Hz and (b) f =300 and 500 Hz

Results and discussion: Minimum fluidization velocity in relation to standing wave characteristic

Table 3 Summary of standing wave properties and corresponding minimum fluidization velocity

Sound frequency (hz)	kh	Harmonic number (n)	Average SPL (dB)	U_{mf} (mm/s)
50	π/2	1	108.15	0.750
80	1.73p/2	1	74.52	0.956
100	2.26p/2	2	76.02	1.100
300	6.22p/2	4	75.13	1.100
500	10.36p/2	6	76.59	1.100

- At sound frequency of 50 Hz;
  - Highest SPL magnitude along distance x of standing wave, as well as theirs average values, causing minimum fluidization velocity to be lowest.
- At other sound frequency:
  - Approximately the same average value of SPL and, hence, minimum fluidization velocity.

Conclusions:

Standing wave characteristics was implemented to explain hydrodynamics behaviors of a sound-assisted fluidization of a rigid-microsized powder under different inlet superficial velocity and sound frequency ranging from 0-500 Hz at a fixed sound pressure level of 80 dB.

- Due to exponential and periodic variation of vibrational strength of standing wave with sound properties, minimum fluidization velocity was, then, varied in the same manner.

- Local minima of minimum fluidization velocities were, thus, multiple values rather than a single value.

Acknowledgment:

Thailand Research Fund and Chiang Mai University.

Reference:

[1] Herrera C.A. and Levy E.K., Characteristics of acoustic standing waves in fluidization beds. American Institute of Chemical Engineers. 2002; 48: 503-513.

APPENDIX B: MANUSCRIPT #1

Gmail Parimanan cherntongchai <parimanan@gmail.com>

Chemical Engineering Science Submission: Manuscript Number Assigned

1 message

Chemical Engineering Science (ELS) <eesserver@eesmail.elsevier.com> 20 December 2017 at 13:25
Reply-To: "Chemical Engineering Science (ELS)" <chemicales@elsevier.com>
To: parimanan@gmail.com, parimanan.ch@cmu.ac.th
Cc: sattawat@kao.th.com, leruk-ae@hotmail.com, jutarat2440@gmail.com, somsiri_s@elearning.cmu.ac.th

Chemical Engineering Science
Ref: CES-D-17-02557
Title: Influence of Standing Wave Characteristics on Hydrodynamics Behaviors in Sound Assisted Fluidization of Geldart's Group A Powder
Authors: Parimanan Cherntongchai, Ph.D; Sattawat Chaiwattana; Rattanaporn Leruk; Jutarat Panyaruean ; Somsiri Sriboonnak
Article Type: Research paper

Dear Dr. Parimanan Cherntongchai,

Your submission entitled "Influence of Standing Wave Characteristics on Hydrodynamics Behaviors in Sound Assisted Fluidization of Geldart's Group A Powder" has been assigned the following manuscript number: CES-D-17-02557.

You may check on the progress of your paper by logging on to the Elsevier Editorial System as an author. The URL is https://ees.elsevier.com/ces/.

Your username is: parimanan@gmail.com
If you need to retrieve password details, please go to:
http://ees.elsevier.com/ces/automail_query.asp

Thank you for submitting your work to this journal. Please do not hesitate to contact me if you have any queries.

Kind regards,

Chemical Engineering Science
E-mail: chemicales@elsevier.com

****

For further assistance, please visit our customer support site at http://help.elsevier.com/app/answers/list/p/7923 Here you can search for solutions on a range of topics, find answers to frequently asked questions and learn more about EES via interactive tutorials. You will also find our 24/7 support contact details should you need any further assistance from one of our customer support representatives.

Elsevier Editorial System(tm) for Chemical Engineering Science
Manuscript Draft

Manuscript Number:

Title: Influence of Standing Wave Characteristics on Hydrodynamics Behaviors in Sound Assisted Fluidization of Geldart's Group A Powder

Article Type: Research paper

Section/Category: Particle Technology

Keywords: Sound; Fluidization; Hydrodynamics; Standing wave; Sound frequency; Pressure drop

Corresponding Author: Dr. Parimanan Cherntongchai, Ph.D

Corresponding Author's Institution: Chiang Mai University

First Author: Parimanan Cherntongchai, Ph.D

Order of Authors: Parimanan Cherntongchai, Ph.D; Sattawat Chaiwattana; Rattanaporn Leruk; Jutarat Tanyaruean ; Sornsiri Sriboonnak

Abstract: An objective of this work was to investigate hydrodynamics behaviors of a sound-assisted fluidization of Geldart's group A powder under effects of standing wave characteristics in which the wave properties were embedded. The sound wave properties used in this work were a sound frequency ranging from 0-500 Hz at a fixed sound pressure level of 80 dB and the hydrodynamics behaviors observed were a total bed pressure drop, a fixed bed pressure drop, an incipient fluidization velocity and a complete fluidization velocity (a minimum fluidization velocity). It was found that, for full fluidization, the total bed pressure drop was always equaled to weight of a bed per cross section area but the fixed bed pressure drop increased with sound frequency, in comparison with a conventional fluidization. This was proved that the sound wave also associated its force on the particle bed. In addition, with increasing sound wave frequency, the minimum fluidization velocity was decreased and reached the local minimum value at sound critical frequency of 50 Hz. After this point, the further increase in the sound frequency caused the minimum fluidization velocity to be increased again and, then, leveled off. This pattern of variation was found to be consistent with the standing wave characteristics in fluidization medium, where an average magnitude of the sound pressure level varied exponentially around the critical frequency and periodically for each harmonic number. It was also pointed out that the local minimum of the minimum fluidization velocity can be multiple values according to this periodic variation pattern of the standing wave in the fluidized bed with the sound wave properties. Finally, by taken into account the gas oscillation velocity caused by a particular pattern of the standing wave travelling inside the fluidized bed, the fixed bed pressure drop correlations based on revised Ergun equation and Ergun equation, including their empirical closure equations, were proposed.

Suggested Reviewers: Stefano Brandani

Professor, School of Engineering, Institute for Materials and Processes, University of Edinburgh
s.brandani@ed.ac.uk

Kai Zhang
Professor, Center of Chem Eng for Clean Energy, North China Electric Power University
kzhang@ncepu.edu.cn

Paola Lettieri
Professor, Department of Chemical Engineering, University College London
p.lettieri@ucl.ac.uk

Quingjie Guo
Professor, Processing, College of Chemistry and Chemical Engineering, University of Petroleum
qjguo@mail.hdpu.edu.cn

Eldin Lim
Senior lecturer, Department of Chemical and Biomolecular Engineering, National University of Singapore
chelwce@nus.edu.sg

Jingxu Zhu
Department of Chemical and Biochemical Engineering, Faculty of Engineering, University of Western Ontario
jzhu@uwo.ca

Opposed Reviewers:

Parimanan Cherntongchai

Department of Industrial Chemistry
Faculty of Science, Chiang Mai University
Chiang Mai, Thailand, 50200
parimanan@gmail.com

18 December 2017

Re: Consideration of a research article publication

Dear Editors,

I am Dr. Parimanan Cherntongchai from Department of Industrial Chemistry, Faculty of Science, Chiang Mai University. I would like to summit a research article in a topic of "**Influence of Standing Wave Characteristics on Hydrodynamics Behaviors in Sound Assisted Fluidization of Geldart's Group A Powder**" to be considered for a publication in "**Chemical Engineering Science**". I, thereby, have enclosed a manuscript for a revision process together with a list of suggested referees, graphical abstract and highlights.

Sound-assisted fluidization has been successfully used to improve the quality of fluidization, induce smaller agglomerate size and reduce particle elutriation. By the same time, the sound vibrational force caused a change in fluidization hydrodynamics. And, the hydrodynamics of sound-assisted fluidization are implicitly related to the characteristics of a standing wave traveling through the fluidizing bed. However, the knowledge of the standing wave characteristics has never been used to explain the fluidization hydrodynamics observed. In this work, the aim was, therefore, to apply the knowledge regarding the standing wave characteristics to explain the influence of sound frequency on the minimum fluidization velocity of sound-assisted fluidization of Geldart's group A powder. Finally, fixed bed pressure drop correlations for sound-assisted fluidization were also developed, in which gas oscillation velocity, which varies according to the characteristics of the standing wave, was taken into account.

I would like to thank in advance for your consideration and hope to have an opportunity to be able to publish in "**Chemical Engineering Science**".

Sincerely yours,
Parimanan Cherntongchai

Graphical Abstract

Graphical abstract

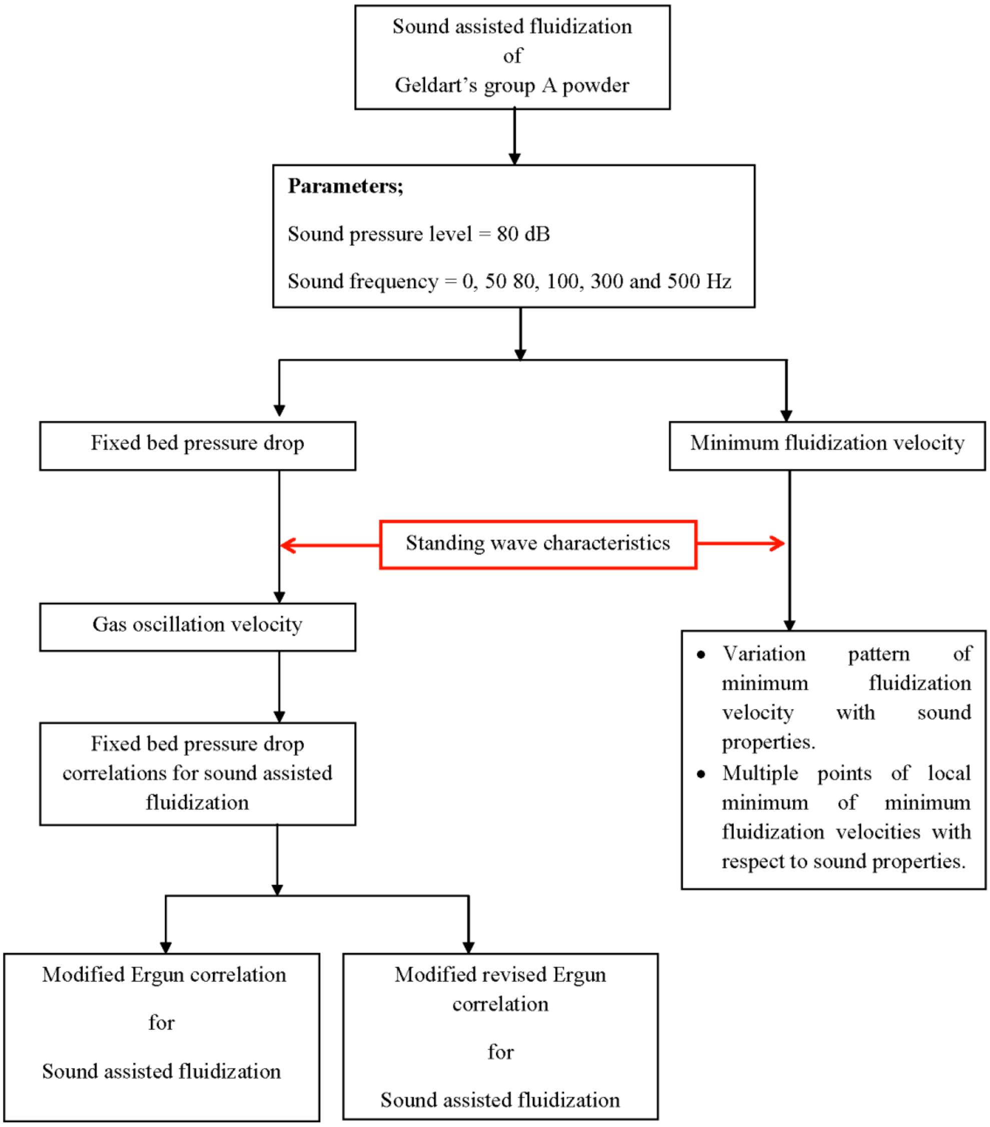

Highlights

- Knowledge of standing wave characteristics explains quantitatively well a variation pattern of minimum fluidization velocity with sound properties.
- Due to an exponential and a periodic variation of vibration strength of a standing wave with the sound properties, the minimum fluidization velocity was varied in the same manner and the local minima of the minimum fluidization velocities were, thus, multiple values rather than a single value.
- By taken into account gas oscillation velocity, calculated using a standing wave theory, fixed bed pressure drop correlations for the sound-assisted fluidization, based on revised Ergun equation and Ergun equation, were purposed, together with their corresponding empirical closure equations.

*Manuscript
Click here to view linked References

Influence of Standing Wave Characteristics on Hydrodynamics Behaviors in Sound Assisted Fluidization of Geldart's Group A Powder

Parimanan Cherntongchai*, Sattawat Chaiwattana, Rattanaporn Leruk, Jutarat Panyaruean

and

Sornsiri Sriboonnak

Department of Industrial Chemistry, Faculty of Science, Chiang Mai University,

Chiang Mai, Thailand, 50200

*Corresponding author (parimanan@gmail.com)

ABSTRACT

An objective of this work was to investigate hydrodynamics behaviors of a sound-assisted fluidization of Geldart's group A powder under effects of standing wave characteristics in which the wave properties were embedded. The sound wave properties used in this work were a sound frequency ranging from 0-500 Hz at a fixed sound pressure level of 80 dB and the hydrodynamics behaviors observed were a total bed pressure drop, a fixed bed pressure drop, an incipient fluidization velocity and a complete fluidization velocity (a minimum fluidization velocity). It was found that, for full fluidization, the total bed pressure drop was always equaled to weight of a bed per cross section area but the fixed bed pressure drop increased with sound frequency, in comparison with a conventional fluidization. This was proved that the sound wave also associated its force on the particle bed. In addition, with increasing sound wave frequency, the minimum fluidization velocity was decreased and reached the local minimum value at sound critical frequency of 50 Hz. After this point, the further increase in the sound frequency caused the minimum fluidization velocity to be increased again and, then, leveled off. This pattern of variation was found to be consistent with the standing wave characteristics in fluidization medium, where an average magnitude

of the sound pressure level varied exponentially around the critical frequency and periodically for each harmonic number. It was also pointed out that the local minimum of the minimum fluidization velocity can be multiple values according to this periodic variation pattern of the standing wave in the fluidized bed with the sound wave properties. Finally, by taken into account the gas oscillation velocity caused by a particular pattern of the standing wave travelling inside the fluidized bed, the fixed bed pressure drop correlations based on revised Ergun equation and Ergun equation, including their empirical closure equations, were proposed.

KEYWORDS: Sound, Fluidization, Hydrodynamics, Standing wave, Sound frequency, Pressure drop

1. INTRODUCTION

Sound-assisted fluidization is a modification of conventional fluidization by implementing sound vibrational force. And, the additional equipment is a sound wave generator, connected to a sound amplifier and a loudspeaker. Sound waves from the loudspeaker can be directed to a fluidized bed from either the top or the bottom of a column. Then, the sound wave which is a pressure wave will propagate through a bed of particles and break up the inter-particle forces, resulting in better fluidization quality, smaller agglomerate size, particle elutriation reduction, and change in the fluidization hydrodynamics.

Sound-assisted fluidization has been successfully used to improve the quality of fluidization since 1955 by Morse for the fluidization of Geldart's group C/A powders, as well as in the works of Kaliyaperumal et al. (2011), Langde et al. (2011), Russo et al. (1995), and Xu et al. (2006). Zhu et al. (2004) was the first to report better fluidization quality in sound-assisted fluidized bed of nanoparticles, followed by Guo et al. (2005), Guo et al. (2006), and Liu et al. (2007). The sound-assisted fluidization of Geldart's group B powder was also investigated by Escudero and Heindel (2013) and Leu et al. (1997) and it was concluded that the sound wave field helped to improve the ease of fluidization.

Numerous hydrodynamic investigations of sound-assisted fluidization have been reported. Upon focusing on the fixed bed region and the transition from the fixed to the fluidized bed under the effect of sound waves, there appeared a range from the incipient fluidization stage to the complete fluidization stage, as reported by Xu et al. (2006). And, the minimum fluidization point has been generally defined to be at the point of complete fluidization (Escudero and Heindel, (2013); Guo et al., (2006); Si et al., 2015), apart from the work of Xu et al. (2006), who defined the minimum fluidization velocity to be at the intersecting point of the defluidization curve with the constant pressure line, and the work of Kaliyaperumal et al. (2011), who proposed a novel curve-fitting iteration method to define the minimum fluidization point. In any case, it has been observed that in the presence of sound, there is significant reduction in the minimum fluidization velocity (Kaliyaperumal et al., 2011; Leu et al., 1997; Si et al., 2015; Zhu et al., 2004).

Variation in minimum fluidization under the influence of the properties of sound waves can be summarized as follows: All previous works have reported that an increase in the sound frequency causes the minimum fluidization point to decrease to the local minima and, then, increase with increase in the sound frequency (Escudero and Heindel, 2013; Guo et al., 2005; Guo et al., 2006; Kaliyaperumal et al., 2011; Liu et al., 2007; Russo et al., 1995; Si et al., 2015; Xu et al., 2006; Zhu et al., 2004;). And, the common explanation involves the resonance behavior between the natural frequency of the fixed bed and the sound frequency.

Under the effect of the sound pressure level, it has been reported, as the sound pressure level increases, the minimum fluidization decreases (Escudero and Heindel, 2013; Guo et al., 2005; Kaliyaperumal et al., 2011; Russo et al., 1995; Si et al., 2015; Xu et al., 2006) because the vibrational forces help to loosen the bed and reduce the energy required for particle fluidization.

Russo et al. (1995) studied the effect of particle loading on sound-assisted fluidization of Geldart's group C powder and reported that with increase in particle loading, the minimum fluidization velocity was observed to increase. They explained that the more the particle loading, the more the sound attenuation and the more the decrease in the sound pressure level, resulting in an increase in the minimum fluidization velocity.

It is well-known that the fixed bed pressure drop undergoes variation in accordance with the sound wave properties. For example, Xu et al. (2006) reported that the fixed bed pressure drop increased significantly with sound frequency for Geldart's group A powders. In order to describe the variation of the fixed bed pressure drop with respect to sound frequency, the force-balance principle as well as the drag force correlation and the acoustic force correlation should be taken into consideration. To the best of the researchers' knowledge, there is no previous report that has purposed an appropriate correlation for the prediction of the fixed bed pressure drop in sound-assisted fluidization. Instead, there have been a number of previous works using the principle of force-balance and the related force correlations for describing sound-assisted fluidization. For example, Russo et al. (1995) developed the cluster/subcluster oscillator model to predict the agglomeration size of Geldart's group C powder in sound-assisted fluidization and implemented Stokes' law to identify the drag force due to gas flow in an acoustic field. Likewise, Si and Guo (2008) and Urciuolo et al. (2008)

also used Stokes' law for drag force under fluid velocity and gas oscillation velocity in force-balance analysis. Wang et al. (2011) used the Ergun equation for drag force correlation and applied the gas oscillation velocity in the same equation for the acoustic force in order to establish the equation of motion for cohesive powder.

The characteristics of sound-assisted fluidization are implicitly related to the characteristics of a standing wave traveling through the fluidizing bed, which has been thoroughly described by Herrera et al. (2002). However, the knowledge has never been used to explain the fluidization characteristics observed. In this work, the aim was to apply the knowledge regarding the standing wave characteristics to explain the influence of sound frequency on the minimum fluidization velocity of sound-assisted fluidization of Geldart's group A powder. Finally, fixed bed pressure drop correlations for sound-assisted fluidization were also developed, in which gas oscillation velocity, which varies according to the characteristics of the standing wave, was taken into account.

2. THOERY: Characteristics of standing wave characteristics in sound-assisted fluidized bed

The concept of pressure wave propagation in fluidization was used to describe sound wave propagation in the fluidization medium. Considering Herrera et al. (2002), they assumed that sound propagation was an adiabatic one-dimensional process; the wave equation in terms of pressure is written as follows:

$$\frac{\partial^2 p}{\partial x^2} = \frac{1}{\varepsilon^2}\frac{\partial^2 p}{\partial t^2} \qquad (1)$$

A known solution to the above equation is as follows:

$$p(x,t) = Ae^{-j(\omega t - kx)} \qquad (2)$$

Transmission of a sound wave in the sound-assisted fluidization system consists of traveling of the sound wave in two media, confined in a vertical column (Fig. 1). One is the top end, where the sound wave is supplied, which was the nitrogen media (in this study), and the other is the bottom end which is the heavier fluidization media supported by a rigid porous distributor. As the sound wave travels through the nitrogen, the incident pressure wave (p_{i1}) reaches the interface between the nitrogen and the fluidized bed. A fraction of the incident wave is reflected (p_{r1}) and the rest (p_t) travels downward through the bed and reaches the distributor. Once the incident wave in the fluidized bed (p_{i2}) reaches the rigid distributor, the reflected wave (P_{r2}) travels backward. The incident wave and the reflected wave then combine to form a steady wave called the "standing wave." The sum of the incident and the reflected waves within the fluidized bed in the form of the total pressure is illustrated in Eq. (3):

$$p(x,t) = Ae^{-j(\omega t - kx)} + Be^{-j(\omega t - kx + \theta)} \tag{3}$$

The amplitude $|p(x,t)|$ can be written as follows:

$$|p(x,t)| = \sqrt{(A+B)^2 \cos^2\left(-kx + \frac{\theta}{2}\right) + (A-B)^2 \sin^2\left(-kx + \frac{\theta}{2}\right)} \tag{4}$$

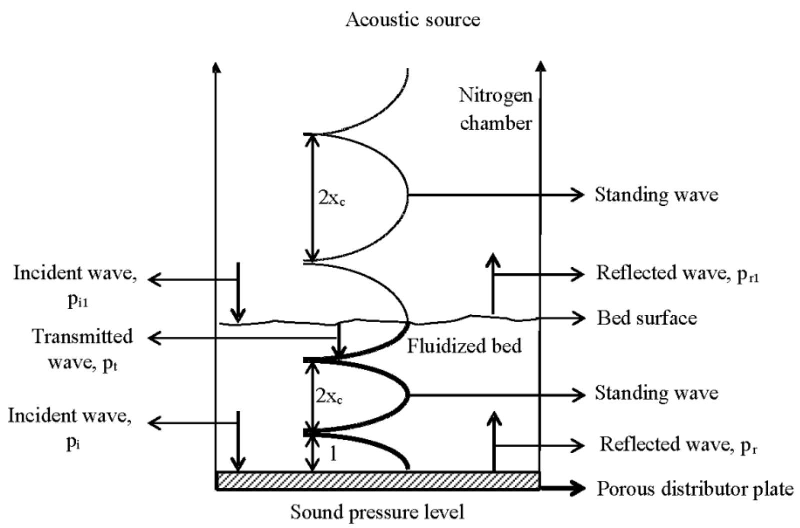

Fig. 1. The standing wave pattern in the fluidization media.

When the reflecting boundary is solid, the incident and the reflected amplitude are equal; therefore, A=B. In addition, assuming that the incident and the reflected waves were in phase (θ=0), the resulting standing wave amplitude becomes

$$|p(x,t)| = 2A\sqrt{\cos^2 kx} \tag{5}$$

At x=h, the pressure was

$$p(h,t) = P_{fs}\cos\omega t \tag{6}$$

P_{fs} is related to the sound pressure level as

$$SPL = -20\log\left[\frac{p_{rms}}{p_{ref}}\right] \tag{7}$$

$$P_{rms} = \frac{|p(x,t)|}{\sqrt{2}} = \frac{P}{\sqrt{2}} \quad (8)$$

Thus, the pressure distribution becomes

$$p(x,t) = P_{fs}\sqrt{\frac{\cos^2 kx}{\cos^2 kh}}\cos\omega t \quad (9)$$

And,

$$|p(x,t)| = P_{fs}\sqrt{\frac{\cos^2 kx}{\cos^2 kh}} \quad (10)$$

$|p(x,t)|$ is very large when cos(kh) = 0, which occurs at

$$kh = (2n-1)\frac{\pi}{2}, \text{for } n = 1,2... \quad (11)$$

This point is called the "critical state," and the critical frequency can be calculated as follows:

$$f_c = \frac{(2n-1)}{4}\frac{C_o}{h}, \text{for } n = 1,2... \quad (12)$$

$$C_o = \sqrt{\frac{\left[\frac{\varepsilon}{K_g} + \frac{(1-\varepsilon)}{K_p}\right]^{-1}}{\varepsilon\rho_g + (1-\varepsilon)\rho_p}} \quad (13)$$

The value of $|p(x,t)|$ can be interchanged using Eqs. (7), (8), and (10), and this would also enable the gas oscillation velocity ($u_{ac}(x,t)$) along the bed height to be calculated thus:

$$u_{ac}(x,t) = U\sin(2\pi ft) = U\sin(kx) \quad (14)$$

And,

$$SPL = 20\log\left[\frac{U}{\sqrt{2}U_{ref}}\right] \quad (15)$$

Finally, the point is reached at which it is possible to explain the characteristics of fluidization under the influence of sound wave properties using the value of $|p(x,t)|$ or $u_{ac}(x,t)$ of the standing wave.

3. MATERIAL AND METHODS

3.1 Experimental setup

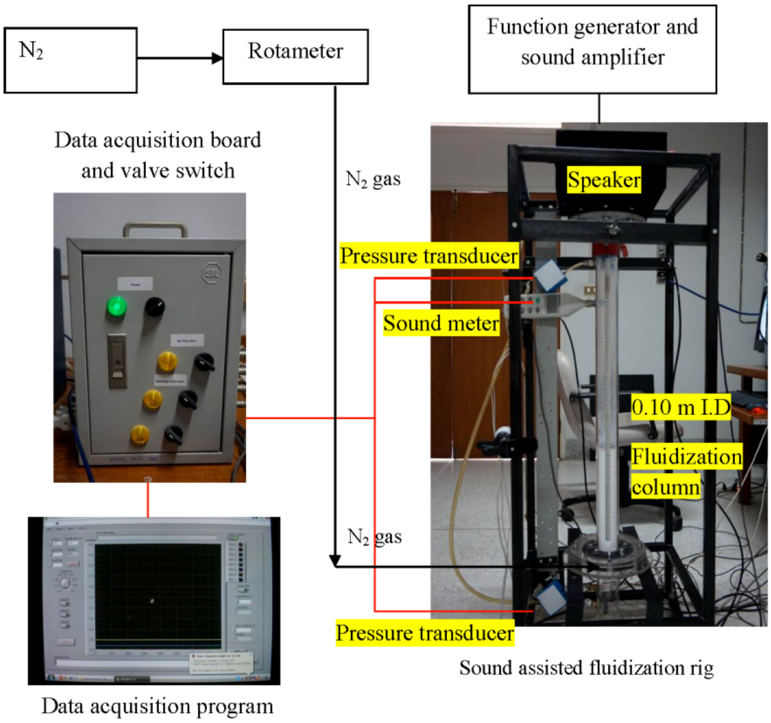

Fig. 2. The sound-assisted fluidization setup for the 0.10 m ID fluidization column.

The sound-assisted fluidization setup (Fig. 2) consisted of 99.99% pure nitrogen gas connected to a rotameter. After metering the gas flow rate, the nitrogen gas line was connected to a 0.10 m ID fluidization column. The column was equipped with a gas distributor, pressure transducers, a sound level meter, and a speaker on top of the column. The pressure transducers and the sound meter were connected to a data acquisition board and, then, to a data acquisition program. The flow range for this setup was 0–30 L/min. The sound pressure level was fixed at 80 dB and the sound frequency was in the range of 0–500 Hz. The data acquisition rate was 100 data points per second. Finally, the measuring range of the pressure transducer was 0–5 psi.

3.2 Material

The powder used was glass ballotini. In this work, the particle density was measured using pycnometer and the laser light scattering method was used for the measurement of the particle size and the particle size distribution. The particle properties are presented in Table 1 and the particle size distribution is illustrated in Fig. 3. The particle loading was 0.8509 kg.

Table 1 Particle Density and Average Particle Size

Material	Apparent density (kg/m^3)	Average particle diameter (μm)
Glass ballotini	2,432	32.61

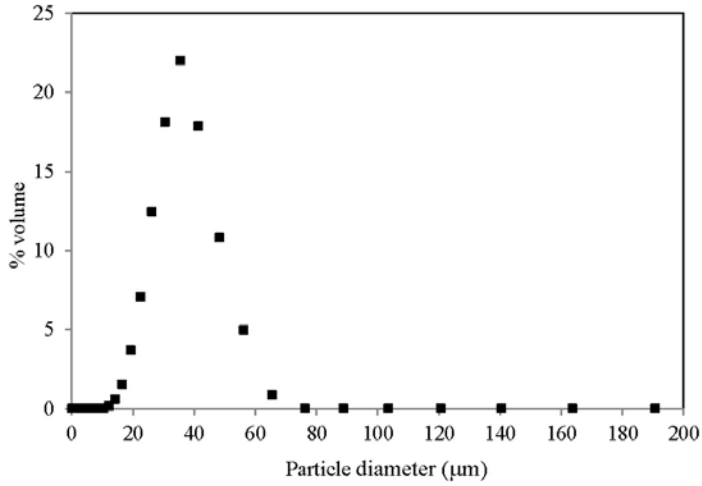

Fig. 3. The particle size distribution of glass ballotini.

3.3 Experimental method

The fluidization experiment was performed by increasing the inlet superficial gas velocity and measuring the bed pressure drop at each gas velocity. On the other hand, the defluidization experiment was carried out by decreasing the inlet superficial gas velocity and, likewise, measuring the bed pressure drop at each velocity. Table 2 presents the summary of the experimental conditions used in this work.

Table 2 Summary of Experimental Conditions

Experimental conditions	Inlet superficial velocity (mm/s)	Sound pressure level (dB)	Sound frequency (Hz)
	0–15	0	0
	0–15	80	50,80,100,300,500

4. RESULTS AND DISCUSSION

4.1 Total bed pressure drop in sound-assisted fluidization

4.1.1 Total bed pressure drop in sound assisted fluidization

Figure 4 presents the total bed pressure drop of both conventional fluidization (Fig. 4(a)) and sound-assisted fluidization at a sound pressure level of 80 dB and a sound frequency of 50 Hz (Fig. 4(b)). It was found that if the particle bed is fully fluidized, the total bed pressure drop can reach the maximum point in both the cases where the total bed pressure drop values were equal to the weight of the bed per cross section area. In addition, it needs to be pointed out that with the application of sound, the flow resistance in the fixed bed was observed to have increased.

4.1.2 Fixed bed pressure drop

Fig. 5 presents the fixed bed pressure drop of the sound-assisted fluidized bed in comparison with the fixed bed pressure drop of the conventional fluidized bed from the fluidization and the defluidization experiments. It can be seen that the increase in the sound frequency resulted in an increase in the fixed bed pressure drop, also reported by Xu et al. (2006). Besides, there was linear relation between the sound frequency and the fixed bed pressure drop resistance, as illustrated in Fig. 6. This can be explained by the fact that gas oscillation velocity due to propagation of sound waves causes higher pressure drop in the fixed bed.

4.2 Transition from fixed bed to fluidized bed

4.2.1 Incipient and complete fluidization

The transition point from the fixed bed to the fluidized bed for the sound-assisted fluidized bed can be observed as a range from the incipient and the complete fluidization points (Fig. 7), also reported by Xu et al. (2006). The incipient fluidization point was defined at the inlet superficial velocity where the fixed bed pressure drop implicitly deviated from the linear trend of the fixed bed pressure drop but was still less than the desired maximum value. As for the complete fluidization point, the value was defined at the first inlet superficial velocity where the total bed pressure reached the maximum value. And, the complete fluidization point is also specified as the minimum fluidization point.

4.2.2 Minimum fluidization point

It is obvious from Fig. 8 that with the application of sound, the particle bed can be fluidized at the lower inlet superficial velocity. The minimum value was found at the sound frequency of 50 Hz. After this, the minimum fluidization velocity increased again and was independent of sound frequency from sound frequency values of 100 Hz to 500 Hz. And, the common explanation for the minimum value found was the resonance behavior between the bed natural frequency and the sound frequency. However, this explanation can be misleading in that the possibility for the minimum value of the minimum fluidization can exist at only one value of the sound frequency. Based on a different point of view, the theory of the standing wave characteristics could claim a better explanation for the observed behavior. Hence, this will be expanded in the following section.

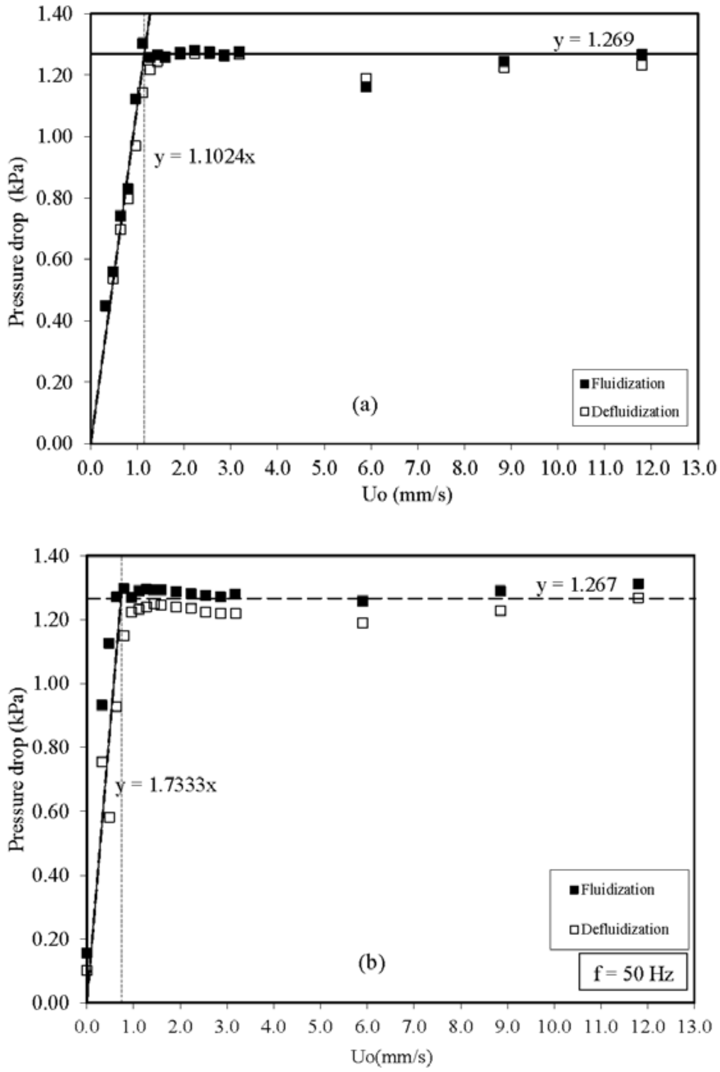

Fig. 4. Total bed pressure drop versus inlet superficial velocity for (a) conventional fluidization and (b) sound-assisted fluidization at sound pressure level = 80 dB and sound frequency = 50 Hz.

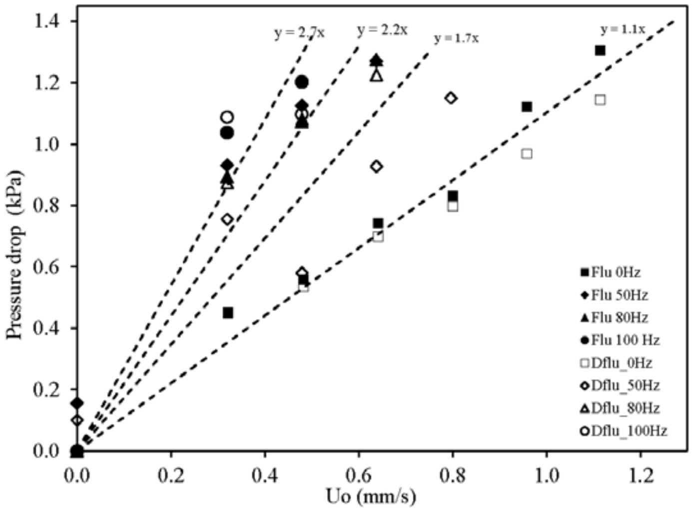

Fig. 5. Fixed bed pressure drop versus inlet superficial velocity of conventional and sound-assisted fluidized beds from the fluidization and the defluidization experiments.

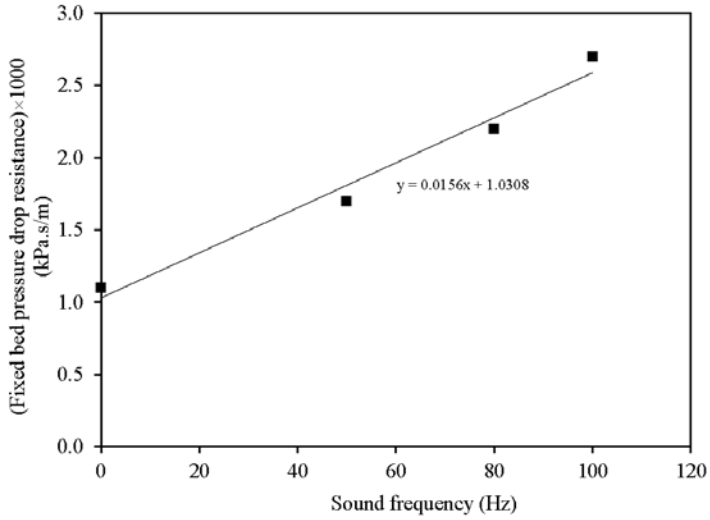

Fig. 6. Relation between sound frequency and fixed bed pressure drop resistance.

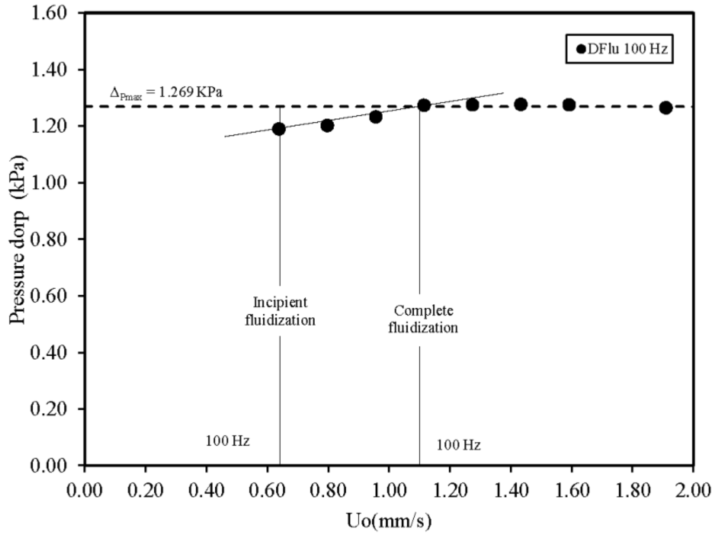

Fig. 7. Incipient and complete fluidization points of sound-assisted fluidization at sound pressure level = 80 dB and sound frequency = 100 Hz for the defluidization experiment.

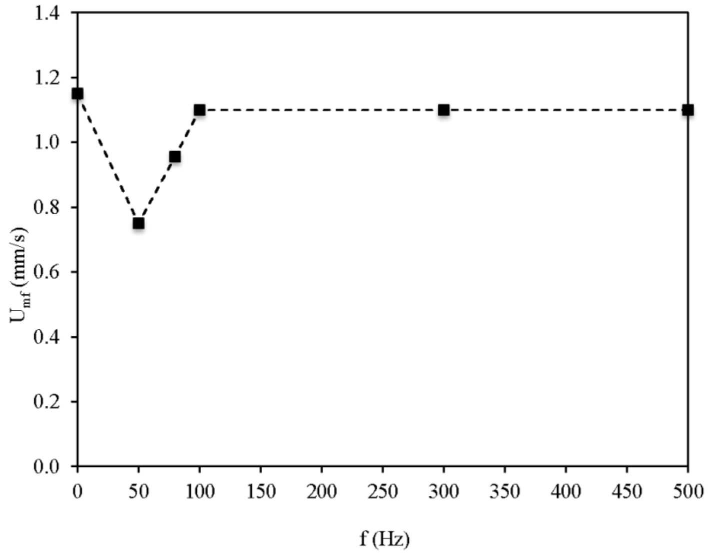

Fig. 8. Minimum fluidization point versus sound frequency for sound-assisted fluidization.

4.3 Standing wave characteristics in sound-assisted fluidization

The standing wave characteristics implicitly influence the fluidization characteristics. In this part, the change in the standing wave characteristics in the fixed bed with the sound wave properties was declared, where the standing wave pattern in the fluidized bed in the form of SPL versus distance from the distributor (x) can be calculated using Eqs. (7), (8), and (10).

A variation in the wave number (kh), according to Eq. (10), for the fixed bed, where h and bed voidage are constant, represents a variation in the sound wave frequency. Furthermore, the standing wave patterns with variation of kh from 0 to $\pi/2$ and kh from $\pi/2$ to π for the harmonic number (n) = 1 are shown in Fig. 9(a) and Fig. 9(b), respectively. It can be seen from Fig. 9(a) that at x= h, or at the bed surface, the SPL was always at 80 dB. With increase in the distance down to the distributor, the SPL increased, and the maximum SPL was at x=0. From Fig. 9(a), it is evident that there is no trough for kh from 0 to $\pi/2$. In addition, it has been illustrated that SPL increases with kh. Besides, when kh approached $\pi/2$, there appeared to be a rapid increase in the SPL, and the maximum SPL was found at kh = $0.99\pi/2$. In contrast, for kh from $\pi/2$ to π (Fig. 9(b)), there appeared to be one trough for kh > $\pi/2$, but there was no trough at kh = $\pi/2$. With increasing kh, the trough tends to move toward the distributor. In addition, at kh = $\pi/2$, the SPL is substantially high in comparison with the SPL for other kh values. This kh value was found to correspond to the critical kh calculated from Eq. (11). From Fig. 9(b), it is clear that for kh higher than the critical value, the SPL decreased implicitly and was distributed approximately over the same average value, even though the decrease with increasing kh can still be observed.

Fig. 10 presents the variation in SPL_o with kh: the figure illustrates that there was a critical kh value for each harmonic number that gave a high magnitude of SPL_o. For n = 1 $(0<kh<\pi)$, the critical kh is at $\pi/2$ and for n = 2 (π<kh<2π), the critical kh is at $3\pi/2$, according to Eq. (11). In addition, for each harmonic number, SPL_o is observed to increase and decrease exponentially with kh for kh of less than the critical value and that of higher than the critical value, respectively. This explains the local minimum point of the minimum fluidization velocity at certain sound frequencies but approximately the same superficial velocity at other values of the sound frequency.

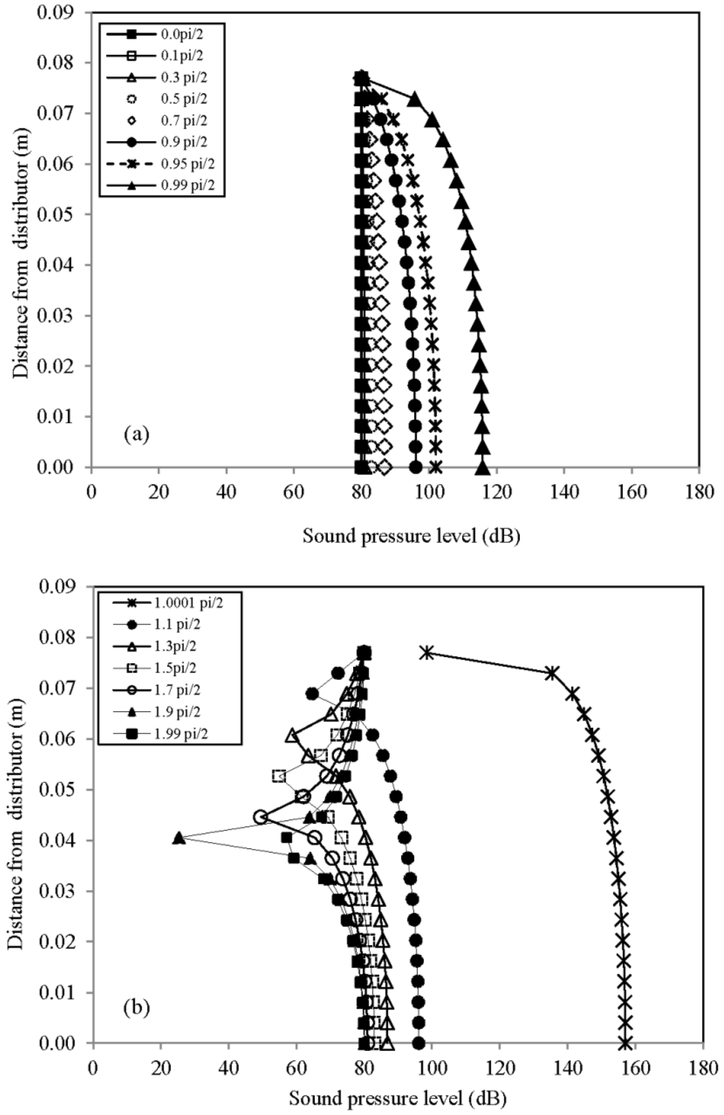

Fig. 9. Variation in the sound pressure level along the bed height (0<x<h): (a) 0<kh<π/2 and (b) π/2<kh<π for n = 1.

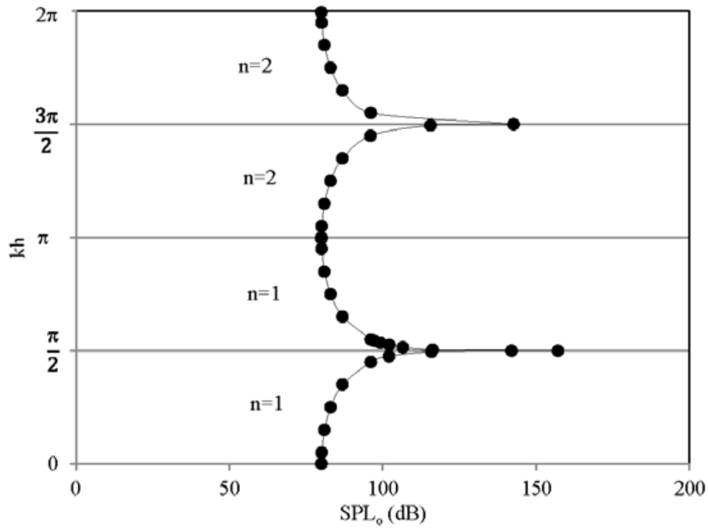

Fig. 10. Variation in SPL_o with kh for $0<kh<\pi$, n = 1 and for $\pi<kh<\pi/2$, n = 2.

4.4 Quantitative relation between minimum fluidization velocity and standing wave characteristics

The magnitude of the SPL along the distance x and the standing wave pattern imparted an effect on the gas oscillation strength and, certainly, the hydrodynamic properties. It can be seen from Fig. 8 that the minimum fluidization velocity decreased with the application of the sound wave and that the local minima was found at the sound frequency of 50 Hz. After this, the minimum fluidization velocity increased again and leveled off at sound frequencies higher than 100 Hz. The standing wave patterns obtained in this study at different sound frequencies are presented in Fig. 11. It can be seen that with the change in the sound frequency, the standing wave pattern and the SPL magnitude had changed in accordance with the explanation, as described above. At the sound frequency of 50 Hz, the SPL magnitude along the distance x of the standing wave was the highest in comparison with those of all the other sound frequencies as well as their average values (Table 3). This caused the minimum fluidization velocity to be the lowest at this particular sound frequency (Table 3). As for other sound frequency values, even though the standing wave patterns were different, the average value of the SPL, as demonstrated in Table 3, was found to be approximately the same and, hence, the minimum fluidization velocity.

The important conclusion from the use of the standing wave characteristics to explain the variation in the minimum fluidization velocity with the sound properties is that the point of local minima of the minimum fluidization velocity can be several points, that is, wherever the kh values hit the critical points, as calculated by Eq. (11). And, this is more pronounced than the explanation using the resonance behavior between the standing wave frequency and the bed natural frequency, where there existed only a single resonance point and only one value of the local minima of the minimum fluidization velocity was possible.

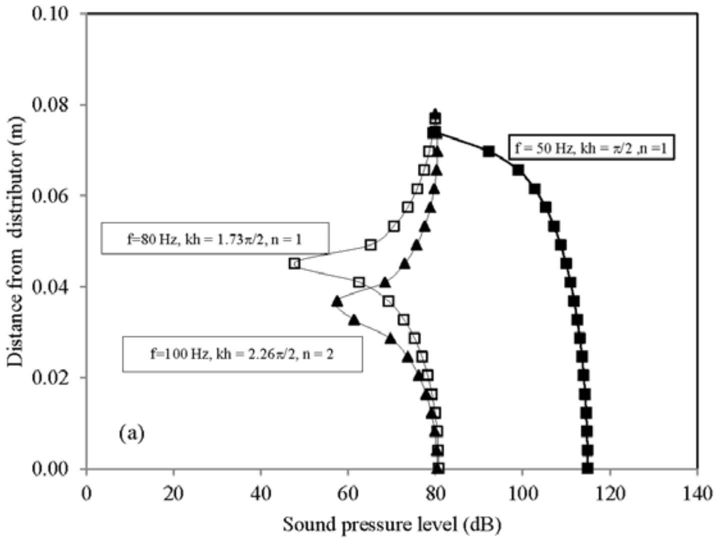

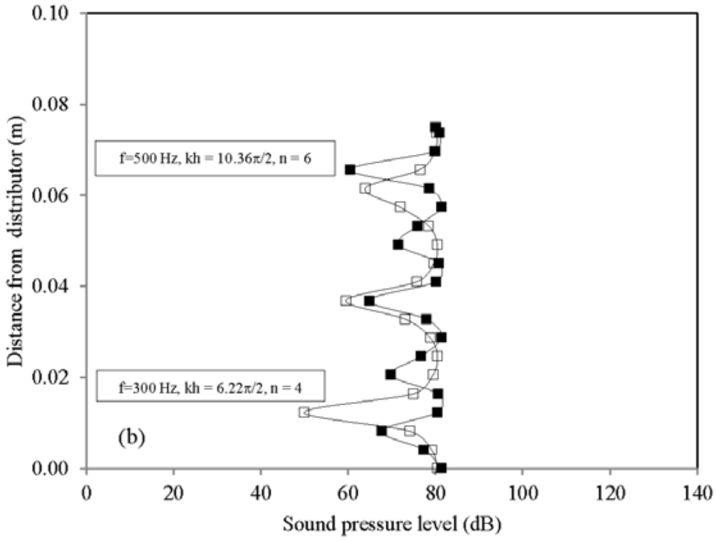

Fig. 11. Sound Pressure Level along Distance for Fixed Bed from Distributor at Different Sound Frequencies: (a) f = 50 Hz, 80 Hz, and 100 Hz; and (b) f = 300 Hz and 500 Hz.

Table 3 Summary of Standing Wave Properties and Corresponding Minimum Fluidization Velocities

Sound frequency (Hz)	kh	Harmonic number (n)	Average SPL (dB)	U_{mf} (mm/s)
50	$\pi/2$	1	108.15	0.750
80	$1.73\pi/2$	1	74.52	0.956
100	$2.26\pi/2$	2	76.02	1.100
300	$6.22\pi/2$	4	75.13	1.100
500	$10.36\pi/2$	6	76.59	1.100

4.5 Fixed bed pressure drop correlation for sound-assisted fluidization

The analysis was based on the force-balance principle, and Fig. 12 shows the schematic diagram of the forces asserted on the particle under the fluid flow and the sound wave pressure.

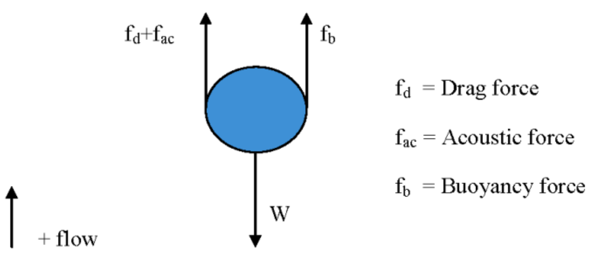

Fig. 12. The schematic diagram of the forces asserted on the particle under fluid flow and sound wave pressure.

According to Fig. 12, the force-balance can be presented as given in Eq. (16)

$$f_d + f_{ac} + w_e = ma \tag{16}$$

when

$$f_b + w = w_e. \tag{17}$$

For fixed bed, the pressure drop was contributed by the drag force due to the flowing of the fluid and the drag force due to the gas oscillation velocity (u_{ac}) on the sound wave field called "acoustic force." These two forces can be defined in terms of the pressure drop, using Eqs. (18) and (19).

$$f_d = \frac{\pi d_P^3 \varepsilon}{6L(1-\varepsilon)} \Delta P_d \tag{18}$$

and

$$f_{ac} = \frac{\pi d_P^3 \varepsilon}{6L(1-\varepsilon)} \Delta P_{ac} \tag{19}$$

Therefore, the fixed bed pressure drop can be written as follows:

$$\Delta P = \Delta P_d + \Delta P_{ac} \tag{20}$$

According to the drag force correlation purposed by Foscolo et al. (1983), who modified the Ergun equation (Ergun, 1952), the pressure drop correlation due to the drag force under the field of the flowing fluid and that under the gas oscillation velocity under the sound wave field for a distance Δx is as presented in Eq. (21).

$$\frac{\Delta P}{\Delta x} = \frac{\rho_F (1-\varepsilon)}{d_P} \left(\frac{17.3\mu_F ((U_o/\varepsilon) + \bar{u}_{ac_{i+1}})}{d_P \rho_F} + \frac{0.336((U_o/\varepsilon)^2 + \bar{u}^2_{ac_{i+1}})}{\varepsilon} \right) \varepsilon^{-3.8} \tag{21}$$

For an overall distance L, the fixed bed pressure correlation can be rewritten as follows:

$$\frac{\Delta P}{\Delta x}=\frac{\rho_F(1-\varepsilon)}{d_P}\left(\frac{17.3\mu_F(\sum_i(U_o/\varepsilon)_{i+1}+\sum_i\bar{u}_{ac_{i+1}})}{d_P\rho_F}+\frac{0.336(\sum_i(U_o/\varepsilon)^2_{i+1}+\sum_i\bar{u}^2_{ac_{i+1}})}{\varepsilon}\right)\varepsilon^{-3.8} \quad (22)$$

The Ergun equation can also be used to represent the pressure drop in the fixed bed for the sound-assisted fluidized bed, which is as presented in Eq. (23) for a distance Δx.

$$\frac{\Delta P}{\Delta x}=\frac{150((U_o/\varepsilon)+\bar{u}_{ac_{i+1}})\mu_F}{g_c\phi_S^2 d_P^2}\frac{(1-\varepsilon)^2}{\varepsilon^2}+\frac{1.75\rho_F((U_o/\varepsilon)^2+\bar{u}^2_{ac_{i+1}})}{g_c\phi_S d_P}\frac{(1-\varepsilon)}{\varepsilon} \quad (23)$$

For the overall distance L, the fixed bed pressure drop correlation based on the Ergun equation can be written as follows:

$$\frac{\Delta P}{\Delta x}=\frac{150(\sum_i(U_o/\varepsilon)_{i+1}+\sum_i\bar{u}_{ac_{i+1}})\mu_f}{g_c\phi_S^2 d_P^2}\frac{(1-\varepsilon)^2}{\varepsilon^2}+\frac{1.75\rho_f(\sum_i(U_o/\varepsilon)^2_{i+1}+\sum_i\bar{u}^2_{ac_{i+1}})}{g_c\phi_S d_P}\frac{(1-\varepsilon)}{\varepsilon} \quad (24)$$

The gas oscillation velocity ($u_{ac}(x,t)$) at distance x along the bed height can be calculated according to Eq. (25):

$$u_{ac}(x,t)=U\sin(2\pi ft) \quad (25)$$

And,

$$SPL=20\log\left[\frac{U}{\sqrt{2}U_{ref}}\right] \quad (26)$$

The average gas oscillation velocity ($\bar{u}_{ac_{i+1}}$) over the distance Δx can be calculated as

$$\bar{u}_{ac_{i+1}}=\frac{u_{ac}(x,t)_i+u_{ac}(x,t)_{i+1}}{2} \quad (27)$$

4.6 Prediction ability of pressure drop correlations

The revised Ergun equation and the Ergun equation were used, firstly, for the prediction of the fixed bed pressure drop for the conventional fluidized bed. It can be seen from Fig. 13(a) for the revised Ergun equation (Eq. (21)) and Fig. 13(b) for the Ergun equation (Eq. (22)) that without the sound vibration, these two original equations can predict perfectly the relation between the fixed bed pressure drop and the inlet superficial velocity. However, when the same correlations were used for sound-assisted fluidization with a sound pressure level of 80 dB and a sound frequency of 80 Hz, deviations between the experimental results and the theoretical prediction were found even though the gas oscillation velocity was taken into account in the correlations, as presented in Fig. 14(a) for the revised Ergun equation (Eq. (21)) and Fig. 14(b) for the Ergun equation (Eq. (22)). Therefore, in order to develop the fixed bed pressure drop correlations appropriately for sound-assisted fluidization, adjustment of the empirical factor of both the correlations is also needed. For the revised Ergun equation, the empirical exponential factor should be modified and for the Ergun equation, the empirical multiplication factor should be modified. Hence, a general form of the correlation should be drawn, as shown in Eq. (28) and Eq. (29), for the revised Ergun equation and the Ergun equation, respectively.

$$\frac{\Delta P}{\Delta x}=\frac{\rho_F(1-\varepsilon)}{d_P}\left(\frac{17.3\mu_F\left(\sum_i (U_o/\varepsilon)_{i+1}+\sum_i \bar{u}_{ac_{i+1}}\right)}{d_P\rho_F}+\frac{0.336\left(\sum_i (U_o/\varepsilon)^2_{i+1}+\sum_i \bar{u}^2_{ac_{i+1}}\right)}{\varepsilon}\right)\varepsilon^{-\beta} \quad (28)$$

$$\frac{\Delta P}{\Delta x}=\frac{X\left(\sum_i (U_o/\varepsilon)_{i+1}+\sum_i \bar{u}_{ac_{i+1}}\right)\mu_F}{g_c\phi_S^2 d_P^2}\frac{(1-\varepsilon)^2}{\varepsilon^2}+\frac{1.75\rho_F\left(\sum_i (U_o/\varepsilon)^2_{i+1}+\sum_i \bar{u}^2_{ac_{i+1}}\right)}{g_c\phi_S d_P}\frac{(1-\varepsilon)}{\varepsilon}$$

(29)

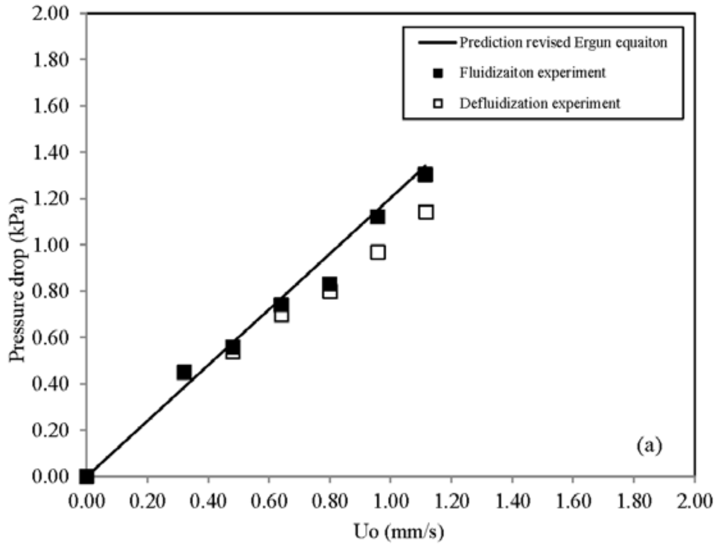

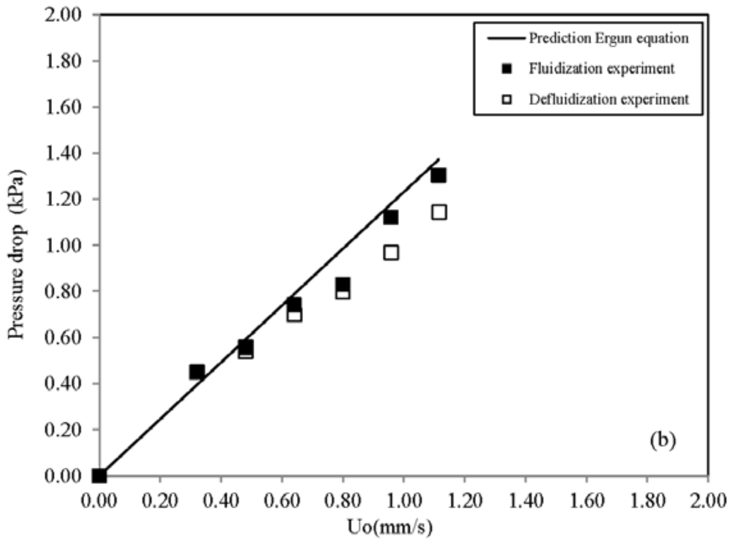

Fig. 13. Comparison between the experimental fixed bed pressure drop from conventional fluidized bed and that from (a) revised Ergun equation prediction and (b) Ergun equation prediction.

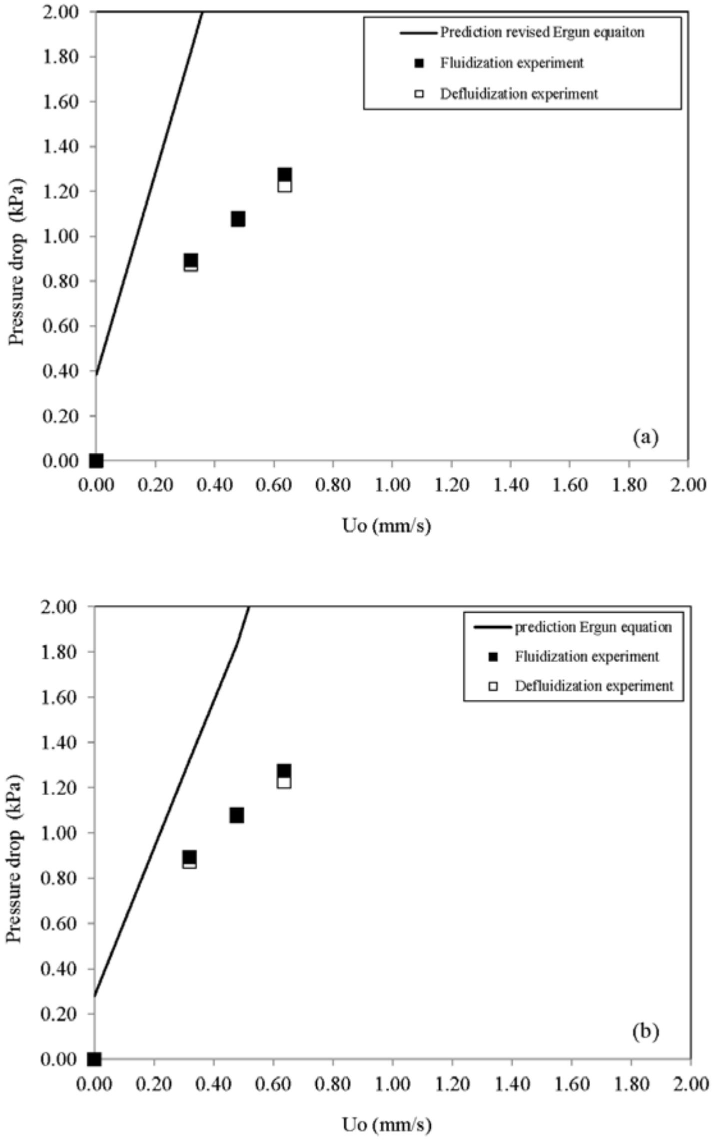

Fig. 14. Comparison between the experimental fixed bed pressure drop from sound-assisted fluidized bed (SPL = 80 dB and f = 80 Hz) and that from (a) the revised Ergun equation prediction and (b) the Ergun equation prediction.

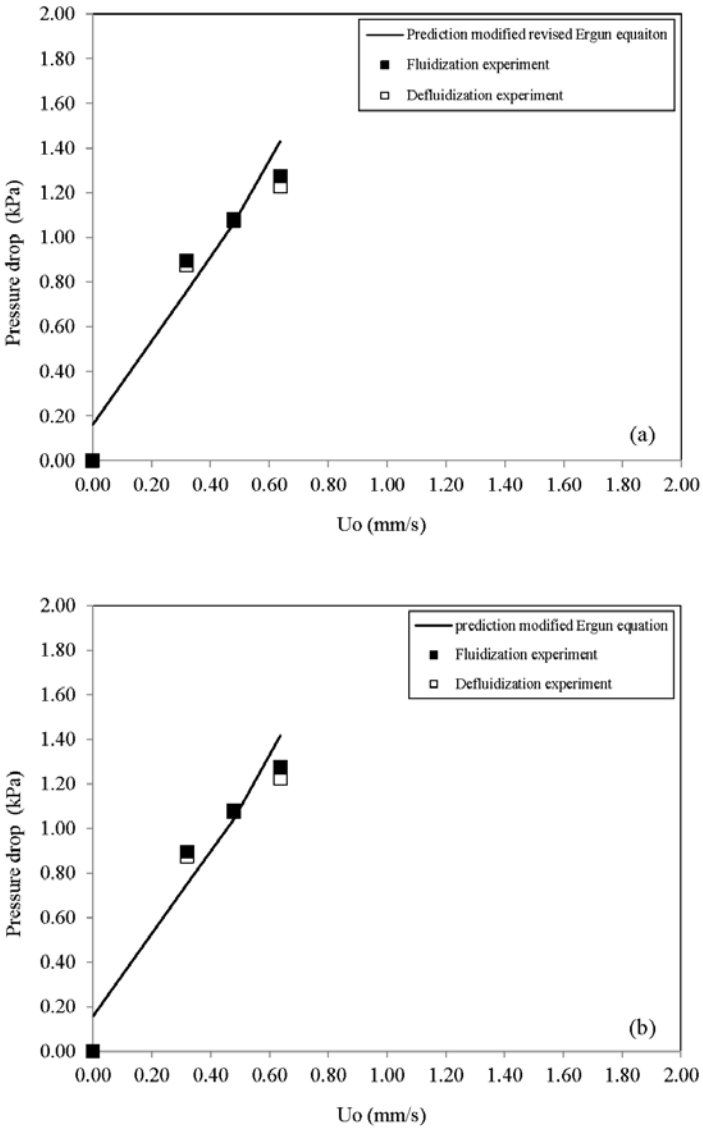

Fig. 15. Comparison between the experimental fixed bed pressure drop from sound-assisted fluidized bed and (a) the modified revised Ergun equation prediction (β = 3.05) and (b) the modified Ergun equation prediction (X = 85).

Fig. 15(a) and (b) present the experimental fixed bed pressure drop under the sound pressure level of 80 dB and sound frequency of 80 Hz from the fluidization and the defluidization experiments in comparison with the theoretical predictions from the modified revised Ergun equation (Eq. (28)) and the modified Ergun equation (Eq. (29)), respectively, when the empirical factors were used. It is obvious that the experimental fixed bed pressure drop was coinciding more with its corresponding theoretical predictions. Besides, it was also found that the empirical values varied with the sound frequency, as shown in Figs. 16 and 17. Fig.16 shows the variation in the empirical exponential factor (β) for the modified revised Ergun equation (Eq. (28)). Fig. 17 shows the variation in the empirical multiplication factor for the modified Ergun equation (Eq. (29)).

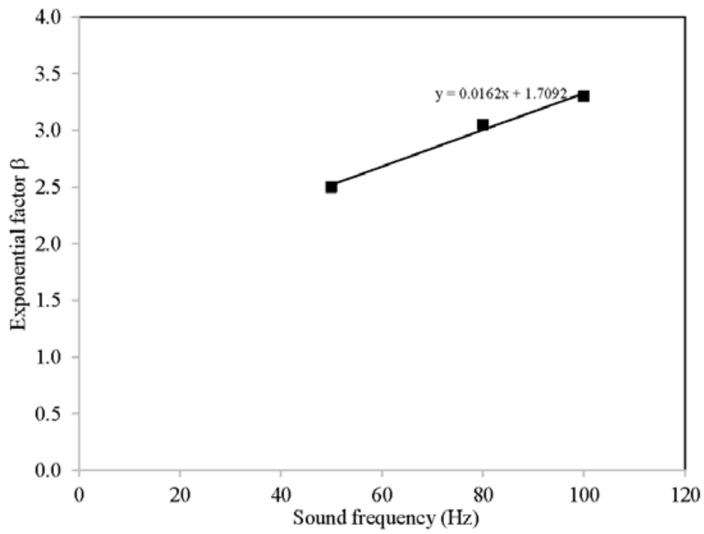

Fig. 16. Variation in the empirical exponential factor (β) for the modified revised Ergun equation (Eq. (28)).

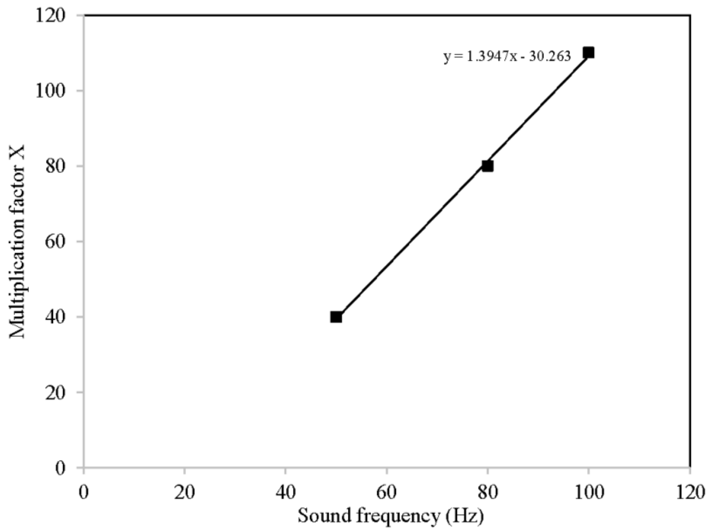

Fig. 17. Variation in the empirical multiplication factor for the modified Ergun equation (Eq. (29)).

For both cases, the linear relation between the factor and the sound frequency were found. Additionally, the closure equations were purposed in Eq. (30) and (Eq. (31).

The closure equation for the modified revised Ergun equation is as follows:

$$\beta = 0.0162(f) + 1.7092\,. \tag{30}$$

And, the closure equation for the modified Ergun equation is as follows:

$$X = 1.3974(f) - 30.263\,. \tag{31}$$

5. CONCLUSIONS

Standing wave characteristics were employed to explain the hydrodynamic behavior of sound-assisted fluidization of a rigid microsized powder under different inlet superficial velocities and sound frequencies ranging from 0 Hz to 500 Hz at a fixed sound pressure level of 80 dB. It can be concluded that due to the exponential and periodic variation of the vibration strength of the standing wave with the sound properties, the minimum fluidization velocity was varied in the same manner. Besides, it can be pointed out that the local minima of the minimum fluidization velocities were, thus, multiple values rather than a single value. To this end, fixed bed pressure drop correlations, based on the revised Ergun equation and the Ergun equation, for sound-assisted fluidization were purposed, where the gas oscillation velocity, calculated using the standing wave theory, was taken into account. It was found that even when the gas oscillation velocity is included, the original revised Ergun equation and the original Ergun equation cannot be used to describe the fixed bed pressure drop in a sound-assisted fluidized bed unless the empirical exponential factor for the revised Ergun equation and the empirical multiplication factor for the Ergun equation are used. In addition, it was observed that these two empirical factors were not a constant value but varied linearly with the sound frequency. Hence, the purposed correlations and their corresponding empirical closure equations can be concluded as follows:

1. Modified revised Ergun equation for the fixed bed pressure drop in sound-assisted fluidization:

$$\frac{\Delta P}{\Delta x} = \frac{\rho_f(1-\varepsilon)}{d_p}\left(\frac{17.3\mu_f\left(\sum_i (U_o/\varepsilon)_{i+1} + \sum_i \bar{u}_{ac_{i+1}}\right)}{d_p\rho_f} + \frac{0.336\left(\sum_i (U_o/\varepsilon)^2_{i+1} + \sum_i \bar{u}^2_{ac_{i+1}}\right)}{\varepsilon}\right)\varepsilon^{-\beta},$$

where

$$\beta = 0.0162(f) + 1.7092$$

2. Modified Ergun equation for the fixed bed pressure drop in sound-assisted fluidization:

$$\frac{\Delta P}{\Delta x}=\frac{X(\sum_{i}(U_o/\varepsilon)_{i+1}+\sum_{i}\bar{u}_{ac_{i+1}})\mu_f}{g_c\phi_S^2 d_P^2}\frac{(1-\varepsilon)^2}{\varepsilon^2}+\frac{1.75\rho_f(\sum_{i}(U_o/\varepsilon)_{i+1}^2+\sum_{i}\bar{u}_{ac_{i+1}}^2)}{g_c\phi_S d_P}\frac{(1-\varepsilon)}{\varepsilon},$$

where

$$X=1.3974(f)-30.263.$$

NOMENCLATURE

A	Constant depending on boundary condition
B	Constant depending on boundary condition
C_o	Standing wave velocity in fluidization media (m/s)
d_P	Particle diameter (μm)
f_c	Critical frequency (Hz)
f	Sound frequency (Hz)
h	Total bed height (m)
i	1, 2, 3, … n
K_g	Bulk modulus of nitrogen gas = 117×10^3 Pa
K_p	Bulk modulus of glass bead = 40×10^9 Pa
k	Wave number = $2\pi f/C_o$
L	Bed height (m)
n	Harmonic number
p	Pressure (Pa)
P_{fs}	Source amplitude at surface boundary at x=h (Pa)
P_{ref}	2×10^{-5} Pa

P_{rms} Root mean square of sound pressure (Pa)

SPL Sound pressure level (dB)

t Time (s)

U Amplitude of gas oscillation velocity (4.83×10^{-8} m/s)

U_o Inlet superficial velocity (m/s)

U_{ref} Reference velocity (m/s)

u_{ac} Gas oscillation velocity (m/s)

$\bar{u}_{ac}$ Average gas oscillation velocity over distance Δx (m/s)

x Axial displacement of wave propagation (m)

Greek letters

ΔP_{ac} Pressure drop due to acoustic force (Pa)

ΔP_d Pressure drop due to drag force (Pa)

ε Bed voidage

ρ_F Fluid density (kg/m^3)

ρ_g Gas density of nitrogen = 1.21 kg/m^3

ρ_P Particle density of glass bead = 2432 kg/m^3

θ Phase angle

ω Angular frequency

μ_F Fluid viscosity (kg/m.s)

ACKNOWLEDGMENTS

Thailand Research Fund and Chiang Mai University are gratefully acknowledged for their financial support. (Contract number: RSA5780008)

REFERENCES

Ergun S., Fluid flow through packed columns, Chemical Engineering Progress 48 (2) (1952) 89– 94.

Escudero D., Heindel T. J., Minimum fluidization velocity in a 3D fluidized bed modified with an acoustic field, Chemical Engineering Journal 213 (2013) 68-75.

Foscolo P.U., Gibilaro L.G., Waldram S.P., A unified model for particulate expansion of fluidised beds and flow in fixed porous media, Chemical Engineering Science 38 (8) (1983) 1251–1260.

Guo Q., Li Y., Wang M., Shen W., Yang C., Fluidization characteristics of SiO2 nanoparticles in an acoustic fluidized bed, Chemical Engineering Technology 26 (1) (2006) 78-86.

Guo Q., Wang M., Li Y., Yang C., Fluidization of ultrafine particles in a bubbling fluidized bed with sound assistance, Chemical Engineering Technology 28 (10) (2005) 1117-1124.

Herrera C.A., Levy E.K., Ochs J., Characteristics of acoustic standing waves in fluidized beds, AIChE Journal 48 (3) (2002) 503–513.

Kaliyaperumal S., Barghi S., Zhu J., Briens L., Rohani S., Effects of acoustic vibration on nano and sub-micron powders fluidization, Powder Technology 210 (2011) 143-149.

Langde M. L., Sonolikar R. L., Dharmaraj J. T., The influence of acoustic field and frequency on hydrodynamics of group B particles, Thermal Science 15(1) (2011) 159-169.

Liu H., Guo Q., Chen S., Sound-assisted fluidization of SiO2 nanoparticles with different surface properties, Industrial & Engineering Chemistry Research 46 (2007) 1345-1349.

Leu L., Li J., Chen C., Fluidization of group B particles in an acoustic field, Powder Technology 94 (1997) 23-28.

Morse R. D., Sonic energy in granular solid fluidization, Industrial & Engineering Chemistry Research 47 (1955) 1170-1175.

Russo P., Chirone R., Massimilla L., Russo S., The influence of the frequency of acoustic waves on sound-assisted fluidization of beds of fine particles, Powder Technology 82 (1995) 219-230.

Si C., Guo Q., Fluidization characteristics of binary mixtures of biomass and quartz sand in an acoustic fluidized bed, Industrial & Engineering Chemistry Research 47 (2008) 9773-9782.

Si C., Wu J., Wang Y., Zhang Y., Liu G., Effect of acoustic filed on minimum fluidization velocity and drying characteristics of lignite in a fluidized bed, Fuel Processing Technology 135 (2015) 112-118.

Urciuolo M., Salatino P., Cammarota A., Chirone R., Development of a sound-assisted fluidized bed filter/afterburner for particle-laden gas clean-up, Powder Technology 180 (2008) 102–108.

Wang S., Li X., Lu H., Liu G., Wang J., Xu P., Simulation of cohesive particle motion in a sound-assisted fluidized bed, Powder Technology 207 (2011) 65–77.

Xu C., Cheng Y., Zhu J., Fluidization of fine particles in a sound field and identification of group C/A particles using acoustic waves, Powder Technology 161 (2006) 227-234.

Zhu G., Liu Q., Yu Q., Pfeffer R., Dave R.N., Nam C.H., Sound assisted fluidization of nanoparticle agglomerates, Powder Technology 141 (2004) 119-123.Zhu et al., (2004)

APPENDIX C: MANUSCRIPT #2

Elsevier Editorial System(tm) for Chemical Engineering Science
Manuscript Draft

Manuscript Number:

Title: Bed Expansion Characteristics in Sound Assisted Fluidization of Geldart's Group A Powder

Article Type: Research paper

Section/Category: Particle Technology

Keywords: Sound; Fluidization; Bed expansion; Bed collapse; Drag force; Stability criterion

Corresponding Author: Dr. Parimanan Cherntongchai, Ph.D

Corresponding Author's Institution: Chiang Mai University

First Author: Parimanan Cherntongchai, Ph.D

Order of Authors: Parimanan Cherntongchai, Ph.D; Sattawat Chaiwattana; Rattanaporn Leruk

Abstract: Intrinsic bed expansion characteristics in a sound assisted fluidization of Geldart's group A powder were investigated. To obtain an accurate bed expansion data, a 1-valve and 2-valve bed collapse experiment, together with a bed collapse model for a correct interpretation of bed collapse curves, was used. It was found that a total bed voidage and a dense phase for the sound assisted fluidization were varied with an inlet superficial velocity in the same fashion as those for a conventional fluidization. Besides, the voidage with respect to the inlet superficial velocity of the sound assisted fluidization was found to be lower, in comparison with those of the conventional fluidization and was independent on the sound frequency. In addition, dense phase voidage and its superficial velocity relations of the sound assisted fluidization at different sound frequencies were approximately on the same trend as that for the conventional fluidization. Finally, a minimum bubbling point, defined using the dense phase voidage and dense phase superficial velocity characteristic curve, was also unaffected by the sound vibration force. These findings suggested that a sound vibrational force tended to create more cavity or bubble phase in the fluidized bed, rather than changing a hydrodynamics relation in the dense phase. Therefore, the same equilibrium of force as that of the conventional fluidization can still be applied for the sound assisted fluidization, as well as stability criteria. Finally, it was proved that the modified revised Ergun drag force correlation, applicable for the conventional fluidization, can describe well the dense phase voidage and the dense phase superficial velocity characteristic curves of the sound assisted fluidization. Likewise, the stability criterion proposed by Cherntongchai and Brandani (2013) can predict excellently the minimum bubbling points for the sound assisted fluidized bed.

Suggested Reviewers: Stefano Brandani
Professor, School of Engineering, Institute for Materials and Processes, University of Edinburgh

s.brandani@ed.ac.uk

Kai Zhang
Professor, Center of Chem Eng for Clean Energy, North China Electric Power University
kzhang@ncepu.edu.cn

Paola Lettieri
Professor, Department of Chemical Engineering, University College London
p.lettieri@ucl.ac.uk

Quingjie Guo
Professor, State Key Laboratory of Heavy Oil Processing, College of Chemistry and Chemical , University of Petroleum
qjguo@mail.hdpu.edu.cn

Eldin Lim
Senior lecturer, Department of Chemical and Biomolecular Engineering, National University of Singapore
chelwce@nus.edu.sg

Jingxu Zhu
Professor, Department of Chemical and Biochemical Engineering, Faculty of Engineering, The University of Western Ontario
jzhu@uwo.ca

Opposed Reviewers:

Parimanan Cherntongchai

Department of Industrial Chemistry
Faculty of Science, Chiang Mai University
Chiang Mai, Thailand, 50200
parimanan@gmail.com

25 December 2017

Re: Consideration of a research article publication

Dear Editors,

I am Dr. Parimanan Cherntongchai from Department of Industrial Chemistry, Faculty of Science, Chiang Mai University. I would like to summit a research article in a topic of "**Bed Expansion Characteristics in Sound Assisted Fluidization of Geldart's Group A Powder**" to be considered for a publication in "**Chemical Engineering Science**". I, thereby, have enclosed a manuscript for a revision process together with a list of suggested referees, graphical abstract and highlights.

Sound-assisted fluidization has been successfully used to improve quality of fluidization, induce smaller agglomerate size and reduce particle elutriation. By the same time, the sound vibrational force causes a change in fluidization hydrodynamics. One of which is a bed expansion characteristics. There are some previous research works studying the bed expansion characteristics of the Geldart's Group A powder in the sound assisted fluidization. However, there is much more comprehension on the bed expansion characteristics in the sound assisted fluidization for a further investigation. Therefore, in our work, the intrinsic bed expansion characteristics of Geldart's group A powder in the sound assisted fluidization were further investigated based on an accurate bed expansion data. And, to obtain such accurate bed expansion data, the 1-valve and 2-valve bed collapse experiment and the bed collapse model (Cherntongchai and Brandani, 2005) were used. Finally, the drag force correlation and the minimum bubbling criterion for the description of the bed expansion characteristics of Geldart's group A powder in the sound assisted fluidization was validated.

I would like to thank in advance for your consideration and hope to have an opportunity to be able to publish in "**Chemical Engineering Science**".

Sincerely yours,
Parimanan Cherntongchai

Graphical Abstract

Graphical abstract

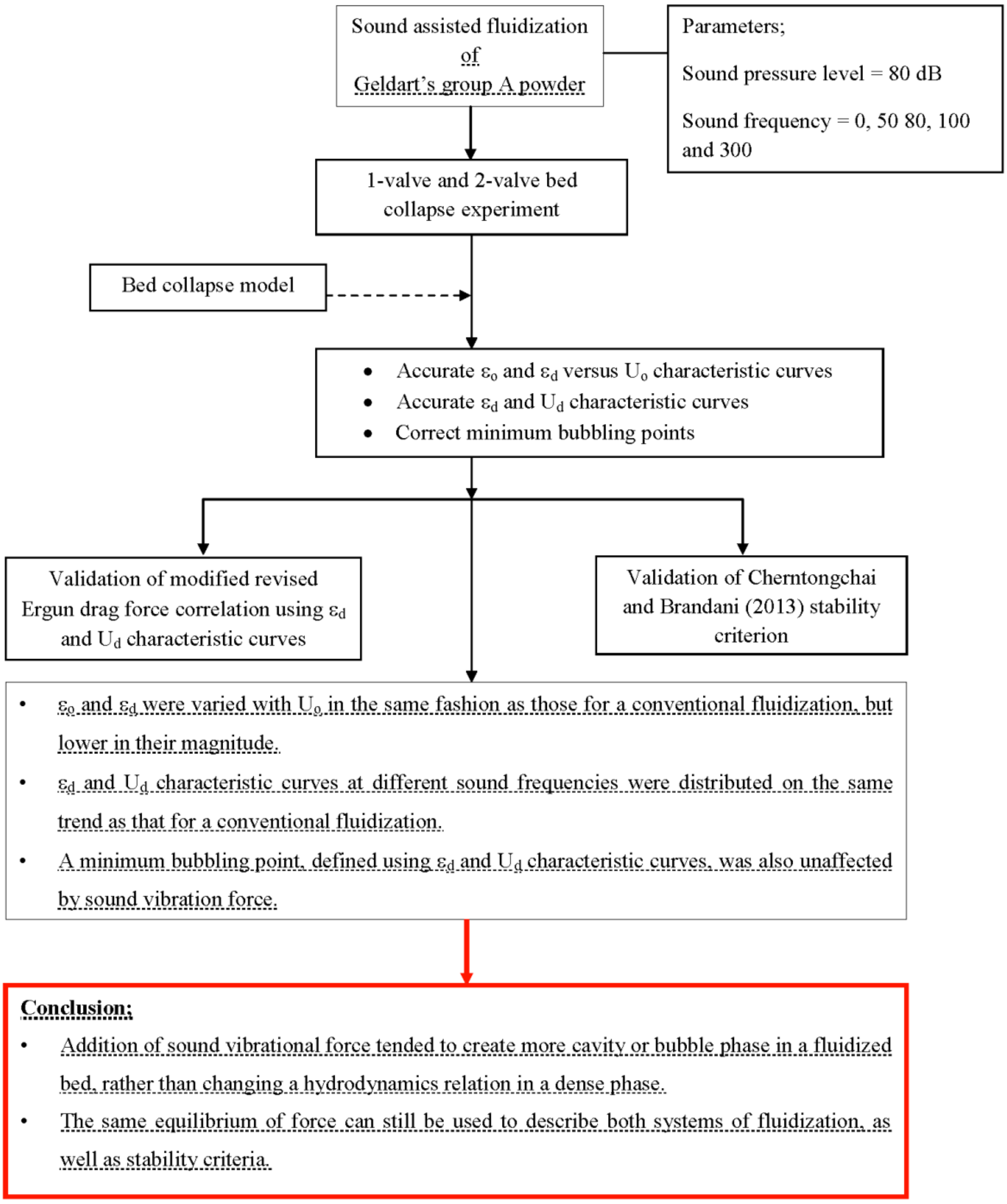

*Highlights

Highlights

- Accurate bed expansion characteristics of Geldart's group A powder were obtained, by the use of 1-valve and 2-valve bed collapse experiment and the bed collapse model for data interpretation.
- An addition of sound vibrational force tended to create more cavity or bubble phase in a sound assisted fluidized bed, rather than changing a hydrodynamics relation in dense phase.
- The same equilibrium of force and stability criteria can be used to describe both conventional fluidization and sound assisted fluidization.
- Modified revised Ergun drag force correlation can describe well the dense phase voidage and the dense phase superficial velocity characteristic curves.
- Stability criterion proposed by Cherntongchai and Brandani (2013) can predict excellently the minimum bubbling points.

*Manuscript
Click here to view linked References

Bed Expansion Characteristics in Sound Assisted Fluidization of Geldart's Group A Powder

Parimanan Cherntongchai*, Sattawat Chaiwattana, and Rattanaporn Leruk

Department of Industrial Chemistry, Faculty of Science, Chiang Mai University

Chiang Mai, Thailand, 50200

*Corresponding author (parimanan@gmail.com)

ABSTRACT

Intrinsic bed expansion characteristics in a sound assisted fluidization of Geldart's group A powder were investigated. To obtain an accurate bed expansion data, a 1-valve and 2-valve bed collapse experiment, together with a bed collapse model for a correct interpretation of bed collapse curves, was used. It was found that a total bed voidage and a dense phase for the sound assisted fluidization were varied with an inlet superficial velocity in the same fashion as those for a conventional fluidization. Besides, the voidage with respect to the inlet superficial velocity of the sound assisted fluidization was found to be lower, in comparison with those of the conventional fluidization and was independent on the sound frequency. In addition, dense phase voidage and its superficial velocity relations of the sound assisted fluidization at different sound frequencies were approximately on the same trend as that for the conventional fluidization. Finally, a minimum bubbling point, defined using the dense phase voidage and dense phase superficial velocity characteristic curve, was also unaffected by the sound vibration force. These findings suggested that a sound vibrational force tended to create more cavity or bubble phase in the fluidized bed, rather than changing a hydrodynamics relation in the dense phase. Therefore, the same equilibrium of force as that of the conventional fluidization can still be applied for the sound assisted fluidization, as well as stability criteria. Finally, it was proved that the modified revised Ergun drag force

correlation, applicable for the conventional fluidization, can describe well the dense phase voidage and the dense phase superficial velocity characteristic curves of the sound assisted fluidization. Likewise, the stability criterion proposed by Cherntongchai and Brandani (2013) can predict excellently the minimum bubbling points for the sound assisted fluidized bed.

KEYWORDS; Sound; Fluidization; Bed expansion; Bed collapse; Drag force; Stability criterion

1. INTRODUCTION

A sound assisted fluidization is a fluidization of a particle bed under a sound vibrational force field due to a propagation of a sound wave through the bed. This sound vibrational force renders a better fluidization quality, a smaller agglomerate size, a particle elutriation reduction and a change in fluidization hydrodynamics. One of which is a bed expansion characteristics, which is involving to a minimum fluidization point, a bed expansion ratio, a total bed voidage, dense phase properties and a minimum bubbling point.

There are still very limit numbers of research works investigating the bed expansion characteristics of the particle bed in the sound assisted fluidization. Currently, some works used a visual observation to obtain a bed expansion ratio and a bed collapse experiment to obtain a bed collapse time and a shape of a bed collapse curve in order to determine a fluidization quality. Russo et al. (1995) studied an influence of a particle loading, a sound pressure level and a sound frequency on the bed expansion ratio of Geldart's group C powder, to determine the fluidization quantity. It was found from this work that, in relation to an inlet superficial velocity, the bed expansion ratio was found to non-monotonically increase with increasing the inlet superficial velocity and, hence, the fluidization quality. Herrera and

Levy (2001) investigated the effect of the sound pressure level on the homogeneous bed expansion and the minimum bubbling point for Geldart's group A powder. The increase of the bed height and the minimum bubbling velocity with increasing the sound pressure level was reported. And, a change in a void structure under the sound vibrational force was an underlined explanation. Zhu et al. (2004) studied the effect of the sound pressure level and the sound frequency on the bed expansion for nanoparticle agglomerates. With an application sound, the bed expansion increased due to the breakup of the large agglomerate under the combined effect of hydrodynamics forces and acoustic excitations. Guo et al. (2006) carried out the bed collapse experiment and used the bed collapse time to identify the de-aeration characteristic of silica nanoparticle with different surface properties in the sound assisted fluidization. It was pointed out that there was a greater bed collapse time under the sound vibrational force. This was due to the more reduction in the van der waals forces between the nanoparticles and the better fluidization quality. Ammendola and Chirone (2010) studied aeration and a mixing behavior of the nano-sized powders under the sound vibration. The bed expansion ratio was also used for an index of the fluidization quality. Under the influence of sound, the fluidization quality was improved. Similar to the previous reports, the higher the sound intensity, the higher the bed expansion, as far as the sound pressure level was higher enough to compensate the sound attenuation. In addition, the optimum sound frequency, giving the maximum bed expansion, was also found. Ammendola et al. (2011) focused on the aeration behavior of the binary mixtures of nanoparticle under acoustic field and reported the better fluidization quality in term of the bed expansion ratio. In this work, they also worked with the homogenous bed expansion data using the Richardson and Zaki correlation at $n \approx 5$ in order to estimate the terminal falling velocity of the agglomerate. Kaliyaperumal et al. (2011) observed the bed expansion ratio for the nano and sub-micron powder under the acoustic vibration to determine the fluidization quality. Similarly, the bed expansion ratio increased with the sound pressure level and was raised with increasing inlet superficial velocity. This was due to the reorientation of the bed voidage under the vibration induced the sound excitation. In addition, the maximum bed expansion ratio was found at a resonance sound frequency. Langde and Sonolikar (2011) investigated the bed expansion of Geldart group C/A powder under the sound field. They reported that the expansion ratio increase non-monotonically with the inlet superficial velocity. Also, the bed expansion ratio was reported to increase with the sound pressure level due to the breaking up of the interparticle forces at higher sound intensity. As a result, more void was created. Under the influence of the sound frequency, the bed expansion ratio reached the maximum point at a certain frequency (120 Hz), where the sound oscillation was the highest and for other sound frequency the bed expansion was approximately the same. Raganati et al. (2014) studied the effect of the CO_2 partial pressure, the sound pressure level and the sound frequency on the fluidization quality using the bed expansion ratio for the CO_2 adsorption on the fine activated carbon. It was pointed out the bed expansion ratio increased with the sound pressure level after the threshold value where the sound intensity overcame the attenuation effect. Under the effect of the sound frequency, the optimum frequency was found for the best fluidization quality and the maximum aggregate break-up. Either too low or too high sound frequency, the fluidization quality failed on the same range. The explanation given was that for too high frequencies the acoustic filed is not able to propagate inside the bed and to promote the break-up of aggregates. On the other hand, for too low frequency, the relative motion between the smaller and the larger sub-aggregates, leading the large aggregates to be broken up, was practically absent.

There is much more comprehension on the bed expansion characteiristics in the sound assisted fluidization for a further interesting investigation. We, therefore, underwent a research work to discover intrinsic bed expansion characteristics of Geldart's group A powder in the sound assisted fluidization. To obtain accurate bed expansion characteristics, the 1-valve and 2-valve bed collapse experiment, together with a bed collapse model for a correct interpretation of bed collapse curves, was used. Finally, the drag force correlation and the minimum bubbling criterion for the description of the bed expansion characteristics of Geldart's group A powder in the sound assisted fluidization was validated.

2. THOERY: 1-valve and 2-valve bed collapse model (Cherntongchai and Brandani, 2005)

1-valve bed collapse experiment is carried out by abruptly shut down an inlet valve. For 2-valve bed collapse experiment, there is a discharged valve attached at a windbox. This valve is synchronized with the inlet valve. Once the inlet valve is abruptly shut down, the discharge valve is opened to vent gas in a bed and the windbox. For both cases, a bed surface starts to collapse with a lapse of time once the valves were energized and a bed collapse structure is presented in Fig. 1. From $0 \leq t \leq t_{bub}$ (Fig. 1(a)), so called "a bubble escape stage", remained bubbles will escape from the collapsing bed. The collapsing bed is comprised of 3 zones. Zone 0 ($\varepsilon = \varepsilon_o$) is the bubbling bed zone, extended from L_o to L_1. This zone is diminished with time due to the escape of the bubbles and the falling down of L_o together with the growing up of L_1. Zone 1 ($\varepsilon = \varepsilon_1 = \varepsilon_d$) is the homogeneous expanded zone, extended from L_1 to L_2, where both L_1 and L_2 moved upward. Zone 2 ($\varepsilon = \varepsilon_2 = \varepsilon_{fixed}$) is the fixed bed zone, formed up from t=0 and growth upward all along the collapsing process. At $t = t_{bub}$, all bubbles disappear and the bed collapse structure is of 2 zones as shown in Fig. 1(b). From $t \geq t_{bub}$ (Fig. 1(c)), this stage is called "a sedimentation stage". L_1 is falling down while L_2 keep growing upward. And, the bed collapse process ends when $L_1 = L_2$. During the entire bed collapse process, the gas flows through the bed are from the gas residue in the windbox and the gas generated at the interface L_2, due to the change in the bed voidage between zone 1 and zone 2. For 1-valve bed collapse process, the gas always flows in an upward direction. On the other hand, for 2-valve bed collapse process, the gas from the windbox and the gas generated at the interface can flow in both upward and downward directions, due to the characteristic of the discharge valve.

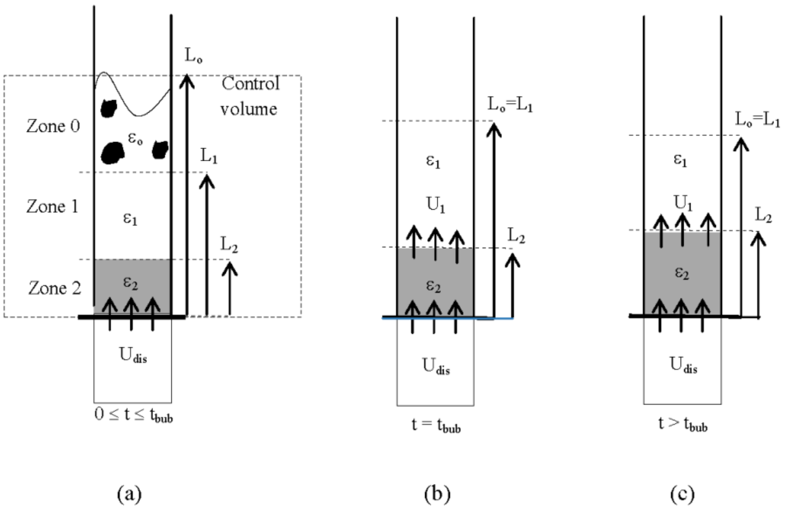

Fig. 1. Schematic of (a) bubble escape stage, (b) and (c) sedimentation stage for 1-valve bed collapse experiment

The main assumptions of the model equations are; one dimensional system, ideal gas, incompressible fluid in the bed section, compressible fluid in the windbox, negligible inertial effects, a constant voidage fraction ε_1 ($\varepsilon_1 = \varepsilon_d$) according to a gas velocity U_d ($U_1 = U_d$).

The bed collapse model can be summarized as follows;

2.1 Sedimentation stage

1-valve configuration

$$\frac{dL_1}{dt} = U_{dis} - U_d \qquad (1)$$

$$\frac{dL_2}{dt} = \frac{(1-\varepsilon_1)(U_{dis} - U_d)}{(\varepsilon_1 - \varepsilon_2)} \qquad (2)$$

$$-\frac{dp_W}{dt} = \frac{p_W}{V_W} U_{dis} A \qquad (3)$$

The bed collapse model can be solved through integration of Eqs. (1) - (3), simultaneously. U_{dis} can be calculated from the knowledge of the distributor pressure drop, determined from the collapsing bed momentum balance (Eq. (4)). The initial condition for L_1 is L_o and for L_2 is zero:

$$\Delta P_{Dist} = (p_W - p_{atm}) - \rho_F g L_c - \Delta P_1 - \Delta P_2 \qquad (4)$$

$$\Delta P_1 = (\rho_P - \rho_F)(1-\varepsilon_1)(L_1 - L_2) g \qquad (5)$$

$$\Delta P_2 = f(U_{dis}) \qquad (6)$$

2-valve configuration

$$\frac{dL_1}{dt} = \pm U_{dis} - U_d \qquad (7)$$

$$\frac{dL_2}{dt} = \frac{(1-\varepsilon_1)(U_{dis} \pm U_d)}{(\varepsilon_1 - \varepsilon_2)} \qquad (8)$$

$$-\frac{dp_W}{dt} = \frac{p_W}{V_W} (\pm U_{dis} A + Q_V) \qquad (9)$$

$$\Delta P_{Dist} = (p_W - p_{atm}) - \rho_F g L_c - \Delta P_1 \pm \Delta P_2 \qquad (10)$$

The solution of the model equations requires the knowledge of the discharge valve pressure drop. A positive sign in Eqs. (7) – (10) applies when the gas is flowing from the windbox to the particle bed.

2.2 Bubble escape stage

1-valve configuration

The properties in the bubbling zone are assumed to be similar to those in the steady state bubbling fluidized bed.

$$\frac{dL_o}{dt} = U_{dis} - U_o \tag{11}$$

$$\Delta P_{Dist} = (p_w - p_{atm}) - \rho_F g L_c - \Delta P_o - \Delta P_1 - \Delta P_2 \tag{12}$$

$$\Delta P_o = (\rho_P - \rho_F)(1 - \varepsilon_o)(L_o - L_1) g \tag{13}$$

Eq. (11) has to be integrated simultaneously with Eqs. (1) – (3). U_{dis} can be calculated using Eq. (12). The initial condition for L_2 and L_1 is zero.

2-valve configuration

A criterion to specify the different bed collapse structures during the bubble escape stage has been added, due to the possibility of the flow reversal of the gas generated at the interface L_2. The first possible structure is as shown in Fig. 1(a), when zone 1 can exist. Another possible structure is when zone 1 cannot exist. To determine whether zone 1 can exist, U_1 is calculated based firstly on the assumption that zone 1 can exist using Eq. (14)

$$U_1 = \varepsilon_1(\pm U_{dis}) + (1 - \varepsilon_1) U_d \tag{14}$$

If U_1 is greater than zero, then zone 1 can exist. And, the bed collapse rate can be expressed as follows;

$$\frac{dL_o}{dt} = U_{dis} - U_o \tag{15}$$

$$\Delta P_{Dist} = (p_w - p_{atm}) - \rho_f g L_c - \Delta P_o - \Delta P_1 \pm \Delta P_2 \tag{16}$$

Eq. (15) has to be integrated simultaneously with Eqs. (7) – (9).

If U_1 is less than zero, the zone 1 cannot exist. In this case Eq. (15) has to be integrated with Eqs. (7), (9) and (17).

$$\frac{dL_2}{dt} = \frac{(1-\varepsilon_o)(U_o - U_{dis})}{(\varepsilon_o - \varepsilon_2)} \qquad (17)$$

2.3 Prediction of dense phase properties using bed collapse model (Cherntongchai et al., 2011)

System configuration information and model parameters, as the required inputs for the bed collapse model, are listed in Table 1.

Table 1 Model input information

System configurations	Parameters
Windbox volume	Fixed bed pressure drop
Distributor pressure drop	Bed voidage, ε_o
Discharge valve pressure drop	Dense phase voidage, ε_d
	Fixed bed voidage, ε_2
	Inlet superficial velocity, U_o
	Dense phase superficial velocity, U_d

All parameters can be achieved independently, except the dense phase voidage and the dense phase superficial velocity, which have to be obtained from the interpretation of the experimental bed collapse curves following the method outlined bellows;

For a homogeneous expanded bed:

- Introducing the system configuration, fixed bed pressure drop, ε_o, ε_2 and U_o
- Initial estimate of ε_d
  - $\Delta P_{Dist}/\Delta P_{Bed}<1$, y-intercept of 1-valve sedimentation curve gives the correct ε_d.
  - $\Delta P_{Dist}/\Delta P_{Bed}>1$, y-intercept of 2-valve sedimentation curve gives the correct ε_d.
- Evaluation of U_d

- $\Delta P_{Dist}/\Delta P_{Bed}<1$, the correct U_d is selected iteratively until the experimental 1-valve sedimentation curve is fitted with the model prediction.
- $\Delta P_{Dist}/\Delta P_{Bed}>1$, the correct U_d is selected iteratively until the experimental 2-valve sedimentation curve is fitted with the model prediction.

- Re-validation of ε_d and U_d

ε_d and U_d from the 1-valve collapse curve ($\Delta P_{Dist}/\Delta P_{Bed}<1$) are used to predict the entire experimental 2-valve sedimentation collapse curve to validate the values obtained. On the contrary, for ε_d and U_d obtained from the 2-valve collapse curve ($\Delta P_{Dist}/\Delta P_{Bed}>1$), the 1-valve sedimentation collapse curve was used to validate the values.

For a bubbling bed, the same procedure can be applied except for ε_o interpretation. ε_o was selected to fit the bubble escape time of the 1-valve collapse curve ($\Delta P_{Dist}/\Delta P_{Bed}<1$). The ε_o, ε_d and U_d from the 1-valve collapse curve were validated by comparing the predictions for the 2-valve collapse curve with the experimental results. On the other hand, ε_o selected from the 2-valve collapse curve for $\Delta P_{Dist}/\Delta P_{Bed}>1$, the ε_o, ε_d and U_d from the 2-valve collapse curve were validated by comparing the predictions for the 1-valve collapse curve with the experimental results.

3. EXPERIMENTS

3.1 Experimental setup

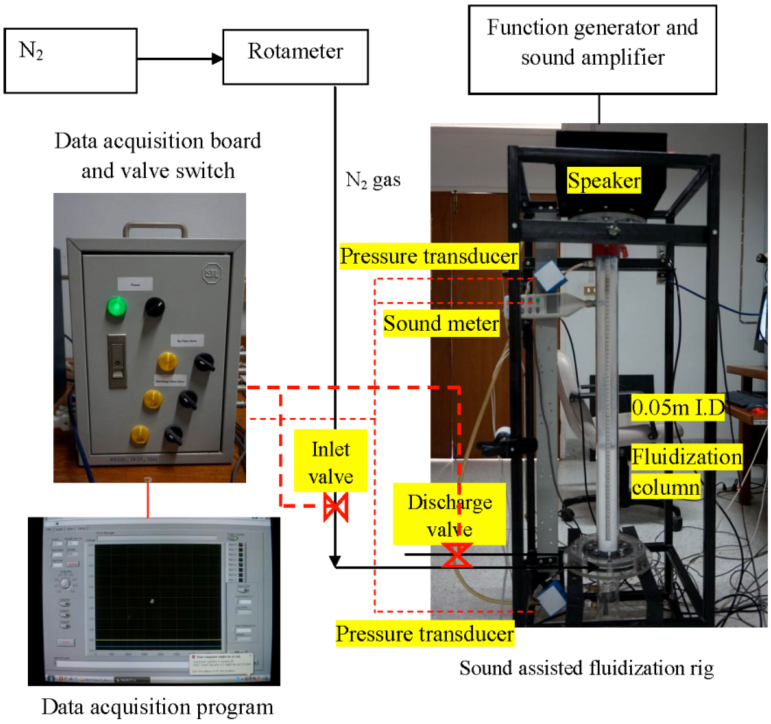

Fig. 2. Sound assisted fluidization setup for 0.05 m ID fluidization column

A sound assisted fluidization setup (Fig. 2) was consisted of 99.99% purity nitrogen gas connected to a rotameter. After metering a gas flow rate, a nitrogen gas line is connected to a 0.05 m ID fluidization column. The column is equipped with a gas distributor, pressure transducers, a sound level meter, a speaker on top of the column, an inlet solenoid valve and a discharge solenoid valve. The pressure transducers and the sound meter are connected to a data acquisition board and, then, a data acquisition program. To carry out 2-valve bed collapse experiment, the discharge valve, attached at the windbox, is synchronized with the inlet valve. These two valves are controlled using a valve switch. A flow range for this setup is from 0-30 L/min. A sound pressure level was fixed at 80 dB and a sound frequency is ranged from 0-300 Hz. A data acquisition rate is 100 data point per second. Finally, a measuring range of a pressure transducer is at 0-5 psi. Empirical correlations of the distributor pressure drop and the discharge valve pressure drop are presented in Eqs. (18) and (19), respectively

$$\Delta P_{Dist}\,(kPa) = 2.28 Q_{Windbox} \tag{18}$$

$$\Delta P_{V}\,(kPa) = 0.0008 Q_{Windbox}^{2} + 0.0046 Q_{Windbox} \tag{19}$$

1-valve bed collapse experimental was carried out by energizing the inlet valve to close while the discharge valve remained closed. For the 2-valve bed collapse experiment, the inlet valve was synchronized to close, with the opening of the discharge valve to release the gas. Then, the particle bed collapsed. A digital camera was used to record the bed surface during the bed collapse process.

3.2 Material

A powder used was a glass ballotini. In this work, a particle density was measured using a pycnometer and a laser light scattering method was used for a measurement of a particle size and a particle size distribution. Particle properties were presented in Table 2 and the particle size distribution was illustrated in Fig. 3. A particle loading was 0.8509 kg.

Table 2 particle density and average particle size

Material	Apparent density (kg/m^3)	Average particle diameter (μm)
Glass ballotini	2,432	32.61

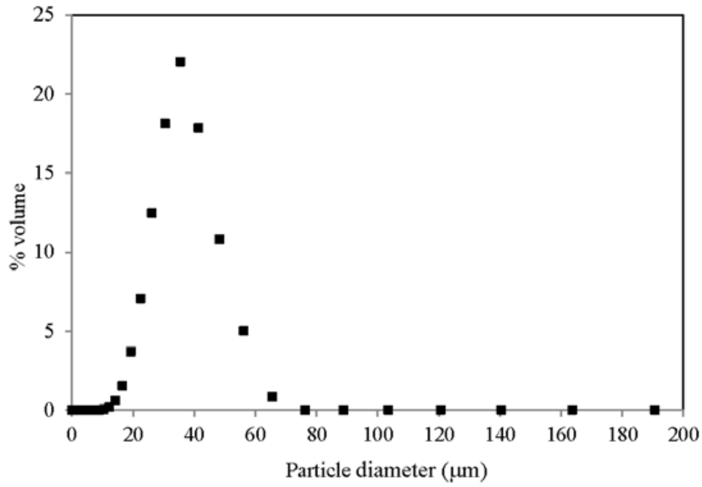

Fig. 3. Particle size distribution of glass ballotini

Table 3 was a summary of experimental conditions used in this work.

Table 3 Summary of experimental conditions

Experimental conditions	Inlet superficial velocity (mm/s)	Sound pressure level (dB)	Sound frequency (hz)
	0-15	0	0
	0-15	80	50,80,100,300

4. RESULTS AND DISCUSSION

4.1 Prediction of total bed voidage and dense phase properties using bed collapse model

An interpretation of ε_o, ε_d and U_d from 1-valve and 2-valve bed collapse curves for a homogeneous expanded bed and a bubbling bed has been explained thoroughly in Cherntongchai and Brandani (2005).

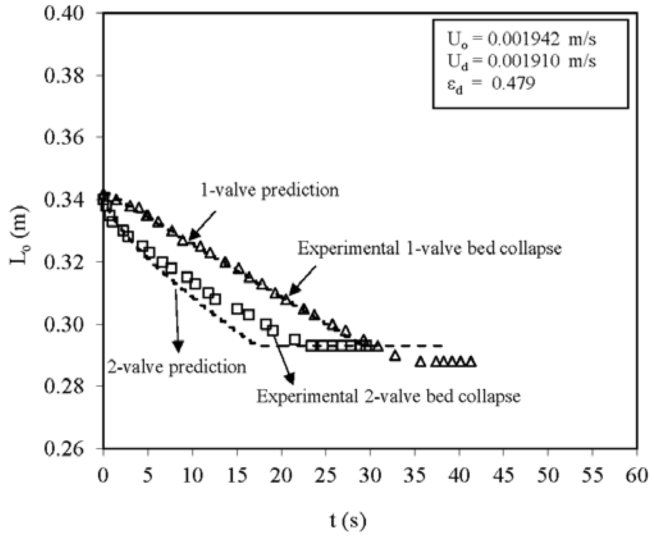

Fig. 4. 1-valve and 2-valved bed collapse curves and model predictions for homogenous expanded bed in sound assisted fluidized bed at SPL = 80 dB and f = 100 Hz

Fig. 4 was the bed collapse curves for the homogeneous expanded bed where there is no bubble escape stage. And, the y-intercept from the 1-valve bed collapse curve was used to determine the correct ε_d. Then, U_d, equivalent to U_o, was used to predict correctly the entire 1-valve collapse curve. The 2-valve collapse curve was fully predicted using ε_d and U_d

obtained from the 1-valve bed collapse curve. By this way, the set of ε_d and U_d was re-validated.

The bubbling bed collapse curves were presented in Fig. 5. ε_o was selected to match with the bubble escape time. ε_d was acquired from the y-intercept of the 1-valve sedimentation state linear extrapolation and U_d was iterated to match the predicted 1-valve sedimentation curve with the experimental curve. As for the homogeneous bed, the entire 2-valve collapse curve was predicted using the same set of ε_o, ε_d and U_d.

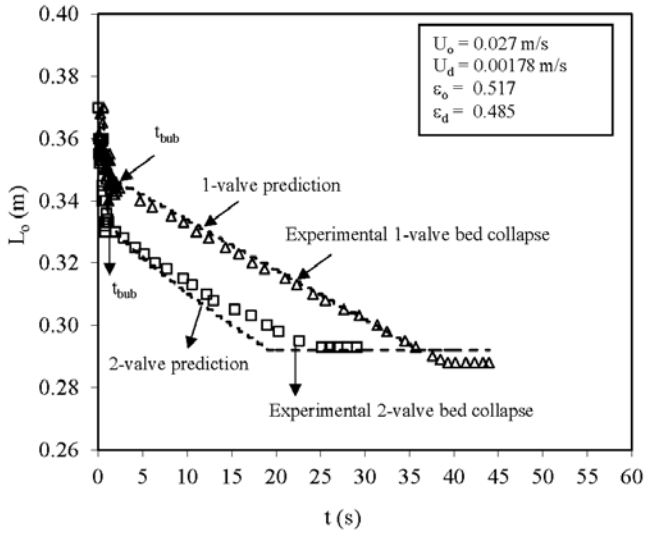

Fig. 5. 1-valve and 2-valved bed collapse curves and model predictions for bubbling bed in sound assisted fluidized bed at SPL = 80 dB and f = 100 Hz

4.2 Total bed voidage and dense phase properties

An aspect of the bed expansion in the sound assisted fluidization has been published by some previous works using the visual observation (Russo et al., 1995; Herrera and Levy, 2001; Zhu et al., 2004; Ammendola and Chirone, 2010; Ammendola et al., 2011; Kaliyaperumal et al., 2011; Langde and Sonolikar, 2011; Raganati et al., 2014). The previous works (Russo et al., 1995; Langde and Sonolikar, 2011) stated that there was a non-monotonically increase with the inlet superficial velocity of the overall bed voidage or the bed expansion ratio obtained visually. And, there was the increase of the bed expansion ratio in the sound assisted fluidization, in comparison with the conventional fluidization. In addition, based on the expansion ratio, the other works reported the existing of the maximum bed expansion at the resonance frequency, usually at 120 Hz. (Ammendola and Chirone, 2010; Kaliyaperumal et al., 2011; Langde and Sonolikar, 2011)

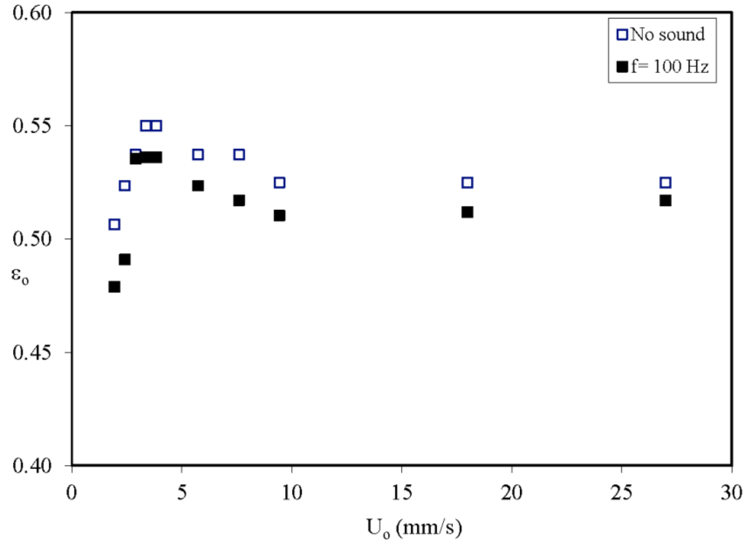

Fig. 6. Total bed voidage and inlet superficial velocity relation for conventional fluidization and sound assisted fluidization at SPL = 80 dB and sound frequency = 100 Hz

Our work using the more accurate method on defining the bed expansion characteristics, as mentioned above. We have found in contrary, for the sound assisted fluidization and the conventional fluidization that the total bed voidage increased with the inlet superficial velocity in the homogeneous expanded bed (Fig. 6). After the minimum bubbling point, where the dense phase voidage is the highest, the total bed voidage decrease with increasing the inlet superficial velocity. At a certain inlet superficial velocity, the total bed voidage reached the minimum and, then, started to increase again. And, this same pattern of variation was also found for the relation between the dense phase voidage and the inlet superficial velocity for both the conventional and the sound assisted fluidization of different sound frequencies (Figs. 7 and 8).

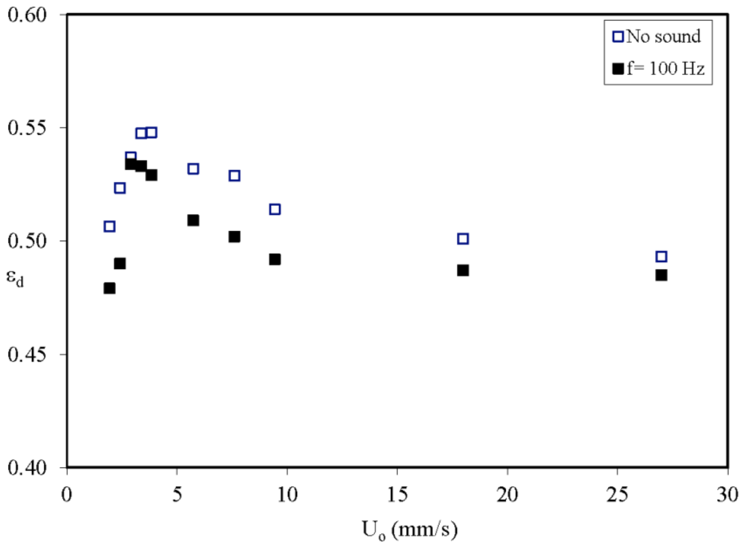

Fig. 7. Dense phase voidage and inlet superficial velocity relation for conventional fluidization and sound assisted fluidization at SPL = 80 db and sound frequency = 100 Hz

It was also proved in our work that the application of the sound vibrational force reduced the dense voidage, as well as the total bed voidage, in comparison with those of the conventional fluidization (Figs. 6, 7 and 8). Besides, under the variation of the sound frequency, the dense phase voidage with respect to the inlet superficial velocity were considered to be randomly distributed over approximately the same values (Fig. 8).

Fig. 9 presented the relation between the dense phase voidage and the dense phase superficial velocity. It was found to be failed on the same trend for both the conventional and the sound assisted fluidization. Even, the dense phase voidage with respect to the inlet superficial velocity (Fig. 7 and Fig. 8) were different, including those for the homogeneous expanded bed.

An explanation of the change of the total bed voidage and the dense phase voidage under the sound vibrational force field was similar to many other reports due to the rearrangement of the bed structure. However, from our results, it was possible to further explain that the gas oscillation under the sound vibrational induced more cavities or bubble phase in the fluidizing bed, and the structure of the dense phase was remained. Therefore, the same force equilibrium relation existed for both systems of fluidization.

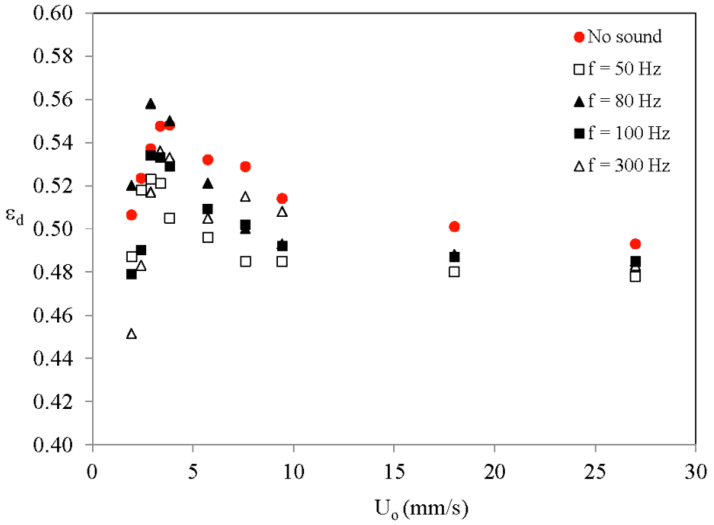

Fig. 8. Dense phase voidage and inlet superficial velocity relation for conventional fluidization and sound assisted fluidization at SPL = 80 dB and sound frequency = 50 Hz, 80 Hz, 100 Hz and 300 Hz

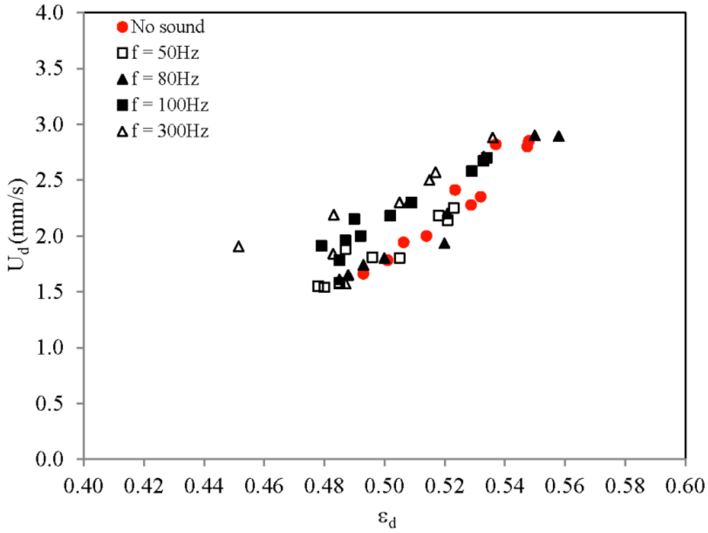

Fig. 9. Dense phase voidage and inlet superficial velocity relation for sound assisted fluidization at SPL = 80 dB and sound frequency = 50 Hz, 80 Hz, 100 Hz and 300 Hz

4.3 Validation of drag force correlation

It is well known that the drag force is the key component on describing the fluidization characteristics. One of which is the revised Ergun drag force correlation (Foscolo et al., 1983) This correlation was applicable for the fixed bed to the fluidized bed for an entire range of flow regime. And, it was proved by Cherntongchai and Brandani (2013) that to apply this correlation more accurately the empirical β should be applied. Therefore, they proposed the modified revised Ergun equation, as presented in Eq. (20) and suggested β value from this work was 4.21 for the conventional fluidization. At equilibrium condition, this drag force correlation is equaled to an effective weight (Eq. (21)). Hence, the relation between the dense phase voidage and its superficial velocity can be described.

$$F_D = \frac{4}{3}\frac{\rho_F}{d_P} C_D U^2 (1-\varepsilon)\varepsilon^{-\beta} \qquad (20)$$

At equilibrium, Eq. (20) is equaled to Eq. (21)

$$F_D = \varepsilon(\rho_P - \rho_F)(1-\varepsilon)g \qquad (21)$$

Richardson and Zaki expansion law (Richardson and Zaki, 1954) (Eq. (22)) is also a basic correlation used to describe the relation between the dense phase voidage and its superficial velocity.

$$\frac{U_d}{U_t} = \varepsilon_d^n \qquad (22)$$

And, the empirical Richardson and Zaki index (n) was recommended, especially for gas fluidization. For a sound assisted fluidization, Ammendola et al. (2011) worked with the homogeneous bed expansion data and gave the suggested value at approximately 5. While n index will be experimentally defined, terminal falling velocity (U_t) can be calculated from Eq. (23). (Dallavalle, 1948).

$$U_t = \left(-3.809 + \sqrt{3.809^2 + 1.832\sqrt{Ar}}\right)^2 \frac{\mu_F}{\rho_F d_P} \qquad (23)$$

Where;

$$Ar = g d_P^3 \rho_F \frac{\rho_P - \rho_F}{\mu_F^2} \qquad (24)$$

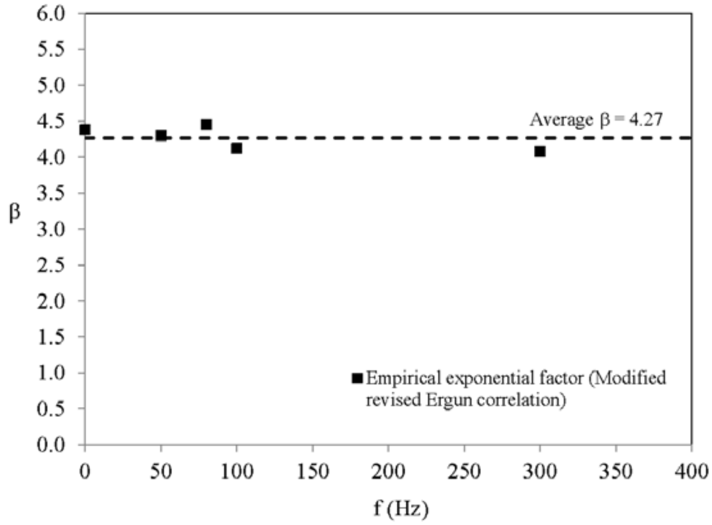

Fig. 10. Empirical exponential factor of revised Ergun correlation for conventional fluidization and sound assisted fluidization at various sound frequencies and SPL = 80 dB

Fig. 10 showed that the empirical β values of the revised Ergun correlation for the conventional fluidization and the sound assisted fluidization at different sound frequencies were distributed over the same average value (β = 4.27). This was considerably very close to the value suggested by Cherntongchai and Brandani (2013) (β=4.21).

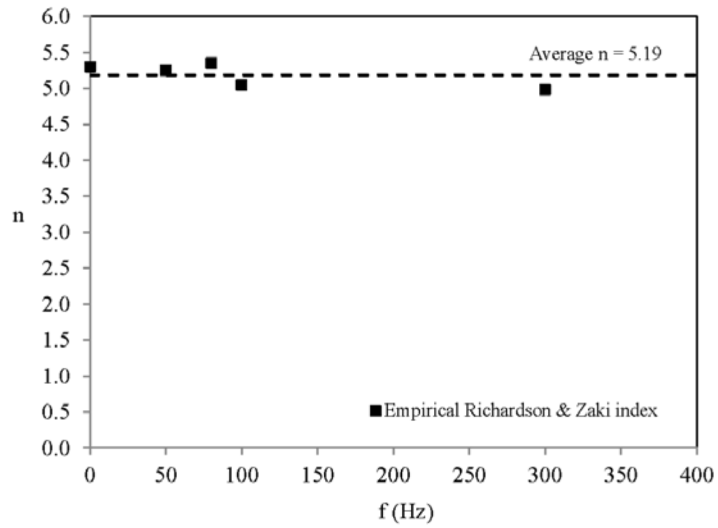

Fig. 11. Empirical Richardson and Zaki index (n) for conventional fluidization and sound assisted fluidization at various sound frequencies and SPL = 80 dB

Fig. 11 presented empirical n index for the Richardson and Zaki expansion law. As for the drag force correlation, the n index of the conventional fluidization and those of the sound assisted fluidization at different sound frequencies were failed on the same average value (n = 5.19)

Fig. 12 showed a good agreement between the prediction by the modified revised Ergun correlation (β = 4.27) and the empirical Richardson and Zaki correlation (n = 5.17) for the conventional fluidization and the sound assisted fluidization at sound pressure level of 80 dB and sound frequency of 50-300 Hz. This consolidated our conclusion that the sound vibration force tended to initiate the cavity or the bubble in the sound assisted fluidized bed rather than causing the change in the dense phase voidage and its superficial velocity relation. Hence, the force equilibrium in the dense phase for the sound assisted fluidized bed is remained as that for the conventional fluidization and the same drag force correlation or the bed expansion law can be applied.

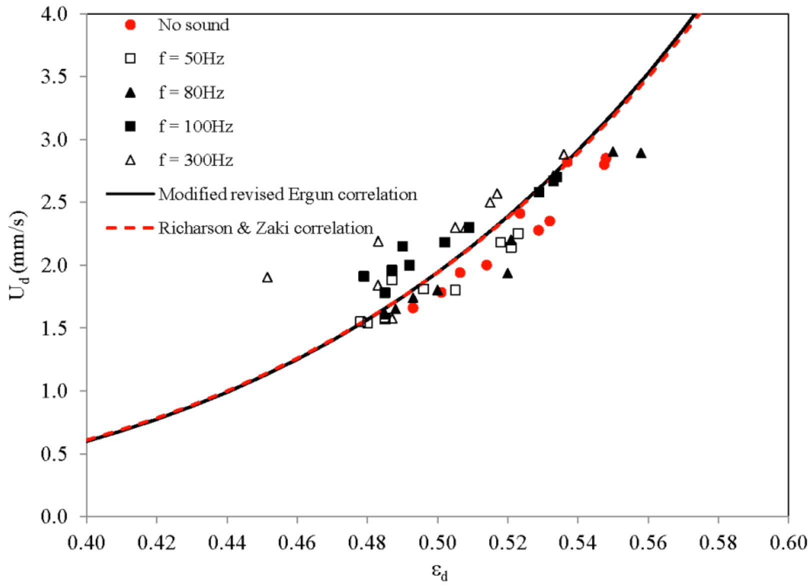

Fig. 12. Predictability of modified revised Ergun correlation and Richardson and Zaki correlation using empirical Richardson and Zaki index for conventional fluidization and sound assisted fluidization at various sound frequencies and SPL = 80 dB

4.4 Minimum bubbling point

A visual observation is the most common method used for an identification of a minimum bubbling point. However, it has been generally known that this method gives a very high degree of uncertainty. By definition, the minimum bubbling point is the point where the very first bubble appears in the particle bed and the dense phase expansion is the highest. To define the minimum bubbling point, it was recommended to use the plot between the dense phase voidage and its superficial velocity (Cherntongchai and Brandani, 2013) and the minimum bubbling point was defined at the maximum dense phase expansion point (Fig. 13).

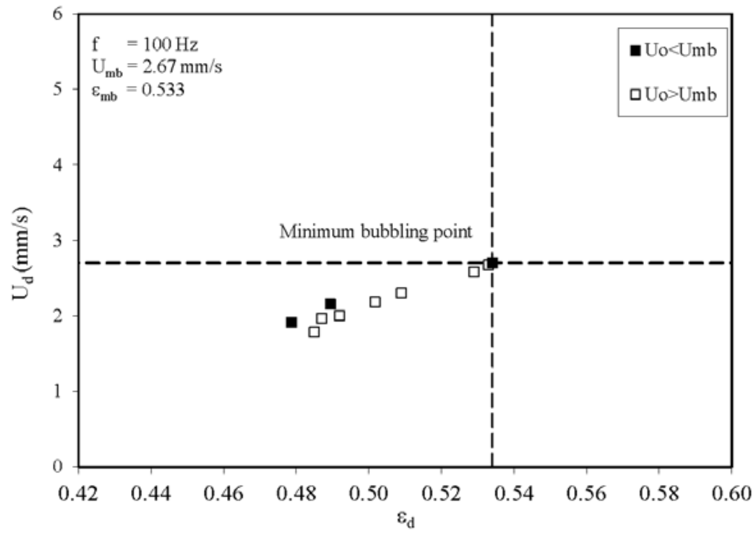

Fig. 13. Minimum bubbling point identification for the sound assisted fluidization at sound pressure level = 80 dB and sound frequency = 100 Hz

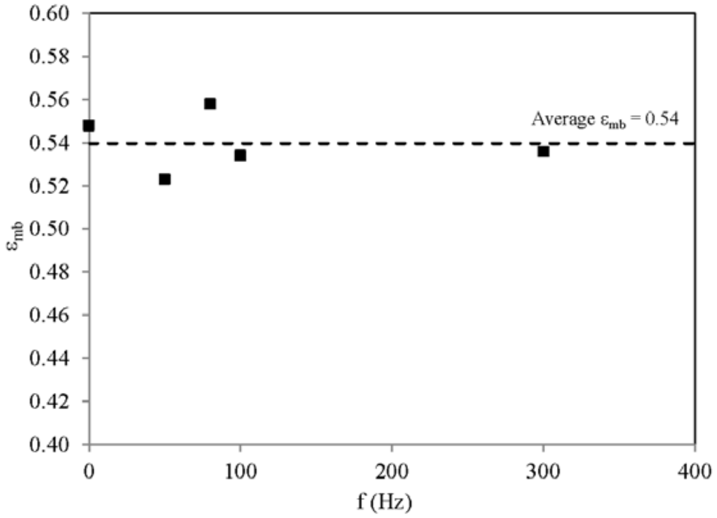

Fig. 14. Minimum bubbling voidage for conventional fluidization and sound assisted fluidization at various sound frequencies and SPL = 80 dB

Fig. 14 showed that the minimum bubbling voidages (ε_{mb}) of the conventional fluidization (f = 0 Hz) and the sound assisted fluidization (f = 50-300 Hz) were distributed on the same average value (ε_{mb}=0.54). Accordingly, their minimum bubbling velocities (Fig. 15) was distributed on the average value (U_{mb} = 2.714 mm/s). This means the sound vibrational force within the range of our study does not affect the bed stability. Again, it rather imparts the effect of creating a premature bubbling in the homogeneous expanded bed or a more bubble fraction in the bubbling bed.

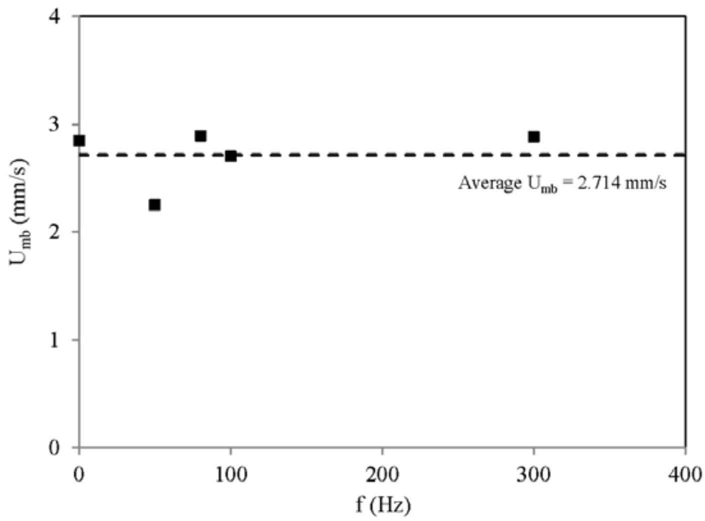

Fig. 15. Minimum bubbling velocity for conventional fluidization and sound assisted fluidization at various sound frequencies and SPL = 80 dB

4.5 Prediction of minimum bubbling point for sound assisted fluidization

The transition from the particulate to the bubbling beds is considered to be an instability problem. The stability criterion developed by Brandani and Zhang (2006) required a correct knowledge of the characteristic length and the drag force correlation. By Cherntongchai and Brandani (2013), the modified revised Ergun drag force correlation was recommended and the characteristic length (δ/d_p) as a function of a voidage was proposed. In this work, the stability criterion of Brandani and Zhang (2006), with a combination of the modified revised Ergun drag force correlation and a voidage dependency of the characteristic (δ/d_p) will be used for a prediction of the minimum bubbling point in a system of the sound assisted fluidization.

The stability criterion can be summarized as follows (Cherntongchai and Brandani, 2013);

$$U_{\varepsilon} = U_{D} \tag{25}$$

$$U_{\varepsilon} = (1-\varepsilon)\left(\frac{\partial U}{\partial \varepsilon}\right)_{Equil} = \frac{1-\varepsilon}{\varepsilon} \cdot \frac{(\beta+1)U}{2 + \frac{dC_{D}}{d\,Re_{P}} \frac{Re_{P}}{C_{D}}} \tag{26}$$

$$U_{D} = \sqrt{V^{2} - G} + V \tag{27}$$

Where β = 4.27 and Dallavalle equation (Dallavalle, 1948) was used for the drag coefficient.

$$C_{D} = \left(0.63 + \frac{4.8}{\sqrt{Re_{P}}}\right)^{2} \tag{28}$$

$$V = \frac{1-\varepsilon}{\varepsilon} \frac{\rho_{F} U}{\varepsilon \rho_{P} + (1-\varepsilon)\rho_{F}} \tag{29}$$

$$G = \frac{\frac{1-\varepsilon}{\varepsilon^{2}} \rho_{F} U^{2} - \delta\left[(1-\varepsilon)\rho_{P} + \varepsilon \rho_{F}\right] g}{\varepsilon \rho_{P} + (1-\varepsilon)\rho_{F}} \tag{30}$$

The empirical correlation for the characteristic length (δ/d_P) as function of the voidage is;

$$\frac{\delta}{d_{P}} = 0.55 + 3.0\left[\exp^{-42(\varepsilon - \varepsilon_{mf})}\right] \tag{31}$$

Table 4 Comparison between model prediction and experimental minimum bubbling point for sound assisted fluidization at various sound frequencies and SPL = 80 dB

Sound pressure level (dB)	Sound frequency (Hz)	Experimental average values		Model prediction	
		ε_{mb}	U_{mb} (mm/s)	ε_{mb}	U_{mb} (mm/s)
80	50-300	0.54	2.714	0.53	2.671

It was presented in Table 4. that the new stability proposed by Cherntongchai and Brandani (2013) can predict excellently the minimum bubbling point of Geldart's group A powder in the sound assisted fluidization.

5. CONCLUSIONS

Intrinsic bed expansion characteristics of Geldart's group A powder in the sound assisted fluidization of a fixed sound pressure level and a varied sound frequency was investigated. To obtain an accurate bed expansion data, the 1-valve and 2-valve bed collapse experiment was carried out and the bed collapse model was used to interpret correctly the bed collapse curves. The bed expansion characteristics were found differently from previous reports. And, the following points can be concluded;

- A total bed voidage and a dense phase voidage for the sound assisted fluidization were varied with an inlet superficial velocity in the same fashion as those for a conventional fluidization.
- The voidage with respect to the inlet superficial velocity of the sound assisted fluidization was found to be lower than that of the conventional fluidization.
- A dense phase voidage and its superficial velocity relations of the sound assisted fluidization at different sound frequencies were found to be approximately on the same trend as that for the conventional fluidization.
- A minimum bubbling point, defined using the dense phase voidage and dense phase superficial velocity characteristic curve, was also unaffected by the sound vibration force.

This suggested that an addition of sound vibrational force tended to create more cavity or bubble phase in the fluidized bed, rather than changing a hydrodynamics relation in the dense phase. Therefore, the same equilibrium of force can still be used to describe both systems of fluidization. Besides, the stability criteria can be applied for both systems.

Finally, it was proved that the modified revised Ergun drag force correlation can describe well the dense phase voidage and the dense phase superficial velocity characteristic curves. And, the stability criterion proposed by Cherntongchai and Brandani (2013) can predict excellently the minimum bubbling points.

NOMENCRATURE

A	=	Bed cross section area (m^2)
Ar	=	Archimedes number
C_D	=	Drag coefficient
d_P	=	Mean particle size (m)
F_D	=	Drag force of particles in suspension/volume (kg/m^2s^2)
f	=	Sound frequency (Hz)
g	=	Acceleration of gravity (m^2/s)
L_o	=	Total bed height from distributor (m)
L_1	=	Height of Zone1 from distributor (m)
L_2	=	Height of Zone 2 from distributor (m)
L_c	=	Column height (m)
n	=	Richardson and Zaki index
P_{atm}	=	Atmospheric pressure (Pa)
P_w	=	Absolute pressure in a windbox (Pa)
Re_P	=	Particle Reynold number = $\frac{d_P U \rho_F}{\mu_F}$
SPL	=	Sound pressure level (dB)

30

t	=	time (s)
t_{bub}	=	Bubble escape time (s)
U	=	Superficial velocity (m/s)
U_D	=	Dynamic wave velocity (m/s)
U_d	=	Dense phase superficial velocity (m/s)
U_{dis}	=	Superficial velocity of gas flowing through a distributor (m/s)
U_{mb}	=	Minimum bubbling velocity (m/s)
U_t	=	Terminal falling velocity (m/s)
U_o	=	Inlet superficial velocity (m/s)
U_1	=	Zone 1 superficial velocity (m/s)
U_ε	=	Continuity wave velocity (m/s)
V_w	=	Windbox volume (m^3)
Q_V	=	Volumetric flow rate of gas through discharge valve (m^3/s)
$Q_{Windbox}$	=	Volumetric flow rate of gas at windbox pressure (m^3/s)

Greek letters

β	=	Exponential factor for modified revised Ergun correlation
ΔP	=	Piezometric pressure drop (Pa)
δ	=	Characteristic length (m)
ε_d	=	Dense phase voidage
ε_{fixed}	=	Fixed bed voidage
ε_{mb}	=	Minimum bubbling voidage
ε_{mf}	=	Minimum fluidization voidage
ε_o	=	Total bed voidage
ε_1	=	Zone 1 bed voidage

ε_2 = Zone 2 bed voidage

ρ_F = Fluid density (kg/m^3)

ρ_P = Particle density (kg/m^3)

μ_F = Gas viscosity (kg/m.s)

ACKNOWLEDGEMENTS

Thailand Research Fund and Chiang Mai University are gratefully acknowledged for their financial support. (Contract number: RSA5780008)

REFERENCES

Ammendola P., Chirone R., Aeration and mixing behaviours of nano-sized powders under sound vibration, Powder Technology 201 (2010) 49-56.

Ammendola P., Chirone R., Raganati F., Fluidization of binary mixtures of nanoparticles under the effect of acoustic fields, Advanced Powder Technology 22 (2011) 174-183.

Brandani S., Zhang K., A new model for the prediction of the behaviour of fluidized beds, Powder Technology, 163(1-2) (2006) 80-87.

Cherntongchai P., Brandani S., A model for the interpretation of the bed collapse experiment, Powder Technology, 151 (2005) 37-48.

Cherntongchai P., Brandani S., Prediction ability of a new minimum bubbling criterion, Advanced Powder Technology, 24 (2013) 1-13.

Cherntongchai P., Innan T., Brandani S., Mathematical description of pressure drop profile for the 1-valve and 2-valve bed collapse experiment, Chemical Engineering Science, 66 (2011) 973-981.

Dallavalle J. M., Micromeritics, Pitman, New York, 1948

Foscolo P.U., Gibilaro L.G., Waldram S.P., A unified model for particulate expansion of fluidised beds and flow in fixed porous media, Chemical Engineering Science 38 (8) (1983) 1251–1260.

Guo Q., Li Y., Wang M., Shen W., Yang C., Fluidization characteristics of SiO_2 nanoparticles in an acoustic fluidized bed, Chemical Engineering Technology 26(1) (2006) 78-86.

Herrera C.A., Levy E.K., Bubbling characteristics of sound-assisted fluidized beds, Powder Technology, 119 (2001) 229-240.

Kaliyaperumal S., Barghi S., Zhu J., Briens L., Rohani S., Effects of acoustic vibration on nano and sub-micron powders fluidization, Powder Technology 210 (2011) 143-149.

Langde M. L., Sonolikar R. L., Dharmaraj J. T., The influence of acoustic field and frequency on hydrodynamics of group B particles, Thermal Science 15(1) (2011) 159-169.

Richardson J.F., Zaki W.N., The sedimentation of a suspension of uniform spheres under conditions of viscous flow, Chemical Engineering Science 3 (1954) 65-73.

Raganati F., Ammendola P., Chirone R., CO_2 adsorption on fine activated carbon in a sound assisted fluidized bed: Effect of sound intensity and frequency, CO_2 partial pressure and fluidization velocity, Applied Energy 113 (2014) 1269-1282.

Russo P., Chirone R., Massimilla L., Russo S., The influence of the frequency of acoustic waves on sound-assisted fluidization of beds of fine particles, Powder Technology 82 (1995) 219-230.

Zhu G., Liu Q., Yu Q., Pfeffer R., Dave R.N., Nam C.H., Sound assisted fluidization of nanoparticle agglomerates, Powder Technology 141 (2004) 119-123.